Structure-preserving Numerical Methods for Engineering Applications

Harsh A. Sharma

Dissertation submitted to the Faculty of the
Virginia Polytechnic Institute and State University
in partial fulfillment of the requirements for the degree of

Doctor of Philosophy
in
Aerospace Engineering

Mayuresh J. Patil, Chair
Craig A. Woolsey, Co-Chair
Taeyoung Lee
Shane Ross
Cornel Sultan

August 7, 2020
Blacksburg, Virginia

Keywords: Structure-preserving methods, Geometric numerical integration, Variational integrators, Lie group methods

Structure-preserving Numerical Methods for Engineering Applications

Harsh A. Sharma

(ABSTRACT)

This dissertation develops a variety of structure-preserving algorithms for mechanical systems with external forcing and also extends those methods to systems that evolve on non-Euclidean manifolds. The dissertation is focused on numerical schemes derived from variational principles – schemes that are general enough to apply to a large class of engineering problems. A theoretical framework that encapsulates variational integration for mechanical systems with external forcing and time-dependence and which supports the extension of these methods to systems that evolve on non-Euclidean manifolds is developed. An adaptive time step, energy-preserving variational integrator is developed for mechanical systems with external forcing. It is shown that these methods track the change in energy more accurately than their fixed time step counterparts. This approach is also extended to rigid body systems evolving on Lie groups where the resulting algorithms preserve the geometry of the configuration space in addition to being symplectic as well as energy and momentum-preserving. The advantages of structure-preservation in the numerical simulation are illustrated by various representative examples from engineering applications, which include limit cycle oscillations of an aeroelastic system, dynamics of a neutrally buoyant underwater vehicle, and optimization for spherical shape correlation and matching.

Structure-preserving Numerical Methods for Engineering Applications

Harsh A. Sharma

(GENERAL AUDIENCE ABSTRACT)

Accurate numerical simulation of dynamical systems over long time horizons is essential in applications ranging from particle physics to geophysical fluid flow to space hazard analysis. In many of these applications, the governing physical equations derive from a variational principle and their solutions exhibit physically meaningful invariants such as momentum, energy, or vorticity. Unfortunately, most traditional numerical methods do not account for the underlying geometric structure of the physical system, leading to simulation results that may suggest nonphysical behavior. In this dissertation, tools from geometric mechanics and computational methods are used to develop numerical integrators that respect the qualitative features of the physical system. The research presented here focuses on numerical schemes derived from variational principles– schemes that are general enough to apply to a large class of engineering problems. Energy-preserving algorithms are developed for mechanical systems by exploiting the underlying geometric properties. Numerical performance comparisons demonstrate that these algorithms provide almost exact energy preservation and lead to more accurate prediction. The advantages of these methods in the numerical simulation are illustrated by various representative examples from engineering applications, which include limit cycle oscillations of an aeroelastic system, dynamics of a neutrally buoyant underwater vehicle, and optimization for spherical shape correlation and matching.

Dedication

To my grandfather, Radheshyam Sharma

Acknowledgments

It has been an honor and a privilege to work with my co-advisors, Dr. Mayuresh Patil and Dr. Craig Woolsey. From my first year, both of them treated me as their colleague and gave me an incredible amount of freedom to explore different research directions at my own pace. In my third year, they also involved me with the proposal writing for NSF and AFOSR funding which was a great learning experience and it is an opportunity for which I owe them a tremendous debt of gratitude. In addition to their technical guidance, both of them have greatly helped me in planning my future steps. Their mentoring has helped me grow as both an academic and a person over these five years and the impact of the things I have learned from them on my life is profound. I must also thank Dr. Shane Ross and Dr. Cornel Sultan for their constructive feedback and suggestions during my committee meetings.

I am incredibly thankful to Dr. Taeyoung Lee for hosting me for research collaborations at the George Washington University during Summer 2018 and Summer 2019. Aside from contributing markedly to my doctoral research, I would also like to thank Dr. Lee for his great hospitality. I cannot overstate my appreciation for his financial support which allowed me to live lavishly in Washington DC. I would also like to thank Kanishke, Chao, Weixin, Mahdis, Shankar, Harshvardhan, and Reza for making me a part of their lab group at GWU. I must also thank Shubhodeep, Sourav, and Debjit for their support during my stay in DC.

I must also thank Dr. Jeff Borggaard for agreeing to mentor me for my MS in Mathematics. His expertise in numerical analysis helped me to give my research work a mathematical flavor. Apart from our research collaboration, I also owe thanks to Dr. Borggaard for his

help with my postdoc search. I am also indebted to Dr. Joseph Schetz with whom I had the honor of working as a GTA during my first three years. Apart from our work interactions, Dr. Schetz has always been really kind to me with his coffee/lunch treats. I will always have fond memories of visiting his house for a party and him giving me a ride to my home from the airport.

I am grateful to Dr. Stephen Prince for allowing me to attend his classes and film screenings during my PhD. Through his classes, I was able to fulfill my long-held wish of learning cinema formally and I got to watch movies from greats like Kurosawa and Ford. I will always cherish the memory of going to Hancock 100 on Tuesday evenings to see some of the greatest movies of all time on the big screen, the way they are meant to be seen.

None of this would be possible without the support of my friends in Blacksburg. I am incredibly thankful for the Blacksburg chapter of Association for India's Development for giving me the opportunity to immerse myself in helping generate funds for grassroots projects in India. I am also grateful to the Bengali community in Blacksburg for treating me as one of their own. I would also like to thank all the friends I made while playing cricket at various basketball and tennis courts in Blacksburg. During these years I have enjoyed visits to movies and sports with Abinash, Aniket, and Apratim. I will also miss hanging out with these friends: Amrita, Rathsara, Jeena, Beth, Kelly, Aarushi, Pranav, Yash, Riya, Adbhut, Shreya, and Varya. Atashi truly deserves separate credit for inviting me to innumerable parties for all these years. I would like to acknowledge my fellow graduate students, Nick, Karanpreet, Deva, Revati, Udit, Poorva, Agastya, Siddharth, and George, for making my graduate experience that much more rich and pleasant. I must also thank my undergraduate friends for their constant support, including my best friends Om, Kushan, Bansal, Akshit, Saurabh, Malhar, Mohit, Atul, and Raj.

I would not be where I am today without the love and support of my family and for that I am sincerely grateful. First of all, I must thank my roommates Pawan, Aarash, Evan, Sheril, Yixiao, Abe, and Anthony for their company during my doctoral study. I must thank my brother Kalpan Sharma and my sister-in-law Rizu Raval for always having my back. My father Apurva Sharma instilled his curiosity and passion for learning in me at a very young age and this played a major part in my choice to pursue a PhD. Finally, I would like to thank my mother Sangita Sharma for believing in me every step of the way.

Contents

List of Figures

List of Tables

Chapter 1

Introduction

1.1 Background and Motivation

Scientists at NASA's Jet Propulsion Laboratory (JPL) [1] recently announced that 2002 AJ129, a Potentially Hazardous Asteroid (PHA), would fly safely past earth on February 4, 2018. Based on their long-time simulation results, they also predicted that the asteroid has zero chance of colliding with Earth any time over next 100 years. At a dramatically different space and time scale, conditions at the subatomic level in the Large Hadron Collider (LHC) are being numerically simulated at a resolution of trillionths of a second to answer fundamental questions about the cosmos [2]. Beyond astrodynamics and particle physics, the study of ocean currents and atmospheric clouds in geophysical fluid dynamics, of energy and momentum transfer processes in plasma physics, and of molecular dynamics with disparate time scales also require very accurate long-time simulation. In many of these applications, the governing physical equations derive from a variational principle and their solutions exhibit physically meaningful invariants such as momentum, energy, or vorticity.

As modern challenges in engineering and science grow in complexity and dimension, the need for sophisticated numerical methods to support model-based design and analysis also grows. With increasing computational power, numerical solutions to increasingly sophisticated problems can be computed over longer time intervals, with millions of time integration steps. For such problems, the qualitative properties of the integrator are critical to the accuracy of the

numerical simulation and reliability of long range predictions. In engineering applications, numerical methods for studying dynamical systems are usually designed to give rapid and robust numerical solutions with small overall error. Traditional numerical schemes do not account explicitly for the qualitative features of the underlying physical system, however, incurring error that may suggest nonphysical behavior.

The field of geometric numerical integration (GNI) is concerned with numerical methods that respect the fundamental physics of a problem by preserving the geometric properties of the governing differential equations. Using ideas from geometric mechanics and differential geometry, the field of GNI has produced a variety of numerical methods for simulating systems described by ordinary differential equations (ODEs), which respect the qualitative features of the dynamical system. GNI methods appeal to physicists, mathematicians, and engineers for many reasons. For physicists, the geometric structure of a dynamical system reveals essential, qualitative features in the system's evolution – features that should appear in an accurate simulation. For mathematicians, numerical methods based on discrete variational principles may exhibit superior numerical stability and structure-preserving capabilities. For engineers, these methods can advance model-based design and analysis by preserving fidelity to the physical, continuous-time system, enabling, for example, more accurate predictions of the energy transfer between subsystems.

Since the emergence of computational methods, fundamental properties such as accuracy, stability, convergence and computational efficiency have been considered crucial for deciding the utility of a numerical algorithm. Recently, various aspects of structure-preservation have emerged as an important addition to these fundamental properties. One of the key ideas of the structure-preserving approach is to treat the numerical method as a discrete dynamical system which approximates the flow of the governing continuous differential equation instead of focusing on numerical approximation of a single trajectory. Such an approach allows a

better understanding of the invariants and qualitative properties of the numerical method. Mechanical systems, in particular, often exhibit physically meaningful invariants such as momentum, energy, or vorticity; the behavior of these invariants in simulation provides an important measure of accuracy. Most traditional numerical methods do not account for the underlying geometric structure of the physical system, however, so these methods introduce numerical dissipation and fail to preserve invariants of the system. A structure-preserving numerical method, on the other hand, can ensure that qualitative features, such as invariants of motion or the structure of the configuration space, are reflected in the simulation and they can provide accurate numerical simulation over exponentially long times.

GNI emerged as a major thread in the development of numerical methods in the 1990s. The field has grown steadily due to the efforts of mathematicians concerned with accurately simulating the behavior of solutions to differential equations, and thus with numerical methods that respect the underlying problem structure. These methods have proven quite useful for conservative Lagrangian/Hamiltonian systems; their numerical stability and accurate prediction of the (constant) system energy make them useful tools for studying complicated dynamical systems. In fact, research over the past two decades has produced GNI methods for finite-dimensional, time-invariant mechanical systems subject to conservative forcing that are so accurate for long-time simulation that they are now used for benchmarking purposes. Even for short-term simulations, it has been frequently observed that the structure-preserving approach enjoys smaller errors per time step compared to traditional methods, especially for problems involving finite-time singularities. Since its advent, the structure-preserving approach has become the new benchmark in the simulation of ODEs, while also making substantial progress in the numerical study of partial differential equations (PDEs).

1.2 Research Objectives

Advances in GNI methods for finite-dimensional, time-invariant mechanical systems subject to conservative forcing have produced algorithms so accurate for long-time simulation that they are now used for benchmarking purposes. There is a present need and opportunity, however, to extend these techniques to time-varying systems subject to non-conservative external forcing. The overarching goal of the current research is to develop and disseminate new structure-preserving numerical methods for mechanical systems with external forcing and time-dependence, which are often found in engineering applications. The specific objectives supporting this goal are:

1. Construct geometric numerical integration schemes based on variational principles – schemes that are general enough to apply to a large class of engineering problems – and investigate the advantages of these tools in comparison with traditional numerical methods.

2. Develop a theoretical framework which *encapsulates* variational integration for mechanical systems with external forcing and time-dependence and which supports the *extension* of these methods to systems that are constrained or that evolve on non-Euclidean manifolds.

3. Taking selected engineering problems with different qualitative features as case studies, apply a variety of structure-preserving numerical methods and investigate their relative performance using relevant metrics (e.g., energy error, computational cost, solvability, numerical stability).

1.3 Summary of Contributions

The main contributions of this dissertation are summarized as follows.

Chapter 2

- Basic differential geometry and geometric mechanics concepts are introduced from a variational point of view.
- A review of various structure-preserving numerical methods is given which covers the basics of variational integrators, energy-momentum integrators and Lie group methods in an accessible way.
- A survey of engineering applications of structure-preserving methods is given for broader use by practitioners.

Chapter 3:

- Energy-preserving, adaptive time step variational integrators for forced Lagrangian systems are derived by discretizing the Lagrange-d'Alembert principle.
- Detailed numerical results with a condition number study are provided.

Chapter 4:

- Hermite polynomial based one-step variational and Galerkin methods are derived for $\mathcal{C}^1$– continuous numerical integration of mechanical systems.

Chapter 5:

- Energy-preserving, adaptive time step Lie group variational integrators are derived for rigid body attitude dynamics.

Chapter 6:

- Energy-preserving, adaptive time step Lie group variational integrators are derived for rigid body motion in $\mathsf{SE}(3)$.

Chapter 7:

- Classical momentum method on $\mathbb{R}^n$ is demonstrated as a variational integrator of a damped harmonic oscillator with a nonlinear potential.
- Symplectic accelerated gradient method on $\mathsf{SO}(3)$ is derived using the Lie group variational integrator framework.

Chapter 8:

- Backward stability of energy-preserving, adaptive time step variational integrators is investigated by interpreting them as fixed time-step variational integrators on a transformed space.

1.4 Publications

This dissertation draws upon the following papers that have or will be submitted for publication, but the contents from these papers have been modified to avoid repetition of material and fit the general theme of this dissertation.

- **Journal Paper:** H. Sharma, J. Borggaard, M. Patil, C. Woolsey, *"Performance Assessment of Energy-preserving, Adaptive Time Step Variational Integrators"* for Journal of Geometric Mechanics (In preparation)

- **Journal Paper:** H. Sharma, M. Patil, C. Woolsey, *"Hermite-based One-step Variational and Galerkin Methods for Mechanical Systems"* for International Journal for Numerical Methods in Engineering (In preparation)

- **Journal Paper:** H. Sharma, M. Patil, C. Woolsey, *"A Review of Structure-preserving Numerical Methods for Engineering Applications"*, Computer Methods in Applied Mechanics and Engineering, Volume 366, 2020

- **Journal Paper:** H. Sharma, M. Patil, C. Woolsey, *"Energy-preserving Variational Integrators for Forced Lagrangian Systems"*, Communications in Nonlinear Science and Numerical Simulation, Volume 64, 2018, pp. 159-177

- **Conference Proceedings:** H. Sharma, T. Lee, M. Patil, C. Woolsey, *"Symplectic Accelerated Optimization on SO(3) with Lie Group Variational Integrators"*, American Control Conference, 2020 (Peer reviewed paper and presentation)

- **Conference Proceedings:** H. Sharma, M. Patil, C. Woolsey, *"Energy-preserving, Adaptive Time-Step Lie Group Variational Integrators for Rigid Body Motion in SE(3)"*, Conference on Decision and Control, 2019 (Peer reviewed paper and presentation)

- **Conference Proceedings:** H. Sharma, T. Lee, *"Energy-preserving, Adaptive Time-Step Lie Group Variational Integrators for the Attitude Dynamics of a Rigid Body"*, American Control Conference, 2019 (Peer reviewed paper and presentation)

Chapter 2

Review of Literature

The main goal of this chapter is to encourage the broader use of structure-preserving numerical methods in engineering applications by providing an overview of existing GNI methods and their capabilities in an accessible way, while adding perspectives and application examples from the literature. In order to be able to use structure-preserving methods in practice, it is necessary to understand their theoretical bases, numerical properties, limitations and computational complexity. This chapter summarizes all these aspects as comprehensively as possible without delving deep into the mathematical details. In the last two decades the field of structure-preserving methods has grown considerably, with many points of view and intricate subtleties. Since this work is intended to provide a gateway into the field for practitioners, we have attempted to address the underlying principles and ideas in this survey, rather than describing specific algorithms and their numerical implementation.

This chapter is organized as follows. In Section 2.1 we give an overview of the geometry and qualitative features of continuous-time dynamical systems with special focus on Lagrangian/Hamiltonian mechanics and mechanical systems evolving on non-Euclidean manifolds. The perspective taken here is to describe in broad brush strokes the different types of qualitative features that can be preserved for mechanical systems found in engineering problems. In Section 2.2 we provide a brief introduction to the formulation of a variety of structure-preserving methods, including symplectic methods, variational integrators, energy-momentum integrators, and Lie group methods. In Section 2.3 we give a selection of appli-

cations from the literature, that may benefit from a structure-preserving approach based on the requirements of a particular application.

2.1 Geometric Structure Underlying Continuous Systems

The geometric structure is a property of the governing differential equation which can be defined independently of particular coordinate representations. The structure-preserving approach to numerical simulation views the numerical method as a discrete dynamical system which inherits this geometric structure from the continuous system. Thus, for a better understanding of structure-preserving numerical schemes, we look at the continuous dynamical systems, governing differential equations and their qualitative properties. Although a lot of methods to be discussed in this chapter can be applied to a broader class of problems, this work pays special attention to Lagrangian/Hamiltonian mechanical systems evolving on manifolds as they are among the most important class of engineering systems in the context of GNI.

2.1.1 Basic Concepts

The modern formulations of Lagrangian and Hamiltonian mechanics [3, 4, 5] utilize the coordinate-free language of differential geometry [6, 7] to provide a unifying framework for many disparate engineering systems. Apart from elegance and precise mathematical formulation, use of differential geometry allows applications to mechanical systems evolving on general manifolds. In this subsection we give a quick review of differential geometry concepts used in the Lagrangian mechanics framework. We emphasize the fundamental concepts

required for the variational mechanics while suppressing the technical details.

The concept of a smooth manifold is central to the geometric treatment of classical mechanics as it generalizes ideas developed on linear vector spaces to non-Euclidean spaces. Manifolds naturally arise as the configuration spaces for a variety of engineering applications, especially for mechanical systems with restrictions on the allowed motion due to physical constraints. For example, the unit sphere $S^2 = \{(x, y, z) \in \mathbb{R}^3 |\ x^2 + y^2 + z^2 = 1\}$ is the configuration space of a spherical pendulum. The sphere S^2 is a two-dimensional manifold embedded in $\mathbb{R}^3$.

Mathematically, manifolds are topological spaces that are locally equivalent to Euclidean spaces - such as $\mathbb{R}^n$. In simple words, for each point on the $n-$dimensional manifold, the points in the neighborhood can be labeled using n local coordinates. The important distinction from the vector spaces is that these coordinates are only valid in a small neighborhood of each point and not globally on manifolds. For most of the mechanical systems evolving on manifolds, the configuration manifolds are equipped with differentiable structure allowing calculus on manifolds.

The Lagrangian and Hamiltonian mechanics formulations defined on vector spaces provide local mathematical formulations of mechanics on manifolds using multiple coordinate maps. From the Lagrangian mechanics perspective, there are two basic requirements for studying the dynamics of mechanical systems. First, we need to identify the set of all possible configurations of the system as the configuration manifold. The second requirement is to develop a Lagrangian function which is a real-valued function defined on the state space. For mechanical systems that are most commonly considered, the Lagrangian function is the difference between the kinetic energy of the system and the potential energy of the system. This Lagrangian function is then used in Hamilton's principle to obtain Euler-Lagrange equations. The Hamiltonian perspective on the other hand utilizes the phase space version

of Hamilton's principle to derive Hamilton's equations.

Consider a mechanical system evolving on a configuration manifold Q. The tangent space to Q at the configuration $\mathbf{q} \in Q$ is the set of all tangent vectors based at $\mathbf{q}$, denoted by $T_{\mathbf{q}}Q$. The dual space of $T_{\mathbf{q}}Q$, i.e. the set of all linear maps from $T_{\mathbf{q}}Q$ to $\mathbb{R}$, is called the contangent space and is denoted by $T^*_{\mathbf{q}}Q$. For the path $\mathbf{q}(t)$ on the manifold Q, the velocity $\dot{\mathbf{q}}(t)$ at time t is a tangent vector to Q, based at the point $\mathbf{q}(t) \in Q$. The tangent bundle of Q, denoted by TQ, is the union of all of the tangent spaces to Q. The configuration and velocity $(\mathbf{q}(t), \dot{\mathbf{q}}(t))$ belong to the tangent space to Q at $\mathbf{q}(t)$ and hence the state space is represented by the tangent bundle TQ. On the other hand, the configuration and the momentum $(\mathbf{q}(t), \mathbf{p}(t))$ belong to the cotangent space, and hence the phase space can be identified with the collection of all the cotangent spaces to Q, namely the cotangent bundle T^*Q. Subsequently, the Lagrangian $L : TQ \to \mathbb{R}$ is defined on the tangent bundle TQ whereas the Hamiltonian $H : T^*Q \to \mathbb{R}$ is defined on the cotangent bundle T^*Q.

It is important to recognise that this geometric formulation can be used to describe and analyze dynamical systems globally without resorting to local coordinate maps that may lead to singularities. In fact this representation is both efficient and advantageous for studying qualitative properties of complex dynamical systems but has not been widely used by the engineering community.

2.1.2 Lagrangian Mechanics

In the late seventeenth century, Newton's laws of motion [8] provided a way to study the dynamics for free point masses but this approach didn't work that well for more complicated mechanical systems such as rigid bodies or connected bodies. Lagrange [9, 10] came up with an elegant way of computing the dynamics of general mechanical systems; he derived

a coordinate-invariant formulation of the equations of motion in terms of the Lagrangian. A few decades later Hamilton [11, 12] simplified the structure of these equations using the variational principle that bears his name. We closely follow [13] to revisit the variational derivation of the Euler-Lagrange equations and their qualitative properties from the Lagrangian point of view.

Consider a time-invariant Lagrangian mechanical system with a finite-dimensional, smooth configuration manifold Q, state space TQ, and Lagrangian $L : TQ \to \mathbb{R}$. Hamilton's principle [14] states that: The motion of the system between two fixed points from t_i to t_f is such that the action integral has a stationary value for the actual path of the motion. For a conservative Lagrangian system, Hamilton's principle characterizes the path $\mathbf{q}(t)$ which passes through $\mathbf{q}(t_i)$ at $t = t_i$ and $\mathbf{q}(t_f)$ at $t = t_f$ as that which satisfies the following condition:

$$\delta\mathfrak{B}(\mathbf{q}) = \delta \int_{t_i}^{t_f} L(\mathbf{q}(t), \dot{\mathbf{q}}(t))\, dt = \int_{t_0}^{t_f} \left[\frac{\partial L(\mathbf{q}(t), \dot{\mathbf{q}}(t))}{\partial \mathbf{q}(t)} \cdot \delta\mathbf{q}(t) + \frac{\partial L(\mathbf{q}(t), \dot{\mathbf{q}}(t))}{\partial \dot{\mathbf{q}}(t)} \cdot \delta\dot{\mathbf{q}}(t) \right] dt = 0 \tag{2.1}$$

Using integration by parts and setting the variations at the endpoints equal to zero gives the Euler-Lagrange equations

$$\frac{\partial L(\mathbf{q}(t), \dot{\mathbf{q}}(t))}{\partial \mathbf{q}} - \frac{d}{dt}\left(\frac{\partial L(\mathbf{q}(t), \dot{\mathbf{q}}(t))}{\partial \dot{\mathbf{q}}} \right) = \mathbf{0} \tag{2.2}$$

Mechanical systems governed by equations (2.2) exhibit important qualitative features. For autonomous Lagrangian systems i.e. no explicit time-dependence in the Lagrangian, the energy is conserved along the solution trajectory. Second, by Noether's theorem [15], there exists an invariant of the motion corresponding to each symmetry that leaves the Lagrangian invariant. Another interesting and useful property is that these Lagrangian mechanical systems conserve a skew-symmetric, bilinear form known as the *symplectic Lagrangian form* along trajectories [3]. For mechanical systems with explicit time-dependence in the La-

grangian, the governing equations and the qualitative features of the nonautonomous system can be studied by utilizing the extended Lagrangian mechanics framework [13]. Unlike standard Lagrangian mechanics, the extended framework accounts for time variations in addition to the configuration variable variations.

The governing equations (2.2) and their properties discussed above can also be derived from the Hamiltonian point of view by considering Hamilton's principle in phase space. Depending on the problem, some properties can be observed and understood from the Lagrangian perspective and others are easier from the Hamiltonian perspective. For most engineering applications, the Lagrangian is hyperregular and it is possible to obtain the governing equations in the Hamiltonian form from (2.2) via Legendre transformation. However, for some applications such as interaction between point vortices [16], the Lagrangian is degenerate and no corresponding Hamiltonian formulation exists. Apart from these two approaches, the Hamilton-Jacobi viewpoint is also very important for developing structure-preserving numerical methods. This theory describes the motion of the system by a characteristic function S that is the solution of a PDE, known as the Hamilton-Jacobi differential equation. This approach is particularly useful in discovering invariants of the motion for mechanical systems without solving the problem completely.

For an autonomous Lagrangian system with time-independent external forcing $\mathbf{f}_L(\mathbf{q}(t), \dot{\mathbf{q}}(t))$, the Lagrange-d'Alembert principle characterizes trajectories $\mathbf{q}(t) \in Q$ as those satisfying

$$\delta \int_{t_i}^{t_f} L(\mathbf{q}(t), \dot{\mathbf{q}}(t))\ dt + \int_{t_i}^{t_f} \mathbf{f}_L(\mathbf{q}(t), \dot{\mathbf{q}}(t)) \cdot \delta\mathbf{q}\ dt = 0 \tag{2.3}$$

where the second term accounts for the virtual work done by the external forces when the path $\mathbf{q}(t)$ is varied by $\delta\mathbf{q}(t)$. Using integration by parts and setting the variations at the

endpoints equal to zero gives the forced Euler-Lagrange equations

$$\frac{\partial L(\mathbf{q}(t), \dot{\mathbf{q}}(t))}{\partial \mathbf{q}} - \frac{d}{dt}\left(\frac{\partial L(\mathbf{q}(t), \dot{\mathbf{q}}(t))}{\partial \dot{\mathbf{q}}}\right) + \mathbf{f}_L(\mathbf{q}(t), \dot{\mathbf{q}}(t)) = \mathbf{0} \tag{2.4}$$

Non-conservative external forcing $\mathbf{f}_L$ violates the symplectic structure and the corresponding Lagrangian system does not preserve the symplectic form. This external forcing will generally break the symmetries of the Lagrangian and that will lead to the corresponding momentum as well as the system energy not being conserved. In the special case that the forcing is orthogonal to the symmetry, the corresponding conserved quantity can be derived from the forced Noether's theorem [13]. Although these forced mechanical systems do not, in general, preserve the invariants or the symplectic form, the variational approach reveals how the external forcing alters these properties over time. This is particularly important for developing numerical methods that capture the evolution of energy or momentum accurately.

2.1.3 Variational Formulation of Different Problems

The variational methodology and the Lagrangian mechanics concepts discussed in Section 2.1.2 have been successfully extended to a variety of mechanical systems. In this subsection, we summarize the qualitative features and the geometric properties of various classes of mechanical problems that are important for engineering applications. To keep this treatise as simple and direct as possible, we have skipped a lot of mathematical details and focused mainly on the key ideas relevant to structure-preserving discretization. For a thorough exposition, the interested reader may consult the standard textbooks [3, 4, 17] and the references cited herein.

Holonomic Constraints: The formulation can be extended to mechanical systems with holonomic constraints, i.e. constraints on the configuration manifold, by the augmented approach using the Lagrange multiplier theorem [17]. For a Lagrangian system with d holonomic constraints $\phi : Q \to \mathbb{R}^d$, the augmented Lagrangian $\bar{L}$ is defined as $\bar{L}(\mathbf{q}(t), \dot{\mathbf{q}}(t), \lambda(t)) = L(\mathbf{q}(t), \dot{\mathbf{q}}(t)) - < \lambda(t), \phi(\mathbf{q}(t)) >$. The configuration $\mathbf{q}(t) \in Q$ along with the Lagrange multipliers $\lambda(t) \in \mathbb{R}^d$ extremize the action integral corresponding to the augmented Lagrangian $\bar{L}(\mathbf{q}(t), \dot{\mathbf{q}}(t), \lambda(t))$ which leads to constrained Euler-Lagrange equations [13].

Nonholonomic Constraints: The theory for mechanical systems with nonholonomic constraints [18], i.e. $\phi : TQ \to \mathbb{R}$, uses theory of Ehresmann connections [19] to describe the constraints. The basic idea is to consider a collection of linear subspaces $\mathcal{D}_{\mathbf{q}} \subset T_{\mathbf{q}}Q$ for each $\mathbf{q}(t) \in Q$ which together describe the velocities attainable by the system under the given constraints. The equations of motion for the mechanical system with nonholonomic constraints are given by the Lagrange-d'Alembert principle where we apply (2.1) with variations of the curve $\mathbf{q}(t)$ satisfying $\delta\mathbf{q}(t) \in \mathcal{D}_{\mathbf{q}}(t)$. The governing equations for the nonholonomic system feature a forcing term which involves the curvature of the connection.

Nonsmooth Problems: The variational approaches discussed so far do not apply directly to nonsmooth problems, such as collision and fragmentation models. This is due to the lack of smoothness of trajectories which prevents the use of differential calculus on manifolds. Using concepts from nonsmooth analysis and extended mechanics framework, the variational approach can be generalized to the nonsmooth setting [20]. Similar to the time-dependent Lagrangian case, the key idea is to treat both configuration variables and time as functions of a fixed parameter space which makes the relevant space of configurations a smooth manifold.

Uncertainty: For mechanical systems with uncertainties, a stochastic action can be defined

based on the stochastic flow of randomly perturbed Hamiltonian systems. The stochastic Hamiltonian systems [21] on manifolds extremize a stochastic action defined on the space of manifold-valued semimartingales. Similar to the deterministic case, the stochastic flow is also symplectic [22] and, by the stochastic Nother's theorem [23], preserves the symmetries as well.

Infinite-dimensional Systems: It is important to note that all the governing equations and geometric properties discussed so far are only applicable to mechanical systems evolving on finite-dimensional manifolds. For infinite-dimensional problems, the governing PDEs can be derived thorugh a variational approach by using the covariant field theory [24] where the dynamics is described in terms of finite-dimensional space of fields at a given event in spacetime. The covariant analogue of the symplecticity property is the multisymplectic form formula [25] and the covariant version of Noether's theorem leads to conservation laws for PDEs in the presence of symmetries.

Nonvariational Problems: An obvious limitation of the variational methodology is that it can be only used for Lagrangian/Hamiltonian systems. Although all conservative [26] and a wide variety of non-conservative problems can be modeled using the Lagrangian formalism, it still excludes a lot of interesting systems, for example the problems found in fluid dynamics and thermodynamics. The inverse problem of the calculus of variations [27] deals with the existence and formulation of variational principles for systems of differential equations. The method of formal Lagrangians [28] can embed certain nonvariational systems into a larger system which admits a Lagrangian formulation. This approach extends the applicability of Noether's theorem [29] to a larger class of problems and is particularly useful for the analysis of conservation laws of arbitrary nonvariational differential equations found in fluid dynamics and plasma physics [30].

2.2 Structure-preserving Methods

Traditional numerical integrators for studying dynamical systems usually take an initial condition and move the dynamical system state in the direction specified by the governing differential equations. This approach to numerical discretization ignores the qualitative properties of the continuous-time systems and hence may introduce spurious nonphysical effects leading to incorrect results. On the other hand, GNI methods preserve the underlying geometric structure and provide qualitatively correct numerical results. The philosophy behind this structure-preserving approach is to identify geometric properties of the continuous-time system and then design numerical methods which possess the same properties in the discrete domain. We focus on mechanical integrators – numerical integration methods that preserve some of the invariants of the mechanical system, such as, energy, momentum, or the symplectic form. Other properties that can be important to preserve are phase-space volume, continuous or discrete symmetries, time-reversibility, Casimirs, the correct physical form of dissipation, etc.

In this section, we provide a brief introduction along with a summary of recent developments in numerical integration of Lagrangian/Hamiltonian mechanical systems. Since our focus is on Lagrangian/Hamiltonian systems, we first look at numerical methods which preserve the symplecticity of the flow. In fact, most of the early developments in the field of GNI methods were related to development of numerical integrators that preserved the symplectic nature of the flow. We then look at the two most important classes of mechanical integrators: variational integrators and energy-momentum integrators. We also discuss Lie group methods for mechanical systems evolving on manifolds.

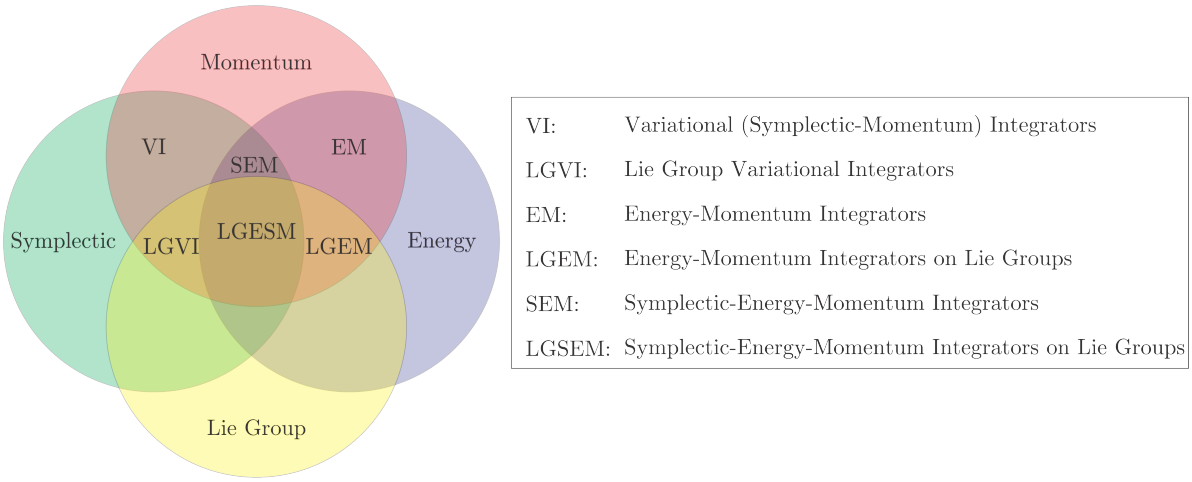

Figure 2.1: The taxonomy of structure-preserving methods based on the qualitative features they preserve for a mechanical system.

2.2.1 Symplectic Methods

As mentioned in Section 2.1.2, the symplectic property has geometric implications regarding the way in which the Lagrangian flow acts on a set of initial conditions. In simple words, symplecticity describes how all motions starting close to the actual motion are constrained in relation to each other. Based on this observation, Vogelaere [31] first developed numerical integrators that preserved this symplectic property of Hamilton's equations in 1950s. Although the symplectic methods for Lagrangian/Hamiltonian problems have a long history with different approaches, modern efforts can be traced to the generating function based methods of Feng *et al* [26] and Ruth [32] where they constructed symplectic methods by computing approximate solutions of the Hamilton-Jacobi equation. Later, Lasagni [33], Sanz-Serna [34], and Suris [35] showed that certain Runge-Kutta methods preserve symplecticity and they constructed symplectic Runge-Kutta methods from different perspectives. Reich [36] showed that the symplectic Runge-Kutta methods conserve the momentum for Hamiltonian problems with linear symmetries.

These methods preserve the symplectic nature of Hamiltonian systems, conserve the momenta and reproduce the dynamic behavior accurately for a long time. The excellent long-time behavior of the symplectic methods can be explained by backward error analysis where instead of asking "What is the numerical error for our problem?", the focus is on "Which nearby problem is solved exactly by our method?". Through backward error analysis of Hamiltonian ODEs, Reich [37] showed that symplectic methods solve a nearby Hamiltonian problem exactly. Thus, despite not conserving the energy of the system exactly, computed trajectories from symplectic methods always remain close to the solution and the energy error remains bounded for an exponentially long time.

Ge and Marsden [38] showed that a fixed time step numerical integrator cannot preserve the symplectic form, momentum, and energy simultaneously for non-integrable systems. Consequently, the structure-preserving fixed time step mechanical integrators can be divided into two categories: (i) energy-momentum and (ii) symplectic-momentum integrators.

2.2.2 Variational Integrators

In comparison to symplectic methods based on the generating functions, variational integrators constitute a more recent approach toward the structure-preserving discretizations of Lagrangian/Hamiltonian mechanical systems. These methods utilize concepts from discrete mechanics, a discrete analogue to continuous-time Lagrangian/Hamiltonian mechanics. Due to their variational nature, these methods can be easily extended to non-conservative mechanical systems by discretizing the Lagrange-d'Alembert principle. The basic idea is to construct a discrete-time approximation of the action integral called the discrete action. Stationary points of this discrete action give discrete-time trajectories of the mechanical system.

Depending on the application, various authors have proposed different versions of discrete mechanics. In fact, discrete-time versions of variational principles are of mathematical interest in their own right. Based on the concept of a difference space, Maeda [39] presented a discrete version of Hamilton's principle and derived discrete Euler-Lagrange equations. Using the same discretization, Maeda [40] later extended Noether's theorem to the discrete setting. Veselov [41, 42] pursued these ideas further in the context of integrable systems and showed that these discrete-time systems preserve a symplectic form. Building on these results, Moser and Veselov [43] presented discrete versions of several classical integrable systems including the free rigid body system.

Based on these concepts, Marsden and West [44] developed a theory of discrete mechanics, from both Lagrangian and Hamiltonian perspectives, and derived variational integrators by considering the discrete analogue of variational principles. Although the derivation of variational integrators from discrete variational principles was first given in [45], we closely follow [44] to give a brief review of the construction of variational integrators from the Lagrangian perspective. The idea behind variational integrators is simple: rather than discretize the governing equations (2.2) or (4.2), one discretizes the underlying variational principle (2.1) or (2.3).

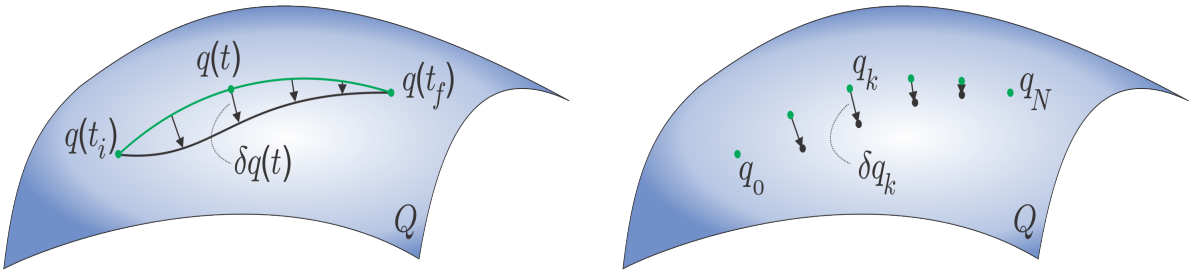

Figure 2.2: A cartoon illustrating the continuous time variational mechanics (left) versus the discrete time variational mechanics (right).

Consider a discrete Lagrangian system with configuration manifold Q and discrete state

space $Q \times Q$. For a fixed time step $h = \frac{t_f - t_i}{N}$, the discrete trajectory $\{ \mathbf{q}_k \}_{k=0}^{N}$ is defined by the configuration of the system at the sequence of times $\{ t_k = t_i + kh \mid k = 0, ..., N \}$. We introduce the discrete Lagrangian function $L_d(\mathbf{q}_k, \mathbf{q}_{k+1})$, an approximation of the action integral along the curve from $\mathbf{q}_k$ to $\mathbf{q}_{k+1}$, which approximates the integral of the Lagrangian in the following sense

$$L_d(\mathbf{q}_k, \mathbf{q}_{k+1}) \approx \int_{t_k}^{t_{k+1}} L(\mathbf{q}(t), \dot{\mathbf{q}}(t))\, dt \tag{2.5}$$

The discrete analogue of Hamilton's principle seeks curves $\{ \mathbf{q}_k \}_{k=0}^{N}$ that satisfy

$$\delta \sum_{k=0}^{N-1} L_d(\mathbf{q}_k, \mathbf{q}_{k+1}) = \sum_{k=0}^{N-1} \left[\frac{\partial L_d(\mathbf{q}_k, \mathbf{q}_{k+1})}{\partial \mathbf{q}_k} \cdot \delta \mathbf{q}_k + \frac{\partial L_d(\mathbf{q}_k, \mathbf{q}_{k+1})}{\partial \mathbf{q}_{k+1}} \cdot \delta \mathbf{q}_{k+1} \right] = 0 \tag{2.6}$$

which gives the discrete Euler-Lagrange equations

$$D_2 L_d(\mathbf{q}_{k-1}, \mathbf{q}_k) + D_1 L_d(\mathbf{q}_k, \mathbf{q}_{k+1}) = \mathbf{0} \quad k = 1, ..., N-1 \tag{2.7}$$

where D_i denotes differentiation with respect to the i^{th} argument of the discrete Lagrangian L_d. Given $(\mathbf{q}_{k-1}, \mathbf{q}_k)$, the above equations can be solved to obtain $(\mathbf{q}_k, \mathbf{q}_{k+1})$. Thus, the discrete Euler-Lagrange equations can be seen as a numerical integrator of (2.2) and these equations can be implemented as a variational integrator for autonomous Lagrangian systems. Using the discrete Legendre transform, we can re-write the discrete Euler-Lagrange equations in the Hamiltonian form as follows

$$-D_1 L_d(\mathbf{q}_k, \mathbf{q}_{k+1}) = \mathbf{p}_k \tag{2.8}$$

$$\mathbf{p}_{k+1} = D_2 L_d(\mathbf{q}_k, \mathbf{q}_{k+1}) \tag{2.9}$$

where the discrete momentum $\mathbf{p}_k$ converges to its continuous counterpart as the fixed time step h approaches zero. Given $(\mathbf{q}_k, \mathbf{p}_k)$, the above equations (2.8)-(2.9) can be solved to

obtain $(\mathbf{q}_{k+1}, \mathbf{p}_{k+1})$.

Since the governing discrete equations are derived from the discrete Lagrangian function, the accuracy of trajectories depends on the order of approximation of the discrete Lagrangian. Marsden and West [44] showed that a discrete Lagrangian of order $r+1$ leads to a variational integrator of order r. Regardless of the choice of the discrete Lagrangian, the fixed time step variational integrators are symplectic [46] and momentum-preserving [44, 47]. The discrete Lagrangian system preserves a discrete symplectic form [45] and when the discrete system has a symmetry, there is a corresponding conserved quantity at the discrete level. While these fixed time step algorithms do not exactly preserve energy, backward error analysis [37, 48] shows that these methods, up to exponentially small errors, exactly integrate a nearby Hamiltonian system. To be more precise, for a small enough fixed time step, the discrete energy computed from the numerical integration will remain close to its initial value for an exponentially long time [46, 49]. In practice, the energy error remains bounded without exhibiting drift. As the fixed time step h decreases, the amplitude of energy error oscillations decrease and the discrete energy approaches the continuous system energy. Because of their excellent long-time stability, these variational integrators – also known as symplectic-momentum integrators – are ideal for long-time simulation of conservative dynamical systems.

Marsden and West [44] showed that the discrete Lagrangian function $L_d(\mathbf{q}_k, \mathbf{q}_{k+1})$ is a generating function for the discrete Lagrangian system. Thus, the discrete equations (2.8)-(2.9) can be seen as a symplectic method with the corresponding discrete Lagrangian as the approximation to the continuous generating function. This way both symplectic methods and variational integrators belong to the same class of structure-preserving methods but their construction is very different. In contrast to symplectic methods, the variational approach extends easily to non-conservative systems and has more theoretical appeal: the symplec-

tic property as well as the conserved discrete quantities can be derived directly from the variational nature of the algorithm as opposed to the trial and error method. In fact, the variational approach has been useful in explaining the excellent numerical performance of widely used integrators such as Newmark methods [50].

To introduce external forcing, we define two discrete forces $\mathbf{f}_d^{\pm} : Q \times Q \to T^*Q$ which approximate the continuous-time force integral that appears in (2.3) over one time step in the following sense

$$\mathbf{f}_d^+(\mathbf{q}_k, \mathbf{q}_{k+1}) \cdot \delta\mathbf{q}_{k+1} + \mathbf{f}_d^-(\mathbf{q}_k, \mathbf{q}_{k+1}) \cdot \delta\mathbf{q}_k \approx \int_{t_k}^{t_{k+1}} \mathbf{f}_L(\mathbf{q}(t), \dot{\mathbf{q}}(t)) \cdot \delta\mathbf{q}\, dt \tag{2.10}$$

The discrete Lagrange-d'Alembert principle seeks curves $\{ \mathbf{q}_k \}_{k=0}^N$ that satisfy

$$\delta \sum_{k=0}^{N-1} L_d(\mathbf{q}_k, \mathbf{q}_{k+1}) + \sum_{k=0}^{N-1} [\mathbf{f}_d^+(\mathbf{q}_k, \mathbf{q}_{k+1}) \cdot \delta\mathbf{q}_{k+1} + \mathbf{f}_d^-(\mathbf{q}_k, \mathbf{q}_{k+1}) \cdot \delta\mathbf{q}_k] = 0 \tag{2.11}$$

which yields the following variational integrator for forced Lagrangian systems:

$$-D_1 L_d(\mathbf{q}_k, \mathbf{q}_{k+1}) - \mathbf{f}_d^-(\mathbf{q}_k, \mathbf{q}_{k+1}) = \mathbf{p}_k \tag{2.12}$$

$$\mathbf{p}_{k+1} = D_2 L_d(\mathbf{q}_k, \mathbf{q}_{k+1}) + \mathbf{f}_d^+(\mathbf{q}_k, \mathbf{q}_{k+1}) \tag{2.13}$$

For forced Lagrangian mechanical systems, variational integrators (2.12)-(2.13) have been shown to exhibit better energy behavior than traditional numerical integrators [44, 50] for weakly dissipative systems. Since the external forcing $\mathbf{f}_L(\mathbf{q}(t), \dot{\mathbf{q}}(t))$ modifies the symplectic structure at every time step, unlike in the conservative case, there are no theoretical results about long-time stable behavior. Despite the lack of theoretical guarantees, the numerical results for a variety of dissipative and forced mechanical systems have demonstrated that

variational integrators track the change in energy more accurately compared to traditional methods. Similar to the continuous case, if the discrete forcing is orthogonal to the symmetry of the discrete Lagrangian then the corresponding momentum is conserved based on the discrete forced Noether's theorem [44].

The variational approach to derive mechanical integrators has been successfully extended to a broad class of problems such as:

- **Energy-preserving, adaptive time step variational integrators:** The strong negative result of Ge and Marsden [38] – that integrators with a fixed time step cannot simultaneously preserve energy, the symplectic structure, and conserved quantities for non-integrable systems – led Kane *et al* [51] to develop energy-preserving variational integrators with adaptive time stepping for conservative systems. Marsden and West [44] derived the same integrators through a variational approach for a more general case of time-dependent Lagrangian systems. Instead of obtaining the adaptive time step by imposing an additional equation, as in [51], they treated time as a discrete dynamic variable [52] and derived governing discrete equations in the extended Lagrangian mechanics framework. These adaptive time step variational integrators are energy and momentum conserving while also preserving the extended symplectic form. These energy-preserving integrators require solving a coupled, nonlinear, ill-conditioned system of equations at every time step and existence of solutions for these discrete trajectories is still an open problem. Shibberu [53] has discussed the well-posedness of these adaptive algorithms and suggested ways to regularize [54] the system of coupled nonlinear discrete equations. Recently, Sharma *et al* [55] derived energy-preserving, adaptive time step variational integrators for forced Lagrangian systems and showed that these adaptive algorithms, for forced Lagrangian systems, capture change in energy more accurately than fixed time step variational integrators.

- **Variational integrators for constrained mechanical systems:** Marsden and West extended the variational integrator framework to account for holonomic constraints [44] and these methods have been utilized in applications ranging from molecular dynamics to planetary motion. Their extension to mechanical systems with nonholonomic constraints remained a challenge for some time though. Equations of motion for a nonholonomic system are derived from the Lagrange-d'Alembert principle which means that the nonholonomic flow does not preserve the symplectic flow [56]. Cortes and Martinez [57] obtained nonholonomic integrators by discretizing the Lagrange-d'Alembert principle and they also extended adaptive time step variational integrators to nonholonomic systems using the extended Lagrangian mechanics framework from [44]. Kobilarov *et al* [58] developed nonholonomic integrators for mechanical systems with symmetries and applied them to robotic car and snakeboard examples to demonstrate the advantages compared to standard methods.

- **Stochastic variational integrators:** Based on the foundational work in the field of stochastic geometric mechanics by Bismut [22], Milstein *et al* [59, 60] developed mean-squared symplectic integrators for stochastic Hamiltonian systems and showed that these integrators capture the correct energy behavior even in presence of dissipation. Bou-Rabee and Owhadi [23] discretized the variational principle for stochastic mechanical systems on manifolds to derive stochastic variational integrators. Similar to their deterministic counterparts, these algorithms are symplectic and satisfy the discrete analogue of Noether's theorem in presence of symmetries. Bou-Rabee and Owhadi [61] also derived constrained, stochastic, variational, partitioned Runge-Kutta methods for stochastic mechanical systems with holonomic constraints. Holm and Tyranwoski [62] utilized the Galerkin type of discretization to derive a more general class of stochastic variational integrators.

- **Variational integrators for impact problems:** Building on the nonsmooth variational mechanics principles, Fetecau *et al* [63] developed variational collision integrators. In addition to the discrete trajectory points, this methodology introduces a collision point and the corresponding collision time, which are solved variationally. These algorithms retain the symplectic structure as well as the excellent energy behavior for nonsmooth cases. One of the drawbacks of this approach is that solving for each individual collision becomes cumbersome in situations involving many bodies undergoing collision sequences. For such complex multibody collisions, Johnson *et al* [64] developed discontinuous variational integrators by incorporating incremental energy minimization in the discrete mechanics framework.

- **Hamiltonian variational integrators:** As mentioned in Section 2.1.2, Lagrangian and Hamiltonian dynamics are not equivalent when the system is not hyperregular. For such cases, Lall and West [65] developed discrete Hamiltonian mechanics from the Hamiltonian side, without recourse to the Lagrangian formulation. In contrast to the Lagrangian approach to derive variational integrators, Leok *et al* [66] developed Hamiltonian variational integrators from the Hamiltonian point of view by discretizing the Hamiltonian. These Hamiltonian variational integrators are particularly useful for mechanical systems with degenerate Hamiltonian, such as interacting point vortices. In fact, Schmitt and Leok [67] investigated numerical properties of the Hamiltonian variational integrators and showed that, even for the same approximation method, the Lagrangian and Hamiltonian approach may lead to different symplectic-momentum integrators.

- **Multisymplectic variational integrators:** Marsden *et al* [25] developed the geometric foundations for variational integrators for variational PDEs. Using ideas from multisymplectic geometry [68], they developed numerical methods that are multisym-

plectic and preserve discrete momentum maps corresponding to symmetries. Lew *et al* [69] developed asynchronous variational integrators for solid mechanics problems. These asynchronous algorithms are based on the spacetime form of the discretized Hamilton's principle and allow the selection of independent time steps in each spatial element. Recently Kraus and Maj [30] extended the variational integrator framework to nonvariational PDEs by utilizing the method of formal Lagrangian.

2.2.3 Energy-momentum Integrators

Conventional numerical methods for ODEs when applied to Lagrangian/Hamiltonian systems conserve the total energy and momenta only up to the order of truncation error. These invariants of motion capture important qualitative features of the long-term dynamics. Aside from their physical significance, from a computational point of view conserved quantities often lead to enhanced numerical stability. For example, algorithmic conservation of energy leads to unconditional stability for nonlinear structural dynamics [70]. In fact, the majority of development on this topic was due to the discovery that numerical methods with unconditional stability for linear dynamics may lose this stability in the non-linear regime [71]. Energy-momentum integrators, in contrast to variational integrators (symplectic-momentum integrators), are designed to preserve the momentum and total energy of the system simultaneously.

Labudde and Greenspan [72, 73, 74] developed discrete mechanics based on difference equations and developed energy-momentum conserving algorithms for particle mechanics problems. Simo *et al* [75, 76] developed a more general methodology to construct energy-momentum integrators for a wide class of mechanical systems. We closely follow [76] to explain the key idea behind these methods.

Consider a finite-dimensional mechanical system with configuration manifold Q and canonical phase space T^*Q. For the simple case of a separable Hamiltonian/Lagrangian system with constant mass matrix M, kinetic energy $K(\mathbf{p}) = \frac{1}{2}\mathbf{p}^T M^{-1}\mathbf{p}$, and potential energy $V(\mathbf{q})$, the governing equations of motion are given by

$$\dot{\mathbf{q}} = M^{-1}\mathbf{p} \qquad \dot{\mathbf{p}} = -\nabla V(\mathbf{q}) \tag{2.14}$$

It is well-known that the system energy (i.e. the Hamiltonian $H = K + V$) and momentum $J(\mathbf{q}, \mathbf{p})$ (corresponding to symmetries) are conserved along the solution trajectory. Given $(\mathbf{q}_k, \mathbf{p}_k)$, the energy-momentum approach designs an approximation $(\mathbf{q}_{k+1}, \mathbf{p}_{k+1})$ such that the system energy $H_{k+1} = H_k$ and momentum $J_{k+1} = J_k$ are conserved. The strategy in the formulation of energy-momentum integrators is to first consider the class of exact momentum conserving schemes and then enforce the additional constraint of exact energy conservation. For the mechanical system described above, the family of exact momentum conserving algorithms , with fixed time step h, given by

$$\mathbf{q}_{k+1} = \mathbf{q}_k + h\kappa_1 M^{-1}\left[\alpha\mathbf{p}_k + (1-\alpha)\mathbf{p}_{k+1}\right] \tag{2.15}$$

$$\mathbf{p}_{k+1} = \mathbf{p}_k - h\kappa_2 \nabla V\left(\alpha\mathbf{q}_{k+1} + (1-\alpha)\mathbf{q}_k\right) \tag{2.16}$$

exactly conserve the momentum J corresponding to the symmetry for arbitrary real-valued functions κ_1 and κ_2 and scalar parameter $\alpha \in [0, 1]$. For exact energy conservation, we enforce the law of conservation of energy on the momentum conserving algorithm (2.15)-(2.16).

As discussed in [76], this constraint can be implemented via a number of different ways. The projection methods fix the collocation parameter to $\alpha = \frac{1}{2}$ and obtain κ_1 and κ_2 such that the energy constraint is satisfied. From a geometric point of view, the resulting energy-momentum integrator can be seen as an implicit projection of the mid-point rule from the

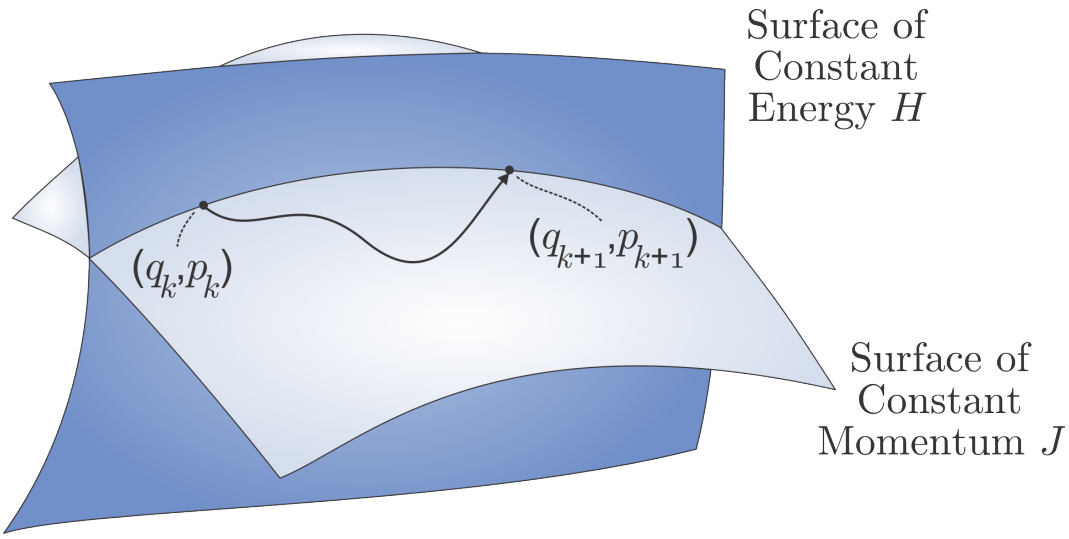

Figure 2.3: A cartoon illustrating the use of energy-momentum method where conservation of energy is achieved by an implicit momentum-preserving projection onto the surface of constant energy H

level set of conserved momentum onto the constant energy surface. The collocation methods, on the other hand, fix the real valued constants $\kappa_1 = \kappa_2 = 1$ and solve the energy constraint equation for the collocation parameter $\alpha \in [0, 1]$.

It is important to note that the energy-momentum approach requires solving an implicit equation and the stability of these methods depends on the solvability of the energy equation. Assuming the energy equation is solvable, the resulting algorithms are exactly energy and momentum preserving. In addition to the favorable conservation properties, these algorithms are unconditionally stable in the nonlinear regime. Simo and Gonzalez [77] showed that the unresolved high frequencies are controlled by exact energy conservation whereas the symplectic-momentum approach can lead to instability in such cases. These numerical properties make the energy-momentum integrators ideal for numerical simulation of highly oscillatory mechanical systems. Since the early development of energy-momentum integrators was based on the idea of modifying the midpoint rule, all of the energy-momentum

conserving algorithms were symmetric. Hairer *et al* [46] showed that the good long-time behavior of energy-momentum integrators was due to their reversibility and not the conserving properties. They also numerically demonstrated that the non-symmetric energy-momentum integrators do not exhibit good long-time behavior.

Betsch and Steinmann [78, 79] presented a unifying approach to derive energy-momentum integrators by discretizing the weighted residual of Hamilton's equations using continuous Galerkin methods. Unlike the finite difference approach taken by Simo and colleagues, they employed the finite element method for the temporal discretization process and devised quadrature rules that lead to energy-momentum integrators. Betsch and Steinmann [80] also extended this Galerkin-based approach to mechanical systems with holonomic constraints by introducing the mixed Galerkin method based on mixed finite elements in time. Later, Groß *et al* [81] modified the continuous Galerkin method and derived higher order energy-momentum integrators for multi-dimensional mechanical systems.

For dynamic problems involving high frequency content such as constrained, flexible, multi-body problems, the high frequency oscillations can lead to convergence issues for the energy-momentum integrators due to their lack of high frequency numerical dissipation. Armero and Petocz [82] introduced numerical dissipation in the energy-momentum integrators to derive modified energy-momentum integrators. These energy decaying schemes eliminate the energy associated with vibratory motions at high frequency while still preserving the momentum. Instead of satisfying a discrete energy conservation law, the energy decaying schemes are based on the energy decay inequality given by Hughes [83]. Kuhl and Crisfield [84] proposed an alternate strategy based on controllable numerical dissipation to derive generalized energy-momentum integrators. This generalization of the energy conserving/decaying algorithms allows larger time steps, due to numerical damping characteristics and these algorithms are easier to extend to adaptive time-stepping.

2.2.4 Discrete Gradient Methods

The construction of energy-momentum integrators is related to the concept of discrete gradients. The discrete gradient method is a general technique for deriving integral-preserving integrators. Gonzalez [85] introduced discrete Hamiltonian systems as formal abstractions of conserving algorithms based on the idea of discrete directional derivatives. Using this discrete derivative idea, McLachlan *et al* [86] developed the discrete gradient methods for the more general case of dynamical stems with a Lyapunov function.

The discrete gradient methods are applicable to systems with differential equation $\dot{y} = A(y)\nabla H(y)$ where $A(y)$ is a skew-symmetric matrix. For Lagrangian/ Hamiltonian mechanical systems, the vector $y = (\mathbf{q}, \mathbf{p})$ belongs to the phase space with the constant symplectic matrix J as the skew-symmetric matrix $A(y)$ and the Hamiltonian of the system as the energy function $H(y)$. The discrete gradient methods are of the form

$$y_{k+1} = y_k + h\bar{A}(y_{k+1,y_k})\bar{\nabla}H(y_{k+1}, y_k) \tag{2.17}$$

where $\bar{A}(\hat{y}, y)$ is a skew-symmetric matrix for all $\hat{y}, y$, and $\bar{\nabla}H(\hat{y}, y)$ is the discrete gradient satisfying

$$\bar{\nabla}H(\hat{y}, y)^T(\hat{y} - y) = H(\hat{y}) - H(y) \qquad \bar{\nabla}H(y, y) = \nabla H(y) \tag{2.18}$$

These numerical methods are symmetric and are both energy- and momentum-preserving. It has been shown that the projection method approach to derive energy-momentum integrators is a special case of discrete gradient methods. In fact, the symmetric nature of discrete gradient methods played an important role in explaining the good long-time behavior of energy-momentum integrators. For Hamiltonian systems with holonomic constraints, Gonzalez [87] applied the discrete gradient approach to the governing differential algebraic equations to derive energy-momentum integrators for constrained mechanical systems. Re-

cently, Celledoni [88] applied the discrete gradient approach to numerical integration of nonholonomic systems. The resulting algorithms exhibit exact energy preservation while ensuring the nonholonomic constraints are satisfied. For PDEs, McLachlan and Quispel [89] showed that discrete gradient methods preserve energy conservation laws and conserve the energy exactly when the symplectic structure is constant. Celledoni *et al* [90] applied these methods to PDEs with constant dissipative structure and the numerical results demonstrated that the algorithms capture the correct monotonic decrease in energy.

2.2.5 Lie Group Methods

In many engineering applications, the governing differential equations evolve on a non-Euclidean manifold and there are two main numerical approaches for such problems, embedded and intrinsic methods. In the first of these approaches, as the name suggests, one embeds the manifold in $\mathbb{R}^n$ and applies a traditional numerical integration scheme. The drawback of this approach is that, except in special cases, traditional numerical methods are unlikely to provide solutions that remain exactly on the correct manifold. The alternative approach uses intrinsic operations on the group to make sure the computed trajectories are guaranteed to lie on the manifold.

A Lie group G is a group which is also a differentiable manifold, and for which the group operation $G \times G \to G$ and inverse operation are smooth maps. The tangent space $\mathfrak{g} = T_I G$ at the identity of a Lie group G is closed under commutation of its elements making it an algebra, the Lie algebra $\mathfrak{g}$ of the Lie group G. For a differential equation on Lie group G, the continuous trajectory remains on the Lie group for any initial condition on G and the flow map of the system can be seen as group operation. For example, the attitude dynamics of a rigid body can be described as differential equations on the special orthogonal group

$\mathsf{SO}(3)$, the group of proper orthogonal linear transformations.

Consider a dynamical system whose configuration evolves on a differentiable manifold $\mathcal{M}$ subject to the action of some Lie group $\mathcal{G}$. Given an initial condition $y_0 \in \mathcal{M}$, rather than ask "What is the the state y at time t?", the Lie group approach asks an equivalent question [91]: "What is the group action that takes the system from y_0 to $y(t)$?". Posing the question in terms of the group action helps one relate it to the underlying Lie algebra, which is a linear space. Thus, Lie group methods include an intrinsic and consistent strategy for the parametrization of the nonlinear manifold $\mathcal{M}$ in their algorithmic structure. In simple words: Instead of solving the original ODE on $\mathcal{M}$, Lie group methods solve the corresponding problem in the Lie algebra, ensuring that the solution remains on the manifold $\mathcal{M}$.

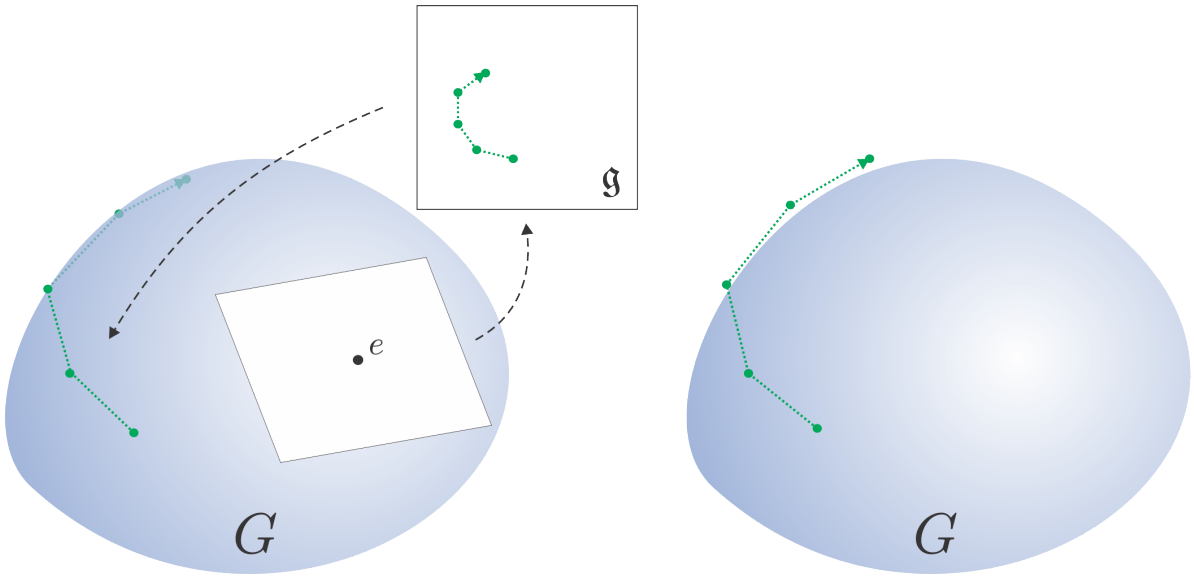

Figure 2.4: A cartoon illustrating the use of a Lie group method (left) versus a conventional method (right) in the case $\mathcal{M} = \mathcal{G}$. (The Lie algebra $\mathfrak{g}$ is the tangent space to $\mathcal{G}$ at the identity $e \in \mathcal{G}$.)

For dynamical systems evolving on non-Euclidean manifolds, the governing differential equations are intimately connected to Lie groups. Although the mathematical properties of differ-

ential equations on manifolds were well understood already by early twentieth century, it is only in last few decades that numerical methods utilizing these aspects have been developed. Crouch and Grossman [92] wrote an influential paper on numerical integrators for ODEs on manifolds where they computed the numerical solution by computing flows of vector fields in the Lie algebra. Munthe-Kaas [93] constructed generalized Runge-Kutta methods on general Lie groups, now known as the Runge-Kutta-Munthe-Kaas (RKMK) methods, and then derived RKMK methods of arbitrarily high order [94] on homogeneous manifolds. The essential aspects of Lie group methods can be reviewed in [95] and a recent survey paper by Celledoni *et al* [96] covers the more recent developments and potential applications.

Although the Lie group methods are applicable to any dynamical system evolving on a manifold, for this particular review, we focus on Lie group methods in the context of mechanical systems. The energy-momentum or variational integrators developed for mechanical systems evolving on vector spaces in general will not retain their conservation properties when applied to systems with nonlinear configuration space of a non-Euclidean manifold. For engineering applications, there are two important classes of conserving schemes for mechanical systems evolving on non-Euclidean manifolds: variational (symplectic-momentum) integrators and energy-momentum integrators.

Simo *et al* [76] extended the exact energy-momentum methods to classical rigid body dynamics for which the configuration manifold is the rotation group $\mathsf{SO}(3)$. They exploited knowledge of the Lie group's role in rigid body motion, using the exponential map from the Lie algebra to the Lie group in order to numerically integrate the dynamic equations. Lewis and Simo [97] developed energy-momentum and symplectic integrators for the general case of Hamiltonian systems evolving on Lie groups i.e. nonlinear configuration spaces with a group structure.

Bobenko and Suris [98] extended the discrete mechanics ideas in [43] to the Lie group setting.

Variational integrators for the reduced dynamics of a mechanical system with a Lie group symmetry were first derived by Marsden *et al* [99]. By incorporating ideas from Lie group methods in the variational integrator framework, Leok [66] developed the general theory of Lie group variational integrators. Lee *et al* [100, 101, 102] adapted the Lie group variational integrators to rigid body dynamics applications. As the name "Lie group variational integrator" suggests, these methods essentially combine the structure-preserving features of Lie group methods and variational integrators. The resulting integrators are thus symplectic and momentum-preserving *and* they preserve the structure of the configuration space. Lie group variational integrators have recently been extended to the infinite-dimensional setting of beam and plate dynamics by Demoures *et al* [103, 104, 105].

Lie group methods discussed so far, in addition to preserving the nonlinear configuration space structure and momentum, conserve either the energy or the symplectic form. These Lie group methods can not preserve all three elements - energy, momentum and symplectic form - simultaneously. For the special case of a rigid body system, Lewis and Simo [97] presented a strategy for deriving algorithms that preserve energy, momentum and symplectic form while also making sure the computed trajectory lies on the correct manifold. Based on the strong negative result for fixed step algorithms by Ge and Marsden [38], we know that this approach does not work for the more general case of non-integrable systems. Recently, Sharma *et al* [106, 107] developed the extended Lagrangian mechanics framework on $\mathsf{SO}(3)$ and $\mathsf{SE}(3)$, and derived energy-preserving, adaptive time step Lie group variational integrators for rigid body dynamics.

2.3 Science and Engineering Applications

The numerical methods covered in Section 2.2 have been successfully applied to a wide range of problems in engineering. In this section, we give examples from the literature where these structure-preserving methods have been utilized in physics, mechanics and dynamics.

2.3.1 Celestial Mechanics and Dynamical Astronomy

Celestial mechanics and dynamical astronomy apply the principles of classical mechanics to solve problems concerning the motion of objects in space. These problems involve determining long-term trajectories of bodies such as stars, planets, and asteroids as well as computing spacecraft trajectories, from launch through atmospheric re-entry, including the orbital maneuvers. Similarly, interplanetary trajectory and planetary protection applications also require accurate long-time numerical simulations. Symplectic methods due to their symplectic and momentum-preserving nature along with long-time stability are ideal for numerical simulation of such problems.

Based on the symplectic method proposed by Ruth [32], various symplectic algorithms for canonical integration of Hamiltonian systems were proposed by Feng and Qin [108], Channell and Scovel [109], and Forest and Routh [110]. Wisdom and Holman [111], building on the previous work by Wisdom [112, 113], developed symplectic algorithms for N-body problems with a large central mass such as planetary systems or satellite dynamics. Yoshida [114] applied symplectic methods to study the motion of minor bodies in the solar system and the long-term evolution of outer planets. These methods came to the attention of the celestial mechanics [115] and dynamical astronomy [116] community in the early 1990s and have now become the benchmark in the study of orbit propagation [117], close encounters [118], asteroid [119, 120] dynamics, cometary orbits [121, 122], long-term formation flight dynamics

[123] and N-body dynamics [111, 124].

Since the development of discrete mechanics and variational integrators, a variety of symplectic algorithms, derived from the variational point of view, have been applied to celestial mechanics, spacecraft dynamics and orbital propagation problems. Farr and Bertschinger [125] developed adaptive variational integrators for N-body problems with superior symplecticity and momentum preservation. Lee *et al* applied Lie group variational integrators to study the complex dynamics of a tethered spacecraft system [126] and spacecraft with imbalanced reaction wheels [127]. Hall and Leok [128] applied spectral variational integrators to solar system simulation and obtained closed, extremely stable and precession free orbits, even for large time steps. Recently, Palacios and Gurfil [129] developed variational integrators for satellite relative orbit propagation including atmospheric drag.

2.3.2 Elastodynamics

Formulation of dynamic problems in nonlinear solid mechanics is built on energy and momentum conservation laws and these fundamental properties of the continuum dynamics play a key role in many engineering applications. Customary temporal and spatial finite difference/finite element discretizations of the continuum dynamics do not always inherit the conservation properties. The construction of robust spacetime discretizations of these problems has been a long-standing goal in the field of computational mechanics.

For nonlinear elastodynamics problems, especially stiff systems possessing high-frequency contents, energy-momentum schemes are known to possess enhanced numerical stability properties in the nonlinear regime [71]. In most of the applications, the semidiscrete equations resulting from a finite element discretization are viewed as a finite-dimensional Hamiltonian system with symmetry and are solved in time using energy-momentum integrators.

In the context of nonlinear elastodynamics, Simo and Tarnow [75] first developed numerical methods for Saint Venant-Kirchhoff model and later, Simo and Gonazalez [130, 131] extended these methods to the more general case of hyperelastic materials. Based on this pioneering work, a variety of energy-momentum algorithms have been designed for structural elements such as beams [132], plates [133] and shells [134].

Unlike the energy-momentum integrator applications, variational integrators use the space-time approach for elastodynamics problems. Lew *et al* [69] developed asynchronous variational integrators (AVI) for nonlinear elastodynamics that permit independent time steps in each spatial element. Based on this work, Lietz *et al* [103] developed AVIs for geometrically exact beam and plate dynamics. Lew [135] used AVIs to study rotor blade dynamics and contained detonation of a highly-explosive material. Kale and Lew [136] developed scalable parallel AVI algorithms and applied them to study the interaction dynamics involved in atomic force microscopy.

2.3.3 Multibody Dynamics

Multibody dynamics applications often involve a system consisting of rigid bodies and elastic bodies undergoing large displacements and rotations and the numerical simulation of these systems require advanced modeling strategies. Space discretization for these problems usually results in stiff, nonlinear, differential-algebraic equations and energy-momentum schemes are well-suited for such nonlinear systems due to their algorithmic conservation and numerical stability properties. A variety of energy preserving/decaying schemes were presented in the late 1990s by a number of authors for multibody systems.

Ordern and Goicolea [137] utilized discrete gradient ideas to develop energy-momentum integrators for constrained dynamics of flexible multibody systems. Betsch and Lyndecker

[138] developed energy-momentum integrators in the discrete null space setting for multibody dynamics and later Leyendecker *et al* [139] applied these methods to flexible multibody dynamics. Based on the work by Betsch and Steinmann [140], Betsch and Uhlar [141] developed a rotationless formulation for energy-momentum conserving integration of multibody systems. Uhlar and Betsch [142] extended this method to non-conservative systems and applied it to a double wishbone suspension of a car.

Although the multibody dynamics field has mainly used energy-momentum integrators for computational studies, recently some researchers have also used variational integrators and Lie group methods in the context of multibody dynamics. Leyendecker *et al* [143] adapted the discrete null space method to the discrete mechanics framework and applied the variational discrete null space method to a kinematic chain of rigid bodies and flexible multibody systems. Leyendecker and Ober-Blöbaum [144] applied multirate variational integrators to study constrained systems with dynamics on strongly varying time scales. For systems with large displacements and rotations, various Lie group methods for complex flexible multibody dynamics have been developed by Bruls *et al* [145, 146], Park and Chung [147], and Terze *et al* [148].

2.3.4 Fluid Dynamics

Computational methods for fluid dynamics problems typically discretize the governing equations through finite volume, finite element or finite difference methods and are rarely designed with structure preservation in mind, leading to spurious numerical artifacts such as energy and circulation drift. In sharp contrast to these traditional methods, structure-preserving methods based on the geometric nature of Euler fluids (adiabatic and inviscid) have recently become popular in the context of numerical methods for fluid dynamics. Perot *et al* [149]

studied conservation properties of unstructured staggered mesh schemes and constructed numerical methods that conserve kinetic energy, vorticity, and momentum in 2D. Elcott *et al* [150] proposed numerically stable integrators for fluids that satisfy the discrete version of Kelvin's circulation theorem.

Based on the pioneering work by Arnold [151], Euler fluids have been extensively studied in the literature from the geometric-differential standpoint. Cotter *et al* [152] provided multisymplectic formulation of fluid dynamics using the inverse map approach. In the variational description of fluid dynamics [153], the configuration space is defined as the volume-preserving diffeomorphisms, and Kelvin's circulation theorem is seen as a consequence of Noether's theorem associated with the particle relabeling symmetry. This variational formulation provides a powerful framework to construct structure-preserving methods for fluid dynamics.

Mullen *et al* [154] constructed time-reversible integrators that preserve energy for inviscid fluids (or capture the correct energy decay for viscous fluids) and are particularly useful for fluid animation by maintaining the liveliness of fluid motion without recourse to corrective devices. Pavlov *et al* [155] derived fluid mechanics equations from Hamilton's principle and derived Lie group variational integrators for incompressible Euler fluids by constructing a finite-dimensional approximation to the volume-preserving diffeomorphism group for the discretization. The resulting scheme exhibits energy conservation over long simulations, time reversibility, and circulation preservation. Using similar ideas, Gawlik *et al* [156] derived variational discretizations of continuum theories arising in fluid dynamics, magnetohydrodynamics (MHD), and the dynamics of complex fluids. Kraus and his colleagues [30] have utilized the formal Lagrangian approach to develop variational integrators for a variety of MHD models. Similarly, Desbrun *et al* [157] developed structure-preserving space-time discretization schemes for rotating and/or stratified flows which are relevant for modeling

large-scale atmospheric or oceanic flows. Recently, Bauer *et al* [158] have developed a framework for geometric variational discretization of compressible fluids in the context of rotating shallow water equations.

(a) Wheelbone suspension [142]

(b) Tethered dynamics [127]

(c) Rotor blade dynamics [69]

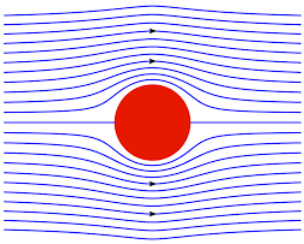

(d) Fluid flow animation [154]

(e) Little dog robot [159]

Figure 2.5: GNI applications from literature

2.3.5 Optimal Control

The optimal control of a mechanical system is an important engineering problem in application areas such space mission design, robotics and biomechanics. The numerical solution to the optimal control problem involves the discretization of the infinite-dimensional optimization problem and one has to repeatedly solve a sequence of nearby systems approximately. Using the discrete mechanics framework on the dynamic level in the optimal control problem leads to structure-preserving time-stepping equations and these equations act as equality constraints on the final finite-dimensional nonlinear optimization problem. Besides the structure-preserving aspect, both optimal control and variational mechanics have their

roots in calculus of variations. Junge *et al* [160] exploited this connection and developed the Discrete Mechanics and Optimal Control (DMOC) method, in which both the dynamics and optimization are discretized variationally.

Building on this work, Ober-Blöbaum *et al* [161] showed that the DMOC approach is equivalent to time discretization of Hamilton's equations using a symplectic method and utlilized the structure-preserving nature of discretization to provide proof of convergence. Leyendecker *et al* [162] formulated the dynamics subject to holonomic constraints and controls by applying a constrained version of Lagrange-d'Alembert principle for the optimal control of constrained systems. Kobilarov and Sukhatme [163] applied the DMOC framework to nonholomonic mechanical systems using nonholonomic variational integrators and later Kobilarov *et al* [58] also extended the framework to mechanical systems with symmetries. Manns and Mombaur [164] showed that the DMOC method offers competitive performance for complex models with large degrees of freedom by taking advantage of the parallel computer architecture.

Although the DMOC method is relatively new, since its introduction it has been utilized in a variety of problems from diverse fields. In spaceflight mechanics, the DMOC method has been applied to problems like low thrust orbital transfer [165], attitude maneuvers of spacecraft [166] and formation flying satellites [160]. For robotics applications, the DMOC method has been applied successfully to simultaneous path planning and trajectory optimization [167], periodic gait optimization [168, 169] and robot planning [170] problems. Manchester *et al* [159, 171] have developed trajectory optimization algorithms using the DMOC framework and applied them in handling the contact constraints found in robot planning problems. Apart from these, the DMOC method has also been used for problems like hybrid systems control [172], vibration suppression control of a film [169], and image analysis [173].

Chapter 3

Energy-preserving Variational Integrators

The purpose of this chapter is twofold. First, we develop variational integrators for time-dependent Lagrangian systems with non-conservative forces based on the discretization of the Lagrange-d'Alembert principle in extended phase space. We modify the Lagrange-d'Alembert principle to include time variations in the extended phase space and derive the extended forced Euler-Lagrange equations. We then present a discrete variational principle for time-dependent Lagrangian systems with forcing and derive extended forced discrete Euler-Lagrange equations. We use the extended discrete mechanics formulation to construct adaptive time step variational integrators for nonautonomous Lagrangian systems with forcing that capture the rate of energy evolution accurately. Second, we consider three numerical examples to understand the numerical properties of the adaptive time step variational integrators and compare the results with fixed time step variational integrators to illustrate the advantages of using adaptive time-stepping in variational integrators. We also study the effect of initial time step and initial conditions on the numerical performance of the adaptive time step variational integrators.

This chapter is organized as follows. In Section 3.1, we review the basics of extended Lagrangian mechanics and discrete mechanics. We also discretize Hamilton's principle to derive adaptive time step variational integrators. In Section 3.2, we modify the Lagrange-

d'Alembert principle in the extended phase space and derive extended forced Euler-Lagrange equations. In Section 3.3, we derive the extended forced discrete Euler-Lagrange equations and obtain adaptive time step variational integrators for time-dependent Lagrangian systems with forcing. In Section 3.4, we give numerical examples to understand the numerical performance of the adaptive time step variational integrators. Finally, in Section 3.5 we provide concluding remarks and suggest future research directions.

3.1 Background: Adaptive Time Step Variational Integrators

In this section, we review the basics of Lagrangian mechanics and derivation of adaptive time step variational integrators. Drawing on the work of Marsden *et al* [13, 44, 51], we first derive equations of motion in continuous-time from the variational principle and then derive variational integrators by considering the discretized variational principle in the discrete-time domain. To this end, we first derive continuous-time Euler-Lagrange equations of motion from Hamilton's principle. After deriving equations of motion, we use concepts of discrete mechanics developed in [44] to derive discrete Euler-Lagrange equations and then write them in the time-marching form to obtain adaptive time step variational integrators for Lagrangian systems.

3.1.1 Extended Lagrangian Mechanics

Hamilton's principle of stationary action is one of the most fundamental results of classical mechanics and is commonly used to derive equations of motion for a variety of systems. The forces and interactions that govern the dynamical evolution of the system are easily

determined through Hamilton's principle in a formulaic and elegant manner. Hamilton's principle [174] states that: The motion of the system between two fixed points from t_i to t_f is such that the action integral has a stationary value for the actual path of the motion. In order to derive the Euler-Lagrange equations via Hamilton's principle, we start by defining the configuration space, tangent space and path space.

Consider a time-dependent Lagrangian system with configuration manifold Q and time space $\mathbb{R}$. In the extended Lagrangian mechanics framework [44], we treat time as a dynamic variable and define the extended configuration manifold $\bar{Q} = \mathbb{R} \times Q$; the corresponding state space $T\bar{Q}$ is $\mathbb{R} \times TQ$. The extended Lagrangian is $L : \mathbb{R} \times TQ \to \mathbb{R}$.

In the extended Lagrangian mechanics framework, t and $\mathbf{q}$ are both parametrized by an independent variable a. The two components of a trajectory c are $c(a) = (c_t(a), c_{\mathbf{q}}(a))$. The extended path space is

$$\bar{\mathcal{C}} = \left\{ c : [a_0, a_f] \to \bar{Q} |\ c \textit{ is a } C^2 \textit{ curve and } c_t'(a) > 0 \right\} \tag{3.1}$$

For a given path $c(a)$, the initial time is $t_0 = c_t(a_0)$ and the final time is $t_f = c_t(a_f)$. The extended action $\bar{\mathfrak{B}} : \bar{\mathcal{C}} \to \mathbb{R}$ is

$$\bar{\mathfrak{B}} = \int_{t_0}^{t_f} L(t, \mathbf{q}(t), \dot{\mathbf{q}}(t)) dt \tag{3.2}$$

Since time is a dynamic variable in this framework, we substitute $(t, \mathbf{q}(t), \dot{\mathbf{q}}(t)) = \left(c_t(a), c_{\mathbf{q}}(a), \frac{c_{\mathbf{q}}'(a)}{c_t'(a)} \right)$ in the above equation to get

$$\bar{\mathfrak{B}} = \int_{a_0}^{a_f} L \left(c_t(a), c_q(a), \frac{c_q'(a)}{c_t'(a)} \right) c_t'(a)\ da \tag{3.3}$$

We compute variations of the action

$$\delta\bar{\mathfrak{B}} = \int_{a_0}^{a_f} \left[\frac{\partial L}{\partial t}\delta c_t + \frac{\partial L}{\partial \mathbf{q}} \cdot \delta c_{\mathbf{q}} + \frac{\partial L}{\partial \dot{\mathbf{q}}} \cdot \left(\frac{\delta c'_{\mathbf{q}}(a)}{c'_t} - \frac{c'_{\mathbf{q}}\delta c'_t(a)}{(c'_t)^2}\right)\right] c'_t(a)da + \int_{a_0}^{a_f} L\delta c'_t(a)\ da \quad (3.4)$$

Using integration by parts and setting the variations at the end points to zero gives

$$\delta\bar{\mathfrak{B}} = \int_{a_0}^{a_f} \left[\frac{\partial L}{\partial \mathbf{q}}c'_t - \frac{d}{da}\frac{\partial L}{\partial \dot{\mathbf{q}}}\right] \cdot \delta c_{\mathbf{q}}(a)da + \int_{a_0}^{a_f} \left[\frac{\partial L}{\partial t}c'_t + \frac{d}{da}\left(\frac{\partial L}{\partial \dot{\mathbf{q}}} \cdot \frac{c'_{\mathbf{q}}}{c'_t} - L\right)\right] \delta c_t(a)\ da \quad (3.5)$$

Using $dt = c'_t(a)da$ in the above expression gives two equations of motion. The first is the Euler-Lagrange equation of motion

$$\frac{\partial L}{\partial \mathbf{q}} - \frac{d}{dt}\left(\frac{\partial L}{\partial \dot{\mathbf{q}}}\right) = \mathbf{0} \quad (3.6)$$

which is the same as the equation obtained using the classical Lagrangian mechanics framework. The second equation is

$$\frac{\partial L}{\partial t} + \frac{d}{dt}\left(\frac{\partial L}{\partial \dot{\mathbf{q}}} \cdot \dot{\mathbf{q}} - L\right) = 0 \quad (3.7)$$

which describes how the energy of the system evolves with time.

3.1.2 Energy-preserving Variational Integrators

For the extended Lagrangian mechanics, we define the extended discrete state space $\bar{Q} \times \bar{Q}$. The extended discrete path space is

$$\bar{\mathcal{C}}_d = \{\ c : \{\ 0, ..., N\} \to \bar{Q} |\ \ c_t(k+1) > c_t(k)\ \ for\ all\ k\} \quad (3.8)$$

The extended discrete action map $\bar{\mathcal{B}}_d : \bar{\mathcal{C}}_d \to \mathbb{R}$ is

$$\bar{\mathcal{B}}_d = \sum_{k=0}^{N-1} L_d(t_k, \mathbf{q}_k, t_{k+1}, \mathbf{q}_{k+1}) \tag{3.9}$$

where $L_d : \bar{Q} \times \bar{Q} \to \mathbb{R}$ is the extended discrete Lagrangian function which approximates the action integral between two successive configurations. Taking variations of the extended discrete action map gives

$$\begin{aligned}\delta \bar{B}_d = \sum_{k=1}^{N-1} \left[D_4 L_d(t_{k-1}, \mathbf{q}_{k-1}, t_k, \mathbf{q}_k) + D_2 L_d(t_k, \mathbf{q}_k, t_{k+1}, \mathbf{q}_{k+1}) \right] \cdot \delta \mathbf{q}_k \\ + \sum_{k=1}^{N-1} \left[D_3 L_d(t_{k-1}, \mathbf{q}_{k-1}, t_k, \mathbf{q}_k) + D_1 L_d(t_k, \mathbf{q}_k, t_{k+1}, \mathbf{q}_{k+1}) \right] \delta t_k = 0\end{aligned} \tag{3.10}$$

where D_i denotes differentiation with respect to the i^{th} argument of the discrete Lagrangian L_d. Applying Hamilton's principle of least action and setting variations at end points to zero gives the extended discrete Euler-Lagrange equations

$$D_4 L_d(t_{k-1}, \mathbf{q}_{k-1}, t_k, \mathbf{q}_k) + D_2 L_d(t_k, \mathbf{q}_k, t_{k+1}, \mathbf{q}_{k+1}) = \mathbf{0} \tag{3.11}$$

$$D_3 L_d(t_{k-1}, \mathbf{q}_{k-1}, t_k, \mathbf{q}_k) + D_1 L_d(t_k, \mathbf{q}_k, t_{k+1}, \mathbf{q}_{k+1}) = 0 \tag{3.12}$$

Given $(t_{k-1}, \mathbf{q}_{k-1}, t_k, \mathbf{q}_k)$, the extended discrete Euler-Lagrange equations can be solved to obtain $\mathbf{q}_{k+1}$ and t_{k+1}. This extended discrete Lagrangian system can be seen as a numerical integrator of the continuous-time nonautonomous Lagrangrian system with adaptive time steps.

In the extended discrete mechanics framework, we define the discrete momentum $\mathbf{p}_k$ by

$$\mathbf{p}_k = D_4 L_d(t_{k-1}, \mathbf{q}_{k-1}, t_k, \mathbf{q}_k) \tag{3.13}$$

We also introduce the discrete energy

$$E_k = D_3 L_d(t_{k-1}, \mathbf{q}_{k-1}, t_k, \mathbf{q}_k) \tag{3.14}$$

Using the discrete momentum and discrete energy definitions, we can re-write the extended discrete Euler-Lagrange equations (3.11) and (3.12) in the following form

$$-D_2 L_d(t_k, \mathbf{q}_k, t_{k+1}, \mathbf{q}_{k+1}) = \mathbf{p}_k \tag{3.15}$$

$$D_1 L_d(t_k, \mathbf{q}_k, t_{k+1}, \mathbf{q}_{k+1}) = E_k \tag{3.16}$$

$$\mathbf{p}_{k+1} = D_4 L_d(t_k, \mathbf{q}_k, t_{k+1}, \mathbf{q}_{k+1}) \tag{3.17}$$

$$E_{k+1} = -D_3 L_d(t_k, \mathbf{q}_k, t_{k+1}, \mathbf{q}_{k+1}) \tag{3.18}$$

Given $(t_k, \mathbf{q}_k, \mathbf{p}_k, E_k)$, the coupled nonlinear equations (3.15) and (3.16) are solved implicitly to obtain $\mathbf{q}_{k+1}$ and t_{k+1}. The configuration $\mathbf{q}_{k+1}$ and time t_{k+1} are then used in (3.17) and (3.18) to obtain $(\mathbf{p}_{k+1}, E_{k+1})$ explicitly. The extended discrete Euler-Lagrange equations were first written in the time-marching form in [44] and are also known as symplectic-energy-momentum integrators.

3.2 Modified Lagrange-d'Alembert Principle

The extended discrete Euler-Lagrange equations derived in Section 3.1.2 can be used as energy-preserving variational integrators for Lagrangian systems. In order to extend this energy-preserving variational integrator framework to Lagrangian systems with external forcing, we need to discretize the Lagrange-d'Alembert principle in the extended Lagrangian mechanics framework. We first present the Lagrange- d'Alembert principle in extended phase space for time-dependent Lagrangian systems with forcing by considering the variations with respect to time t. Using the extended Lagrangian mechanics framework, we derive the extended Euler-Lagrange equations for time-dependent Lagrangian systems with forcing.

The Lagrange- d'Alembert principle modifies Hamilton's principle of stationary action by considering the virtual work done by the forces for a variation $\delta\mathbf{q}$ in the configuration variable $\mathbf{q}$. Since the standard Lagrangian mechanics framework treats time only as an independent continuous parameter, it does not account for time variations in the Lagrange-d'Alembert principle. Thus, we need to modify the Lagrange-d'Alembert principle in the extended Lagrangian mechanics framework to account for time variations.

We modify the Lagrange-d'Alembert principle by adding an additional term in the variational principle that accounts for virtual work done by the external force $\mathbf{f}_L$ due to variations in the time variable

$$\delta \int_{t_0}^{t_f} L(t, \mathbf{q}(t), \dot{\mathbf{q}}(t))\, dt + \int_{t_0}^{t_f} \mathbf{f}_L(t, \mathbf{q}(t), \dot{\mathbf{q}}(t)) \cdot \delta\mathbf{q}\, dt - \int_{t_0}^{t_f} \mathbf{f}_L(t, \mathbf{q}(t), \dot{\mathbf{q}}(t)) \cdot (\dot{\mathbf{q}}\delta t)\ dt = 0 \quad (3.19)$$

Using the extended Lagrangian mechanics framework discussed in Section 3.1.1 to derive the

equations of motion, we first re-write the modified Lagrange-d'Alembert principle

$$\delta \int_{a_0}^{a_f} L\left(c_t(a), c_{\mathbf{q}}(a), \frac{c'_{\mathbf{q}}(a)}{c'_t(a)}\right) c'_t(a)\, da + \int_{a_0}^{a_f} f_L\left(c_t(a), c_{\mathbf{q}}(a), \frac{c'_{\mathbf{q}}(a)}{c'_t(a)}\right) \cdot (\delta c_{\mathbf{q}} - \dot{\mathbf{q}}\delta c_t)\, c't(a) da = 0 \tag{3.20}$$

Taking variations of the discrete action with respect to both configuration $\mathbf{q}$ and time t gives

$$\int_{a_0}^{a_f} \left[\frac{\partial L}{\partial t}\delta c_t + \frac{\partial L}{\partial \mathbf{q}} \cdot \delta c_{\mathbf{q}} + \frac{\partial L}{\partial \dot{\mathbf{q}}} \cdot \left(\frac{\delta c'_{\mathbf{q}}(a)}{c'_t} - \frac{c'_{\mathbf{q}}\delta c'_t(a)}{(c'_t)^2}\right)\right] c'_t(a) da + \int_{a_0}^{a_f} L\delta c'_t(a)\, da + \int_{a_0}^{a_f} (f_L \cdot \delta c_{\mathbf{q}})\; c't(a) da - \int_{a_0}^{a_f} (f_L \cdot \dot{\mathbf{q}})\, \delta c_t\; c't(a) da = 0 \tag{3.21}$$

Using integration by parts and setting variations at the end points to zero gives

$$\int_{a_0}^{a_f} \left[\frac{\partial L}{\partial \mathbf{q}} c'_t - \frac{d}{da}\frac{\partial L}{\partial \dot{\mathbf{q}}} + \mathbf{f}_L\right] \cdot \delta c_{\mathbf{q}}(a) da + \int_{a_0}^{a_f} \left[\frac{\partial L}{\partial t} c'_t + \frac{d}{da}\left(\frac{\partial L}{\partial \dot{\mathbf{q}}} \cdot \frac{c'_{\mathbf{q}}}{c'_t} - L\right) - \mathbf{f}_L \cdot \dot{\mathbf{q}}\right] \delta c_t(a)\, da = 0 \tag{3.22}$$

Using $dt = c'_t(a)da$ in the above expression gives two equations of motion for the forced time-dependent Lagrangian system. The first equation is the well-known forced Euler-Lagrange equation for a time-dependent system

$$\frac{\partial L}{\partial \mathbf{q}} - \frac{d}{dt}\left(\frac{\partial L}{\partial \dot{\mathbf{q}}}\right) + \mathbf{f}_L = \mathbf{0} \tag{3.23}$$

whereas the second equation is the energy evolution equation

$$\frac{\partial L}{\partial t} + \frac{d}{dt}\left(\frac{\partial L}{\partial \dot{\mathbf{q}}}\dot{\mathbf{q}} - L\right) - \mathbf{f}_L \cdot \dot{\mathbf{q}} = 0 \tag{3.24}$$

Thus, for the forced case, the energy evolution equation describes how the energy of the Lagrangian system depends on the input power by the external force $\mathbf{f}_L$. If we consider an associated curve $\mathbf{q}(t)$ satisfying the forced Euler-Lagrange equations and compute the energy

evolution equation we get

$$\frac{\partial L}{\partial t}+\frac{d}{dt}\left(\frac{\partial L}{\partial \dot{\mathbf{q}}}.\dot{\mathbf{q}}-L\right)-\mathbf{f}_L.\dot{\mathbf{q}}=\frac{\partial L}{\partial t}+\frac{d}{dt}\left(\frac{\partial L}{\partial \dot{\mathbf{q}}}\right).\dot{\mathbf{q}}+\frac{\partial L}{\partial \dot{\mathbf{q}}}.\ddot{\mathbf{q}}-\frac{dL}{dt}-\mathbf{f}_L.\dot{\mathbf{q}} \tag{3.25}$$

which after substituting $\frac{d}{dt}\left(\frac{\partial L}{\partial \dot{\mathbf{q}}}\right)=\frac{\partial L}{\partial \mathbf{q}}+\mathbf{f}_L$ simplifies to

$$\frac{\partial L}{\partial t}+\frac{d}{dt}\left(\frac{\partial L}{\partial \dot{\mathbf{q}}}.\dot{\mathbf{q}}-L\right)-\mathbf{f}_L.\dot{\mathbf{q}}=\left(\frac{\partial L}{\partial t}+\left(\frac{\partial L}{\partial \mathbf{q}}+\mathbf{f}_L\right).\dot{\mathbf{q}}+\frac{\partial L}{\partial \dot{\mathbf{q}}}.\ddot{\mathbf{q}}\right)-\frac{dL}{dt}-\mathbf{f}_L.\dot{\mathbf{q}}=0 \tag{3.26}$$

which shows that (3.23) implies (3.24). Thus, for continuous-time forced Lagrangian systems, the additional energy evolution equation obtained by taking the variation with respect to time does not provide any new information concerning the forced Euler-Lagrange equations.

Remark 1. It should be noted that both (3.23) and (3.24) depend only on the associated curve $\mathbf{q}(t)$ and the time component $c_t(a)$ of the extended path cannot be determined from the governing equations. Thus, the "velocity" of time, i.e. $c_t'(a)$, is indeterminate in the continuous-time formulation of time-dependent Lagrangian systems with forcing.

3.3 Energy-preserving Variational Integrators

In this section, we derive the extended discrete Euler-Lagrange equations for time-dependent Lagrangian systems with forcing by discretizing the modified Lagrange-d'Alembert principle given in Section 3.2. The key difference from the extended discrete Euler-Lagrange equations derived in Section 3.1.2 is that we will have additional discrete terms accounting for the virtual work done by the external forcing.

The modified Lagrange-d'Alembert principle presented in Section 3.2 has two continuous-

time force integrals in the variational principle. In order to derive the extended forced discrete Euler-Lagrange equations, we define two discrete force terms $f_d^{\pm} : \bar{Q} \times \bar{Q} \to T^*\bar{Q}$ which approximate the virtual work done due to variations in $\mathbf{q}$ in the following sense

$$f_d^+(t_k, \mathbf{q}_k, t_{k+1}, \mathbf{q}_{k+1}) \cdot \delta\mathbf{q}_{k+1} + f_d^-(t_k, \mathbf{q}_k, t_{k+1}, \mathbf{q}_{k+1}) \cdot \delta\mathbf{q}_k \approx \int_{t_k}^{t_{k+1}} \mathbf{f}_L(t, \mathbf{q}(t), \dot{\mathbf{q}}(t)) \cdot \delta\mathbf{q}\, dt \quad (3.27)$$

We also define two discrete power terms $g_d^{\pm} : \bar{Q} \times \bar{Q} \to \mathbb{R}$ which approximate the virtual work done due to time variations in the following sense

$$g_d^+(t_k, \mathbf{q}_k, t_{k+1}, \mathbf{q}_{k+1})\delta t_{k+1} + g_d^-(t_k, \mathbf{q}_k, t_{k+1}, \mathbf{q}_{k+1})\delta t_k \approx \int_{t_k}^{t_{k+1}} -\mathbf{f}_L(t, \mathbf{q}(t), \dot{\mathbf{q}}(t)) \cdot (\dot{\mathbf{q}}\delta t)\ dt \quad (3.28)$$

For the time-dependent Lagrangian system with forcing, we seek discrete-time paths which satisfy

$$\delta \sum_{k=0}^{N-1} L_d(t_k, \mathbf{q}_k, t_{k+1}, \mathbf{q}_{k+1}) + \sum_{k=0}^{N-1} [\mathbf{f}_d^+(t_k, \mathbf{q}_k, t_{k+1}, \mathbf{q}_{k+1}) \cdot \delta\mathbf{q}_{k+1} + \mathbf{f}_d^-(t_k, \mathbf{q}_k, t_{k+1}, \mathbf{q}_{k+1}) \cdot \delta\mathbf{q}_k] + \sum_{k=0}^{N-1} [g_d^+(t_k, \mathbf{q}_k, t_{k+1}, \mathbf{q}_{k+1})\delta t_{k+1} + g_d^-(t_k, \mathbf{q}_k, t_{k+1}, \mathbf{q}_{k+1})\delta t_k] = 0 \quad (3.29)$$

Setting all the variations at the endpoints equal to zero in (3.29) gives the extended forced discrete Euler-Lagrange equations

$$D_4 L_d(t_{k-1}, \mathbf{q}_{k-1}, t_k, \mathbf{q}_k) + D_2 L_d(t_k, \mathbf{q}_k, t_{k+1}, \mathbf{q}_{k+1}) + \mathbf{f}_d^+(t_{k-1}, \mathbf{q}_{k-1}, t_k, \mathbf{q}_k) + \mathbf{f}_d^-(t_k, \mathbf{q}_k, t_{k+1}, \mathbf{q}_{k+1}) = \mathbf{0} \quad (3.30)$$

$$D_3 L_d(t_{k-1}, \mathbf{q}_{k-1}, t_k, \mathbf{q}_k) + D_1 L_d(t_k, \mathbf{q}_k, t_{k+1}, \mathbf{q}_{k+1}) + g_d^+(t_{k-1}, \mathbf{q}_{k-1}, t_k, \mathbf{q}_k) + g_d^-(t_k, \mathbf{q}_k, t_{k+1}, \mathbf{q}_{k+1}) = 0 \quad (3.31)$$

We modify the definitions of the discrete momentum and energy to account for the effect of

forcing

$$\mathbf{p}_k = D_4 L_d(t_{k-1}, \mathbf{q}_{k-1}, t_k, \mathbf{q}_k) + \mathbf{f}_d^+(t_{k-1}, \mathbf{q}_{k-1}, t_k, \mathbf{q}_k) \tag{3.32}$$

$$E_k = -D_3 L_d(t_{k-1}, \mathbf{q}_{k-1}, t_k, \mathbf{q}_k) - g_d^+(t_{k-1}, \mathbf{q}_{k-1}, t_k, \mathbf{q}_k) \tag{3.33}$$

Using the modified discrete momentum and energy definitions (3.32) and (3.33), the extended forced discrete Euler-Lagrange equations can be re-written in the following form

$$-D_2 L_d(t_k, \mathbf{q}_k, t_{k+1}, \mathbf{q}_{k+1}) - \mathbf{f}_d^-(t_k, \mathbf{q}_k, t_{k+1}, \mathbf{q}_{k+1}) = \mathbf{p}_k \tag{3.34}$$

$$D_1 L_d(t_k, \mathbf{q}_k, t_{k+1}, \mathbf{q}_{k+1}) + g_d^-(t_k, \mathbf{q}_k, t_{k+1}, \mathbf{q}_{k+1}) = E_k \tag{3.35}$$

$$\mathbf{p}_{k+1} = D_4 L_d(t_k, \mathbf{q}_k, t_{k+1}, \mathbf{q}_{k+1}) + \mathbf{f}_d^+(t_k, q_k, t_{k+1}, q_{k+1}) \tag{3.36}$$

$$E_{k+1} = -D_3 L_d(t_k, \mathbf{q}_k, t_{k+1}, \mathbf{q}_{k+1}) - g_d^-(t_k, \mathbf{q}_k, t_{k+1}, \mathbf{q}_{k+1}) \tag{3.37}$$

Given a time-dependent Lagrangian system with external forcing, the extended discrete Lagrangian system obtained by solving (3.34)-(3.37) can be used as an adaptive time step variational integrator for the continuous-time system.

Remark 2. The modified discrete energy (3.33) has a contribution from the external forcing which accounts for the virtual work done during the adaptive time step. Thus, the discrete trajectory obtained by solving the extended discrete Euler-Lagrange equations preserves a discrete quantity which is not the discrete analogue of the total energy of the Lagrangian system. This detail becomes important when we simulate a dissipative Lagrangian system with an adaptive time step variational integrator in Section 3.4.3

3.4 Numerical Examples

In this section, we implement the extended forced discrete Euler-Lagrange equations as numerical integrators of continuous dynamical systems. We first consider a nonlinear conservative dynamical system studied in [51] and compare the fixed time step variational integrator results with the corresponding results for the adaptive time step variational integrator. We then study a forced harmonic oscillator, a time-dependent dynamical system, in order to investigate the numerical properties of the adaptive time step variational integrators for forced systems. Finally, we simulate a damped harmonic oscillator to understand the numerical performance of adaptive time step variational integrators for dissipative systems.

3.4.1 Conservative Example

We consider a particle in a double-well potential. The Lagrangian for this conservative one degree of freedom dynamical system is

$$L(q,\dot{q}) = \frac{1}{2}m\dot{q}^2 - V(q) \tag{3.38}$$

where

$$V(q) = \frac{1}{2}\left(q^4 - q^2\right) \tag{3.39}$$

Fixed time step algorithm

For the fixed time step case, we choose a constant time step h. The discrete Lagrangian is obtained using the midpoint rule

$$L_d(q_k, q_{k+1}) = hL\left(\frac{q_k + q_{k+1}}{2}, \frac{q_{k+1} - q_k}{h}\right) \tag{3.40}$$

The discrete momentum p_{k+1} is given by

$$p_{k+1} = m\left(\frac{q_{k+1} - q_k}{h}\right) + h\left(\left(\frac{q_{k+1} + q_k}{4}\right) - \left(\frac{q_{k+1} + q_k}{2}\right)^3\right) \tag{3.41}$$

For given (q_k, p_k) at the k^{th} time step, the implicit time-marching equation for the fixed time step method is

$$m\left(\frac{q_{k+1} - q_k}{h}\right) - h\left(\left(\frac{q_{k+1} + q_k}{4}\right) - \left(\frac{q_{k+1} + q_k}{2}\right)^3\right) = p_k \tag{3.42}$$

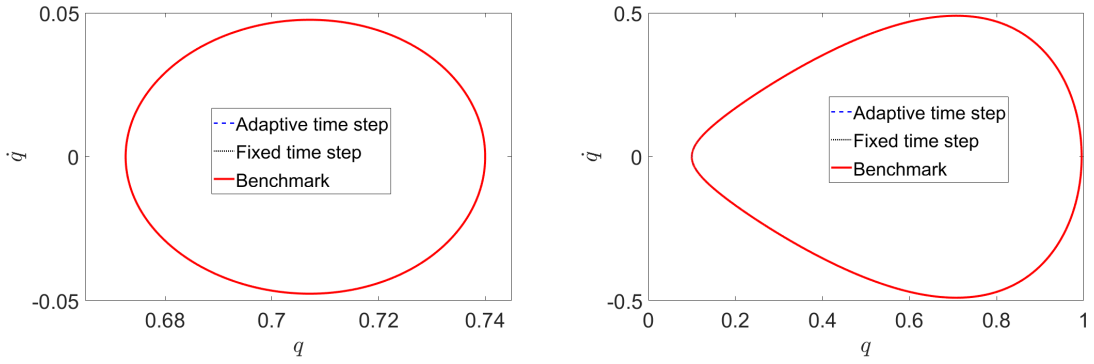

(a) $q(0) = 0.74,\ \dot{q}(0) = 0$ (b) $q(0) = 0.995,\ \dot{q}(0) = 0$

Figure 3.1: Two initial conditions are studied for the particle in double-well potential. An initial time step of $h_0 = 0.01$ is used for the adaptive time step algorithm in both cases. The fixed time step size is chosen such that number of total time steps is same as the adaptive algorithm. Phase space trajectories for both fixed time step and adaptive time step algorithms are compared to the benchmark trajectory. The trajectories in each figure are indistinguishable verifying the equations.

Adaptive time step algorithm

For the adaptive time step case, we have discrete time t_k as an additional discrete variable. We use the midpoint rule to obtain the discrete Lagrangian L_d

$$L_d(t_k, q_k, t_{k+1}, q_{k+1}) = (t_{k+1}-t_k)\left[\frac{1}{2}m\left(\frac{q_{k+1}-q_k}{t_{k+1}-t_k}\right)^2 - \frac{1}{2}\left(\left(\frac{q_{k+1}+q_k}{2}\right)^4 - \left(\frac{q_{k+1}+q_k}{2}\right)^2\right)\right] \tag{3.43}$$

The discrete momentum p_k and discrete energy E_k are obtained by substituting the L_d expression in (3.17) and (3.18)

$$p_{k+1} = m\left(\frac{q_{k+1}-q_k}{t_{k+1}-t_k}\right) + (t_{k+1}-t_k)\left(\left(\frac{q_{k+1}+q_k}{4}\right) - \left(\frac{q_{k+1}+q_k}{2}\right)^3\right) \tag{3.44}$$

$$E_{k+1} = \frac{1}{2}m\left(\frac{q_{k+1}-q_k}{t_{k+1}-t_k}\right)^2 + \frac{1}{2}\left(\left(\frac{q_{k+1}+q_k}{2}\right)^4 - \left(\frac{q_{k+1}+q_k}{2}\right)^2\right) \tag{3.45}$$

The implicit time-marching equations for the adaptive time step algorithm are

$$m\left(\frac{q_{k+1}-q_k}{t_{k+1}-t_k}\right) - (t_{k+1}-t_k)\left(\left(\frac{q_{k+1}+q_k}{4}\right) - \left(\frac{q_{k+1}+q_k}{2}\right)^3\right) = p_k \tag{3.46}$$

$$\frac{1}{2}m\left(\frac{q_{k+1}-q_k}{t_{k+1}-t_k}\right)^2 + \frac{1}{2}\left(\left(\frac{q_{k+1}+q_k}{2}\right)^4 - \left(\frac{q_{k+1}+q_k}{2}\right)^2\right) = E_k \tag{3.47}$$

Since the dynamical system being considered here is time-independent, we rewrite the time-marching equations in terms of $h_k = (t_{k+1}-t_k)$ and $v_k = \left(\frac{q_{k+1}-q_k}{t_{k+1}-t_k}\right)$

$$F(q_k, p_k, h_k, v_k) = mv_k - h_k\left(\left(\frac{v_k h_k + 2q_k}{4}\right) - \left(q_k + \frac{v_k h_k}{2}\right)^3\right) - p_k = 0 \tag{3.48}$$

$$G(q_k, E_k, h_k, v_k) = \frac{1}{2}mv_k^2 + \frac{1}{2}\left(\left(q_k + \frac{v_k h_k}{2}\right)^4 - \left(q_k + \frac{v_k h_k}{2}\right)^2\right) - E_k = 0 \tag{3.49}$$

These time-marching equations are solved using Newton's iterative method with the restriction $h_k > 0$ to obtain discrete trajectories in the extended space. This extended discrete system can be used as a variational integrator for the continuous-time dynamical system.

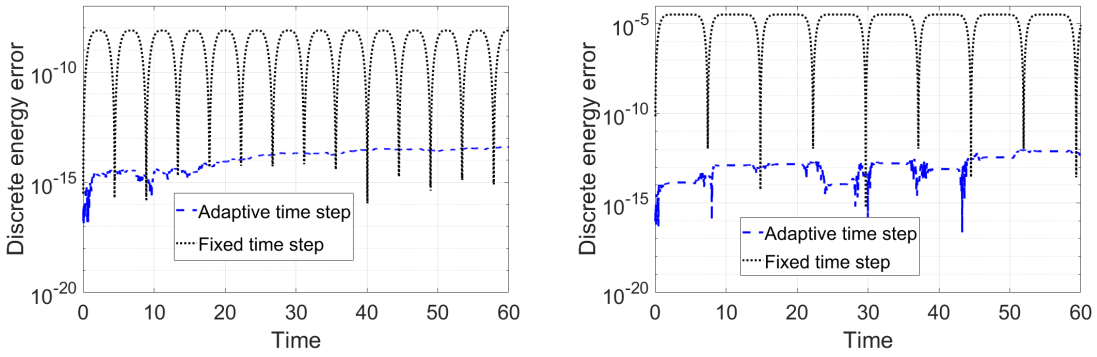

(a) $q(0) = 0.74,\ \dot{q}(0) = 0$ (b) $q(0) = 0.995,\ \dot{q}(0) = 0$

Figure 3.2: Energy error plots for both fixed time step and adaptive time step algorithms are compared for two different initial conditions. Each figure shows the superior energy performance of the adaptive time step algorithm.

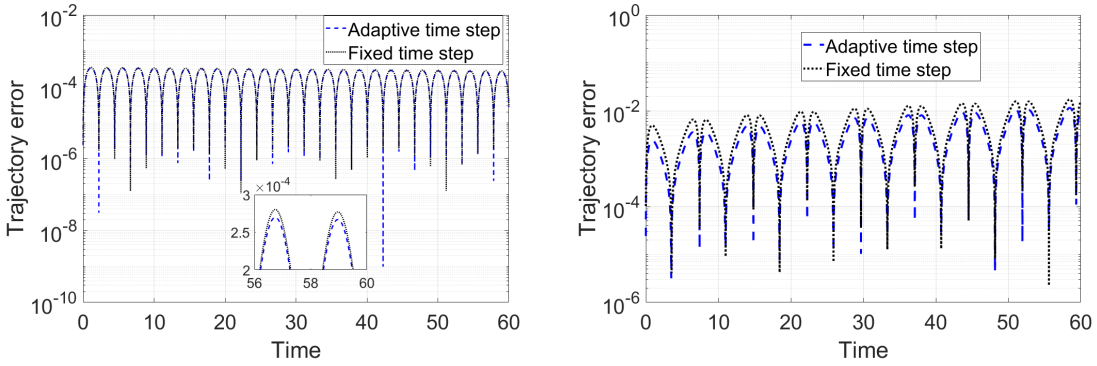

(a) $q(0) = 0.74,\ \dot{q}(0) = 0$ (b) $q(0) = 0.995,\ \dot{q}(0) = 0$

Figure 3.3: Trajectory error plots for both fixed time step and adaptive time step algorithms are compared for two different initial conditions. Each figure, especially the highly nonlinear case (b), clearly shows the superior trajectory performance of the adaptive time step algorithm.

Remark 3. In [51], an alternative optimization method has been implemented where in-

stead of solving the nonlinear coupled equations (3.48) and (3.49), the following quantity is minimized

$$[F(q_k, p_k, h_k, v_k)]^2 + [G(q_k, E_k, h_k, v_k)]^2 \tag{3.50}$$

over the variables v_k and h_k with the restriction $h_k > 0$. The drawback of using this approach is that numerically it violates the energy evolution equation and the underlying structure is no longer preserved. In fact, due to this optimization approach, the energy plots given in [51] do not clearly convey the advantage of energy-preserving variational integrators.

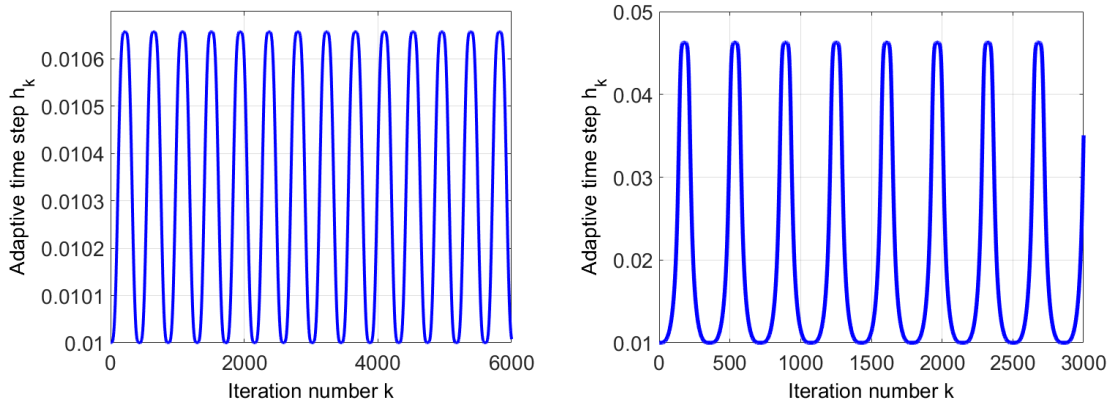

(a) $q(0) = 0.74,\ \dot{q}(0) = 0$ (b) $q(0) = 0.995,\ \dot{q}(0) = 0$

Figure 3.4: Adaptive time step versus iteration number for both initial conditions.

Initial condition

We have considered two regions of phase space, similar to the numerical example in [51], to understand numerical properties of the adaptive time step variational integrator for conservative systems. Since our aim is to use these discrete trajectories as numerical integrators for continuous dynamical systems, instead of starting with two discrete points we consider a continuous-time dynamical system with given initial position $q(0)$ and initial velocity $\dot{q}(0)$

and use the benchmark solution to obtain initial conditions for the adaptive time step variational integrator. Since the adaptive time step changes substantially from the initial time step h_0, for a fair comparison of trajectory accuracy and energy error, we have chosen the fixed time step algorithm in such a way that both fixed and adaptive algorithms take same number total time steps over the numerical simulation.

For a given set of initial conditions, i.e. $(q(0), \dot{q}(0))$, we first decide the initial time step h_0 and then use the benchmark solution to compute discrete configuration q_1 at time $t_1 = h_0$, configuration at first time step. Thus, we have obtained two discrete points in the extended state space (t_0, q_0) and (t_1, q_1) and using these two discrete points we can find discrete momentum p_1 and discrete energy E_1. After obtaining (t_1, q_1, p_1, E_1), we can solve the time-marching equations (3.34)-(3.37) to numerically simulate the dynamical system.

Results

The discrete trajectories for both fixed and adaptive time step algorithms are compared with the benchmark solution in Figure 3.1. The position $q = \frac{q_k+q_{k+1}}{2}$ and velocity $\dot{q} = \frac{q_{k+1}-q_k}{h_k}$ are computed from the discrete trajectories for both fixed and adaptive time step algorithms and compared with continuous time q and $\dot{q}$. For both initial conditions, discrete trajectories from the adaptive time step and fixed time step match the benchmark trajectory.

The energy error plots for both cases in Figure 3.2 show the superior energy behavior of adaptive time step variational integrators for conservative dynamical systems. Instead of using the optimization approach discussed in Remark 3, we have obtained the discrete trajectories by solving the nonlinear coupled equations exactly to preserve the underlying structure. The energy error plots quantify the difference in energy accuracy for fixed time step and adaptive time step method clearly. The energy-preserving performance was not evident in similar re-

sults given in [51] because of the optimization approach used to obtain discrete trajectories instead of solving the implicit equations directly. The energy error comparison in Figure 3.2a shows that the adaptive time step method has energy error magnitude around 10^{-14} whereas the fixed time step method has energy error around 10^{-8}. In Figure 3.2b the energy error for fixed time step increases to 10^{-6} while the adaptive time step method shows nearly exact energy preservation(of the order of computer precision minus the condition number of the equations). Although the magnitude of energy error for fixed time step method is bounded, the magnitude of energy error oscillations depends on where the trajectory lies in the phase space. Thus, for areas in phase space where the magnitude of energy error oscillations is substantial for fixed time step method, the adaptive time step method can be used to preserve the energy of the system more accurately.

Trajectory error plots shown in Figure 3.3 demonstrate the improved accuracy achieved by adaptive time step variational integrators for both cases. In Figure 3.3a both methods exhibit nearly same accuracy with adaptive time step performing marginally better. The trajectory error comparison in Figure 3.3b shows the superior performance of adaptive time step variational integrators for long time simulation. Based on the accuracy results, we believe adaptive time step variational integrators can provide benefits for numerical simulation of regions of phase space which show significant changes in the underlying physics.

Figure 3.4 shows how the adaptive time step oscillates for both cases. The adaptive time step doesn't increase substantially compared to the initial time step of $h_0 = 0.01$ for the first case in Figure 3.4a, while Figure 3.4b indicates the adaptive time step increases by 4 times the initial time step for the second case. The amplitude of adaptive time step oscillations depends on the region of phase space in which the discrete trajectory lies. The adaptive time step algorithm computes the adaptive time step such that the discrete energy is conserved exactly. There is no upper bound on the size of the adaptive time step, but very large adap-

tive time step values make the discretization assumption made in (3.43) erroneous leading to inaccurate discrete trajectories.

Remark 4. It is important to understand that adaptive time step variational integrators are fundamentally different from traditional adaptive time-stepping numerical methods which compute the adaptive time step size based on some error criteria. Adaptive time step variational integrators treat time as a discrete dynamic variable and the adaptive time step is computed by solving the extended discrete Euler-Lagrange equations. Thus, the adaptive time step is coupled with the dynamics of the system whereas, for most of the the adaptive time-stepping numerical methods, the step size computation and dynamics of the system are independent of each other.

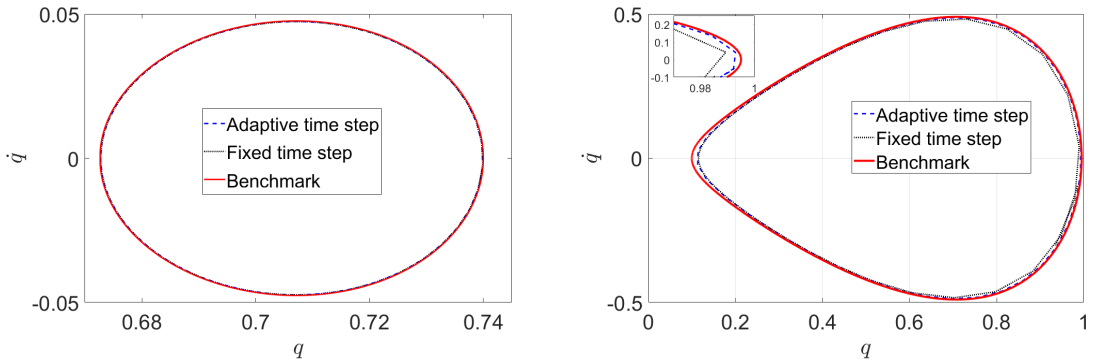

(a) $q(0) = 0.74,\ \dot{q}(0) = 0$ (b) $q(0) = 0.995,\ \dot{q}(0) = 0$

Figure 3.5: In these plots, an initial time step of $h_0 = 0.1$ is used for the adaptive time step algorithm to study the effect of initial time step on the accuracy of discrete trajectories.

Effect of initial time step

From the discrete energy definition it is clear that the initial time step value plays an important role in the adaptive time step algorithm. We study the effect of initial time step on the phase space and energy error plots by simulating the two cases considered in the previous

subsection but with a larger initial time step $h_0 = 0.1$ for the adaptive time step. The fixed time step size is chosen such that number of total time steps is same for both fixed and adaptive time step algorithm.

The phase space trajectories shown in Figure 3.5 show that even with an initial time step of $h_0 = 0.1$ discrete trajectories from both fixed and adaptive time step show good agreement with the benchmark solution. In Figure 3.5a, the discrete trajectories lie on top of the benchmark solution for the first set of initial conditions. In Figure 3.5b, the fixed and adaptive time step discrete trajectories give slightly inaccurate results near the turning point. The discrete energy error plots in Figure 3.6 show that for fixed time step variational integrators, the discrete energy errors increase with increase in the time step size but for the adaptive time step variational integrators, increasing the time step size leads to accurate discrete energy behavior. In fact, the accuracy of energy preservation is slightly better for this case. This unexpected behavior is due to the ill-conditioned nature of the implicit extended discrete Euler-Lagrange equations, which become more ill-conditioned for smaller time steps. The plots of condition number in Figure 3.7 show that the implicit equations become more ill-conditioned as the initial time step value is decreased. Thus, numerical computations with finite precision will lead to higher errors in the solution.

It is important to note that for a conservative system, the continuous-time trajectory preserves the continuous energy which is different from the discrete energy that adaptive time step variational integrators are constructed to preserve. This explains why, despite the superior energy behavior in Figure 3.6b compared to Figure 3.2b, the discrete trajectory in Figure 3.5b is less accurate than the discrete trajectory in Figure 3.1b. We know that as the time step value tends to zero the discrete energy and continuous energy become equal but the condition number analysis and the energy error plots reveal that smaller initial time steps for adaptive time variational integrators lead to ill-conditioning and finite precision

errors in energy. *Thus, there is a trade-off between preserving discrete energy and ensuring overall trajectory accuracy when choosing an initial time step for the adaptive time step variational integrators.*

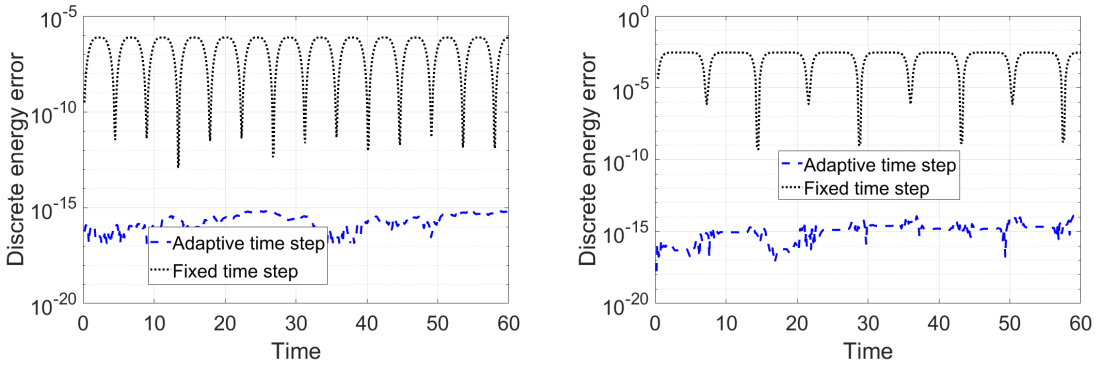

(a) $q(0) = 0.74,\ \dot{q}(0) = 0$ (b) $q(0) = 0.995,\ \dot{q}(0) = 0$

Figure 3.6: The energy error plots with an initial time step of $h_0 = 0.1$ for the adaptive time step algorithm.

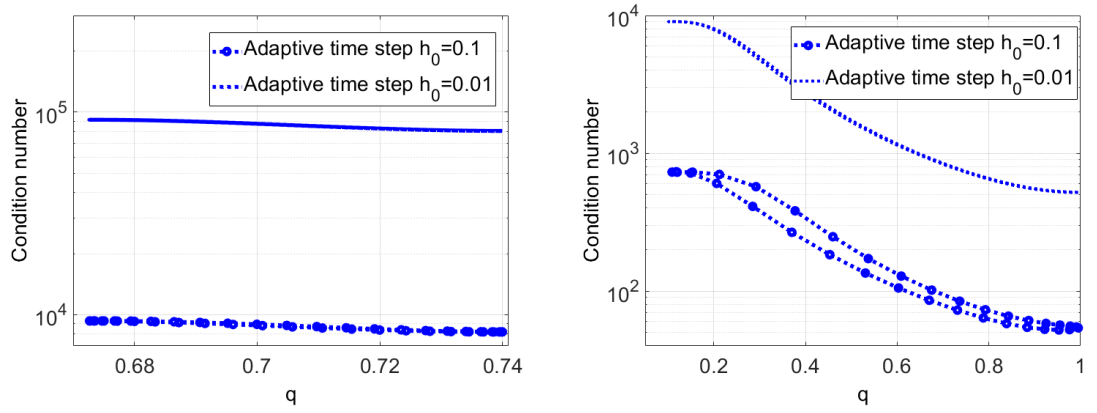

(a) $q(0) = 0.74,\ \dot{q}(0) = 0$ (b) $q(0) = 0.995,\ \dot{q}(0) = 0$

Figure 3.7: The increase in condition number with decrease in initial time step for the adaptive time step algorithm.

Remark 5. The discrete energy error plotted in Figure 3.2 and Figure 3.6 is different from our traditional idea of energy error. We usually define energy error as the difference between the energy of the continuous-time system and the energy obtained from the discrete

trajectories. This traditional energy error can be broken down into *discrete energy error* and *discretization error*. The discrete energy error is the error in preserving the discrete energy of the extended discrete Lagrangian system. The discretization error is the error incurred by discretizing a continuous-time system. Thus, the discretization error is the difference between the continuous energy and the discrete energy that our integrators aim to preserve, whereas the discrete energy error is the error between the true and computed discrete energy.

Remark 6. For a conservative system, we expect discrete energy to be constant and thus the discretization error is also constant. Since this constant discretization error is orders of magnitude larger than the discrete energy error, traditional energy error plots do not show the advantages of using adaptive time-stepping. We evaluate the performance of variational integrators by comparing how well these integrators preserve the discrete energy.

3.4.2 Time-dependent Example

We consider a forced harmonic oscillator to study the numerical performance of the adaptive time step variational integrator for forced Lagrangian systems with explicit time-dependence. The (continuous) Lagrangian for the single degree of freedom system is

$$L(q, \dot{q}) = \frac{1}{2} m \dot{q}^2 - \frac{1}{2} k q^2 \tag{3.51}$$

and the external forcing is

$$f = F_0 cos(\omega_F t) \tag{3.52}$$

where m is the mass, k is the stiffness, F_0 is the magnitude of the force and ω_F is the forcing frequency. For discretization, we use the midpoint rule to obtain the discrete Lagrangian L_d

$$L_d(t_k, q_k, t_{k+1}, q_{k+1}) = (t_{k+1} - t_k)\ L\left(\frac{q_k + q_{k+1}}{2}, \frac{q_{k+1} - q_k}{t_{k+1} - t_k}\right) \tag{3.53}$$

Similarly, we can write the discrete force $f_d^{\pm}$ as

$$f_d^{\pm} = \frac{1}{2}F_0(t_{k+1} - t_k)cos\left(\frac{\omega_F(t_{k+1} + t_k)}{2}\right) \tag{3.54}$$

and the corresponding power term $g_d^{\pm}$ as

$$g_d^{\pm} = -f_d^{\pm}\left(\frac{q_{k+1} - q_k}{t_{k+1} - t_k}\right) = -\frac{1}{2}F_0(t_{k+1} - t_k)cos\left(\frac{\omega_F(t_{k+1} + t_k)}{2}\right)\left(\frac{q_{k+1} - q_k}{t_{k+1} - t_k}\right) \tag{3.55}$$

The discrete momentum p_{k+1} and discrete energy E_{k+1} expressions are

$$\begin{aligned} p_{k+1} &= D_4L_d(t_k, q_k, t_{k+1}, q_{k+1}) + f_d^+ \\ &= m\left(\frac{q_{k+1} - q_k}{t_{k+1} - t_k}\right) - k(t_{k+1} - t_k)\left(\frac{q_k + q_{k+1}}{4}\right) + \frac{F_0(t_{k+1} - t_k)}{2}cos\left(\frac{\omega_F(t_{k+1} + t_k)}{2}\right) \end{aligned} \tag{3.56}$$

$$\begin{aligned} E_{k+1} &= -D_3L_d(t_k, q_k, t_{k+1}, q_{k+1}) - g_d^+ \\ &= \frac{1}{2}m\left(\frac{q_{k+1} - q_k}{t_{k+1} - t_k}\right)^2 + \frac{1}{2}k\left(\frac{q_k + q_{k+1}}{2}\right)^2 + \frac{F_0}{2}cos\left(\frac{\omega_F(t_{k+1} + t_k)}{2}\right)(q_{k+1} - q_k) \end{aligned} \tag{3.57}$$

For given (t_k, q_k, E_k, p_k), the time-marching implicit equations for the forced harmonic oscillator are obtained by substituting the discrete Lagrangian (3.53) and discrete force expressions (3.54)-(3.55) into (3.34) and (3.35)

$$m\left(\frac{q_{k+1} + q_k}{t_{k+1} - t_k}\right) + k(t_{k+1} - t_k)\left(\frac{q_{k+1} + q_k}{4}\right) + \frac{F_0(t_{k+1} - t_k)}{2}cos\left(\frac{\omega_F(t_{k+1} + t_k)}{2}\right) = p_k \tag{3.58}$$

$$\frac{1}{2}m\left(\frac{q_{k+1} - q_k}{t_{k+1} - t_k}\right)^2 + \frac{1}{2}k\left(\frac{q_{k+1} + q_k}{2}\right)^2 - \frac{F_0}{2}cos\left(\frac{\omega_F(t_{k+1} + t_k)}{2}\right)(q_{k+1} - q_k) = E_k \tag{3.59}$$

We re-write the above two coupled nonlinear equations in terms of the k^{th} adaptive time step $h_k = t_{k+1} - t_k$ and $v_k = \left(\frac{q_{k+1}-q_k}{t_{k+1}-t_k}\right)$

$$F(q_k, t_k, p_k, h_k, v_k) = mv_k + \frac{kh_k}{4}(2q_k + h_k v_k) + \frac{F_0 h_k}{2} cos\left(\omega_F\left(t_k + \frac{h_k}{2}\right)\right) - p_k = 0 \quad (3.60)$$

$$G(q_k, t_k, E_k, h_k, v_k) = \frac{1}{2}mv_k^2 + \frac{1}{2}k\left(q_k + \frac{h_k v_k}{2}\right)^2 - \frac{F_0 h_k v_k}{2} cos\left(\omega_F\left(t_k + \frac{h_k}{2}\right)\right) - E_k = 0 \quad (3.61)$$

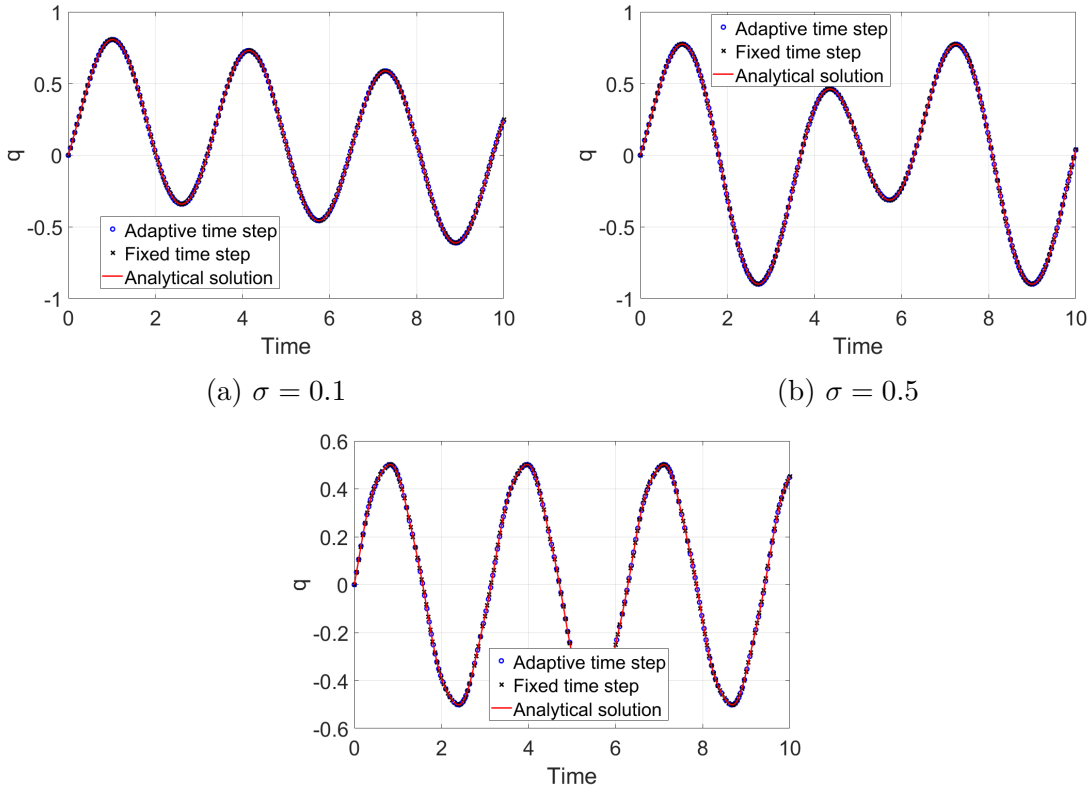

(a) $\sigma = 0.1$ (b) $\sigma = 0.5$

(c) $\sigma = 5$

Figure 3.8: Three forcing frequency ratio values are studied for the forced harmonic oscillator system. Discrete trajectories for both fixed time step and adaptive time step variational integrators are plotted and compared with the analytical solution for an initial time step $h_0 = 0.01$ for the adaptive time step algorithm and natural frequency $\omega_n = 2\ rad/s$.

Results

We have studied the forced harmonic oscillator for three values of the forcing frequency ratio $\sigma = \frac{\omega_F}{\omega_n}$ for $\omega_n = \sqrt{\frac{k}{m}} = 2\ rad/s$ to understand the numerical performance of adaptive time step variational integrators for systems with explicit time-dependence. The discrete trajectories from both fixed and adaptive time step variational integrators are compared in Figure 3.8 and both discrete trajectories agree favorably with the analytical solution for all three cases.

Energy error plots for all three cases in Figure 3.9 show the superior energy behavior of adaptive time step variational integrators for systems with explicit time-dependence. The energy error comparison in Figure 3.9a shows that the adaptive time step method has energy error magnitude around 10^{-4} whereas the fixed time step method has energy error around 10^{-2}. In Figure 3.9b and Figure 3.9c the energy error for fixed time step increases to 10^{-1} with increase in forcing frequency while the adaptive time step method still shows an energy error around 10^{-4}. Thus, adaptive time step method predict change in energy more accurately than fixed time step methods for systems with explicit time-dependence and can be used to numerically simulate nonautonomous oscillatory systems with external forcing.

The trajectory error plots in Figure 3.10 show how both adaptive and fixed time step integrators have similar accuracy for low forcing frequencies but, as the forcing frequency increases, the fixed time step variational integrators show better trajectory accuracy. These trajectory error results in Figure 3.10 are contrary to the trend of superior trajectory performance observed for conservative example in Figure 3.3. In Figure 3.10a both fixed and adaptive time step variational integrators show same trajectory error. The comparison in Figure 3.10b and Figure 3.10c show how adaptive time step variational integrators start with more accurate trajectory but, as we march forward in time, the fixed time step variational integrator ex-

hibits lower trajectory error, especially in the case of $\sigma = 5$. This can be understood if we look at the time step adaptation.

Figure 3.11 shows the change in adaptive time step over the simulation time for different forcing frequencies. For all three cases, the adaptive time step starts from $h_0 = 0.01$ but oscillates significantly for higher σ. $\sigma = 0.1$ leads to a time step range of $0.0095 - 0.0105$ which increases to $0.007 - 0.022$ for $\sigma = 5$. Figure 3.11c shows the adaptive time step for $\sigma = 5$ quickly rise to double its initial time step $h_0 = 0.01$ and the trajectory error (see Figure 3.10c)also rises sharply during the increase in adaptive time step. Since the adaptive time step algorithm captures the flux of energy over an oscillation accurately , the error comes back to zero in every oscillation and hence the trajectory does deviate from the analytical trajectories in Figure 3.10c.

3.4.3 Dissipative Example

We consider a damped harmonic oscillator in order to better understand the numerical behavior of the adaptive time step variational integrator for forced Lagrangian systems. Similar to the time-dependent example, the Lagrangian is given by (3.51) and the dissipative force is

$$f = -c\dot{q} \tag{3.62}$$

where c is the damping parameter of the single degree of freedom system. For the discrete Lagrangian L_d, we use the midpoint rule which gives

$$L_d(t_k, q_k, t_{k+1}, q_{k+1}) = (t_{k+1} - t_k)\ L\left(\frac{q_k + q_{k+1}}{2}, \frac{q_{k+1} - q_k}{t_{k+1} - t_k}\right) \tag{3.63}$$

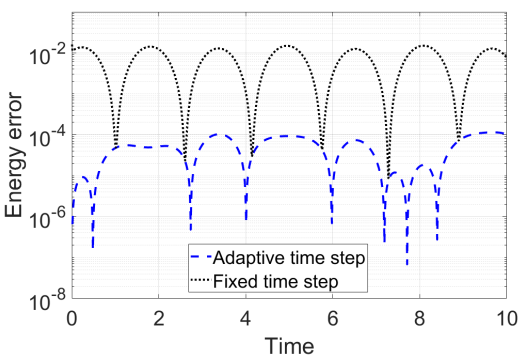

(a) $\sigma = 0.1$

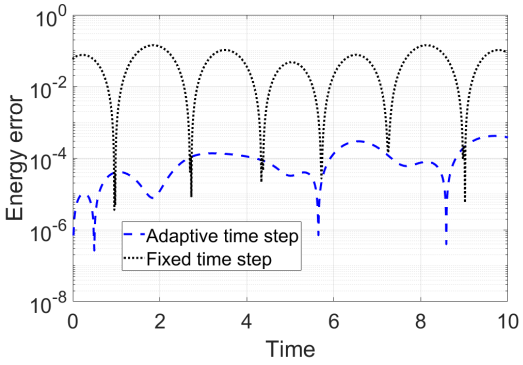

(b) $\sigma = 0.5$

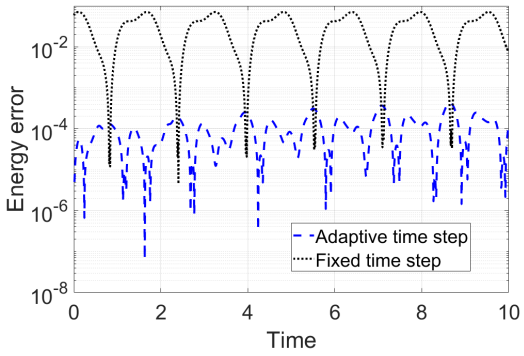

(c) $\sigma = 5$

Figure 3.9: Energy error for fixed time step and adaptive time step variational integrators are compared for three forcing frequencies. Analytical solution at the discrete time instant is used to compute the continuous energy.

Similarly, we can write the discrete force $f_d^{\pm}$ as

$$f_d^{\pm} = -\frac{1}{2}c(t_{k+1} - t_k)\left(\frac{q_{k+1} - q_k}{t_{k+1} - t_k}\right) \tag{3.64}$$

and the corresponding power term $g_d^{\pm}$ is

$$g_d^{\pm} = -f_d^{\pm}\left(\frac{q_{k+1} - q_k}{t_{k+1} - t_k}\right) = \frac{1}{2}c(t_{k+1} - t_k)\left(\frac{q_{k+1} - q_k}{t_{k+1} - t_k}\right)^2 \tag{3.65}$$

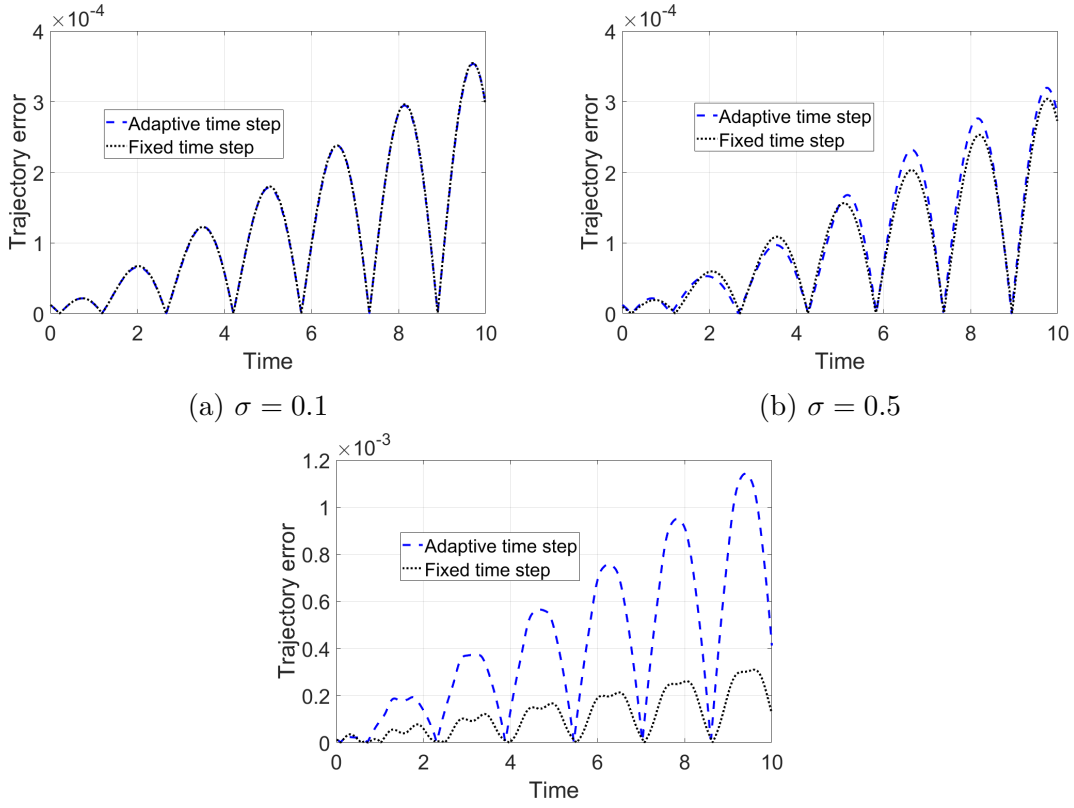

(a) $\sigma = 0.1$ (b) $\sigma = 0.5$

(c) $\sigma = 5$

Figure 3.10: Trajectory error for fixed and adaptive time step variational integrators for the forced harmonic oscillator are compared for three forcing frequency values.

The discrete momentum p_{k+1} and discrete energy E_{k+1} expressions are

$$\begin{aligned} p_{k+1} &= D_4 L_d(t_k, q_k, t_{k+1}, q_{k+1}) + f_d^+ \\ &= m\left(\frac{q_{k+1}-q_k}{t_{k+1}-t_k}\right) - k(t_{k+1}-t_k)\left(\frac{q_k+q_{k+1}}{4}\right) - c\left(\frac{q_{k+1}-q_k}{2}\right) \end{aligned} \tag{3.66}$$

$$\begin{aligned} E_{k+1} &= -D_3 L_d(t_k, q_k, t_{k+1}, q_{k+1}) - g_d^+ \\ &= \frac{1}{2}m\left(\frac{q_{k+1}-q_k}{t_{k+1}-t_k}\right)^2 + \frac{1}{2}k\left(\frac{q_k+q_{k+1}}{2}\right)^2 - \frac{c}{2}\left(\frac{(q_{k+1}-q_k)^2}{t_{k+1}-t_k}\right) \end{aligned} \tag{3.67}$$

For given (t_k, q_k, E_k, p_k), the time-marching implicit equations are obtained by substituting

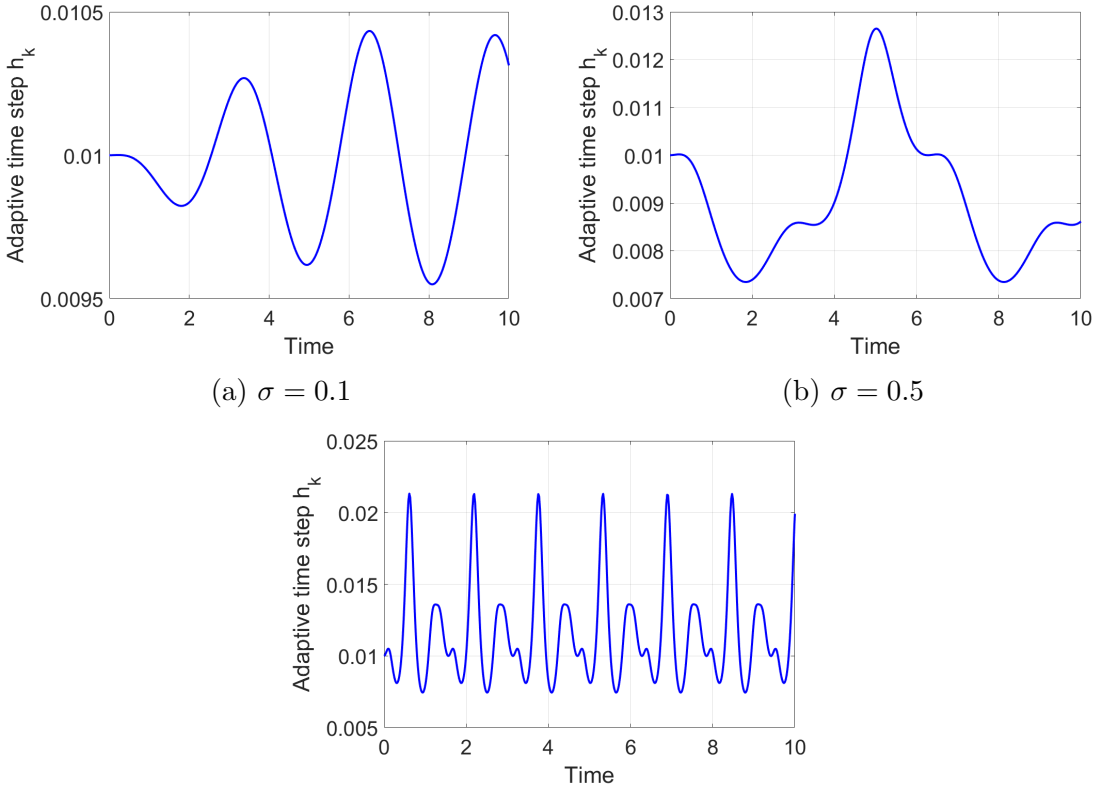

(a) $\sigma = 0.1$ (b) $\sigma = 0.5$

(c) $\sigma = 5$

Figure 3.11: Adaptive time step versus the time for the time-dependent example.

the discrete Lagrangian and discrete force expressions into (3.34) and (3.35)

$$m\left(\frac{q_{k+1}+q_k}{t_{k+1}-t_k}\right)+k(t_{k+1}-t_k)\left(\frac{q_{k+1}+q_k}{4}\right)-c(t_{k+1}-t_k)\left(\frac{q_{k+1}-q_k}{2}\right)=p_k \tag{3.68}$$

$$\frac{1}{2}m\left(\frac{q_{k+1}-q_k}{t_{k+1}-t_k}\right)^2+\frac{1}{2}c(t_{k+1}-t_k)\left(\frac{q_{k+1}-q_k}{t_{k+1}-t_k}\right)^2+\frac{1}{2}k\left(\frac{q_{k+1}+q_k}{2}\right)^2=E_k \tag{3.69}$$

The above two coupled nonlinear equations in q_{k+1} and t_{k+1} are solved with the restriction $t_{k+1} > t_k$ and substituted in (3.66) and (3.67) to obtain the discrete momentum p_{k+1} and discrete energy E_{k+1} for the next step. We re-write the above time-marching equations in

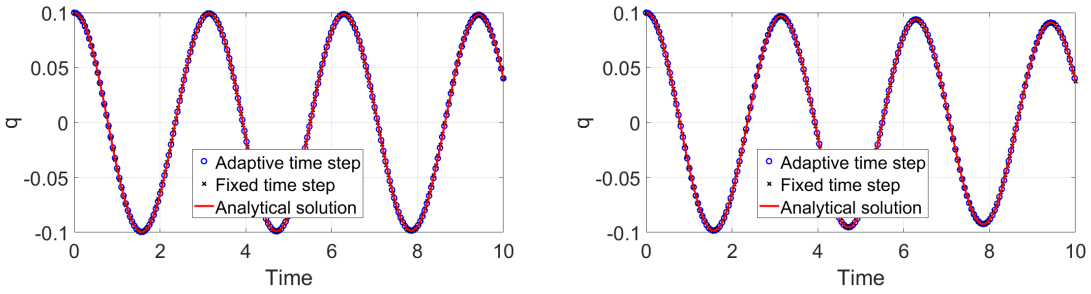

(a) $\zeta = 0.001$ (b) $\zeta = 0.005$

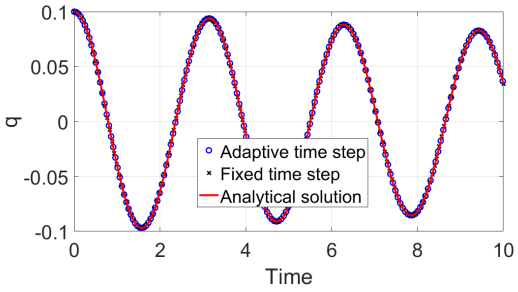

(c) $\zeta = 0.01$

Figure 3.12: Three damping ratio values are studied for the spring mass damper system. Discrete trajectories for both fixed time step and adaptive time step variational integrators are plotted and compared with the analytical solution. The analytical solution is used to prescribe initial conditions for an initial time step $h_0 = 0.01$ for the adaptive time step and natural frequency $\omega_n = 2\ rad/s$.

terms of $h_k = t_{k+1} - t_k$ and $v_k = \left(\frac{q_{k+1}-q_k}{t_{k+1}-t_k}\right)$

$$F(q_k, p_k, h_k, v_k) = mv_k + \frac{h_k}{4}(2q_k + h_k v_k) + \frac{1}{2}ch_k v_k - p_k = 0 \tag{3.70}$$

$$G(q_k, E_k, h_k, v_k) = \frac{1}{2}mv_k^2 + \frac{1}{2}ch_k v_k^2 + \frac{1}{2}k\left(q_k + \frac{h_k v_k}{2}\right)^2 - E_k = 0 \tag{3.71}$$

Remark 7. Since the Lagrangian and the forcing for this example are both time-independent, we can simplify the implicit equations by replacing $t_{k+1} - t_k$ by the k^{th} adaptive time step h_k as shown above. For time-dependent mechanical systems with either time-dependent Lagrangian or time-dependent forcing, this simplification cannot be made and discrete time terms can not be eliminated from the implicit equations, as shown in forced harmonic oscil-

lator numerical example in Section 3.4.2.

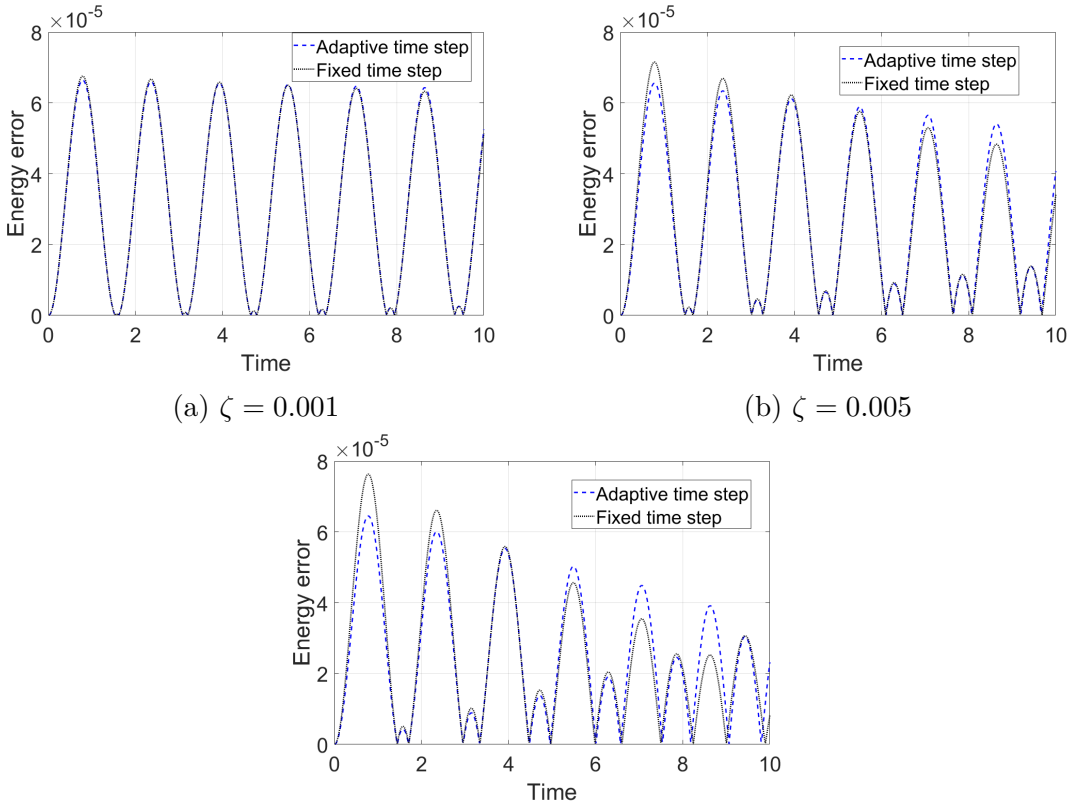

(a) $\zeta = 0.001$ (b) $\zeta = 0.005$

(c) $\zeta = 0.01$

Figure 3.13: Energy error for fixed time step and adaptive time step variational integrators are compared for three cases. Analytical solution at the discrete time instant is used to compute the continuous energy.

Results

We have studied the damped simple harmonic oscillator for three small damping values of the damping ratio $\zeta = \frac{c}{2\sqrt{km}}$ for a single natural frequency $\omega_n = \sqrt{\frac{k}{m}} = 2\ rad/s$ to understand the numerical properties of adaptive time step variational integrators derived for forced systems in Section 3.3. Just like the conservative case, our aim is to simulate the continuous-time dynamical system using discrete trajectories obtained from the adaptive time step variational integrator. The discrete trajectories from both fixed and adaptive time

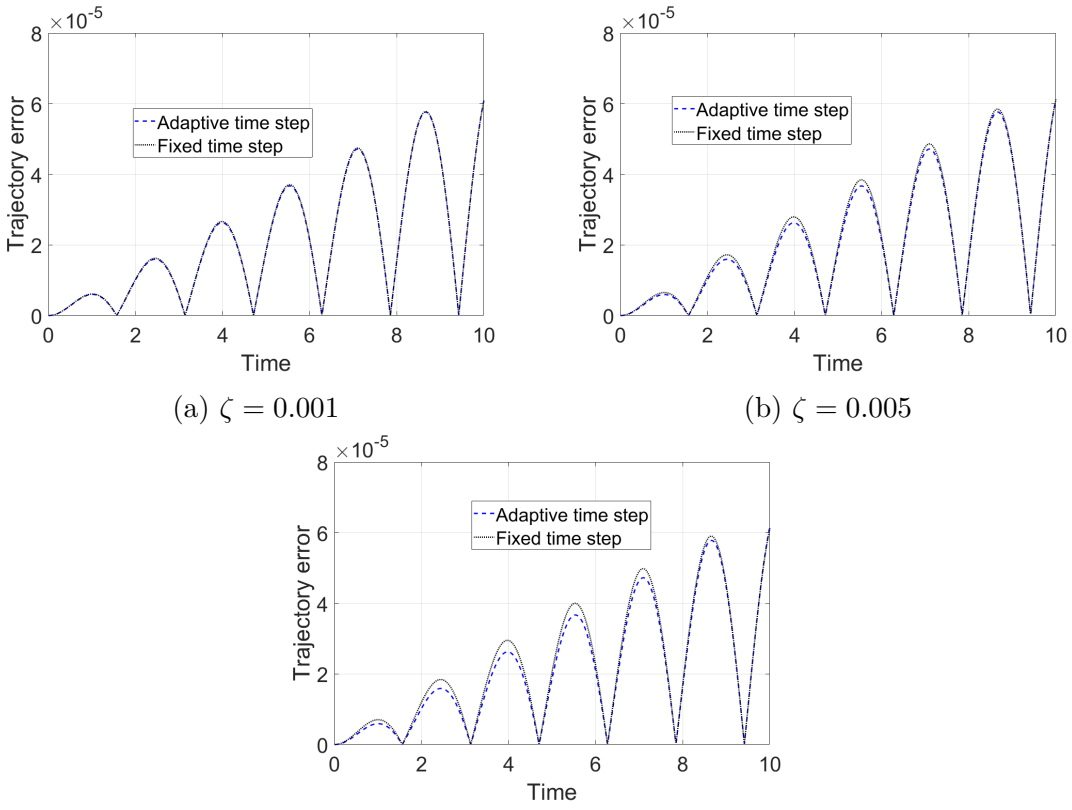

(a) $\zeta = 0.001$ (b) $\zeta = 0.005$

(c) $\zeta = 0.01$

Figure 3.14: Trajectory error for fixed and adaptive time step variational integrators for the damped harmonic oscillator are compared for three damping ratio values.

step algorithms are compared in Figure 3.12. Both are nearly indistinguishable from the analytical solution for all three cases.

The energy error plots in Figure 3.13 show how both adaptive and fixed time step variational integrators start with same energy accuracy for all three cases with adaptive time step performing better initially. As we march forward in time, the fixed time step variational integrator outperforms the adaptive time step variational integrator. *The amplitude of the energy error oscillations for the fixed time step algorithm decreases faster than it does for the adaptive time step algorithm which suggests that for long-time simulations the energy behavior of fixed time step variational integrator is better than the adaptive time step variational*

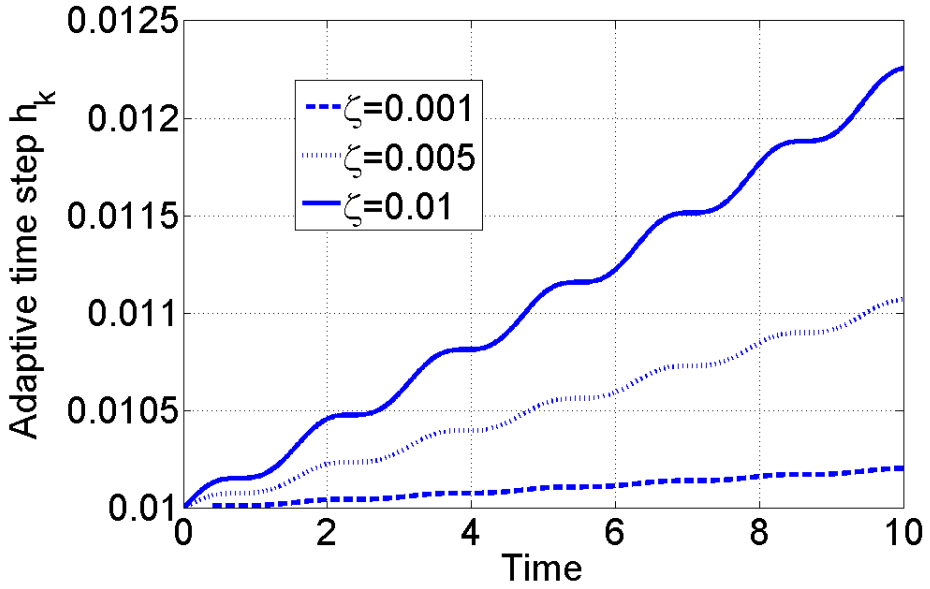

Figure 3.15: Adaptive time step versus the time for the dissipative example.

integrator. This is contrary to what we expected because the adaptive step variational integrator solves an additional discrete energy evolution equation to capture the change in energy of the forced system accurately.

These unexpected results can be understood by looking at the two components of the energy error discussed in the Remark 5. Due to exact preservation of discrete energy, the discrete energy error for adaptive time step variational integrators is orders of magnitude lower than it is for the fixed time step variational integrator. Unlike the conservative system example considered in Section 3.4.1, the continuous energy and the corresponding discrete energy, for this dissipative system, are not constant. Thus, the energy errors are computed by comparing the continuous energy with the discrete counterpart. The discrete energy for forced Lagrangian systems has terms accounting for virtual work done by the external force during the adaptive time step and hence the adaptive time step variational integrators are preserving a discrete quantity which is not analogous to the continuous time energy. Since the difference between continuous and discrete energy is orders of magnitude larger than

the discrete energy error of the variational integrator, the resulting energy error plots do not reflect the advantage of using adaptive variational integrators over fixed time step variational integrators.

Another reason behind the higher energy error for adaptive time step variational integrators is the monotonically increasing adaptive time step shown in Figure 3.15. The velocity approximation $\dot{q} \approx \frac{q_{k+1}-q_k}{h_k}$ used in computing the discrete energy becomes more inaccurate as the adaptive time step increases. As we go forward in time, the adaptive time step h_k keeps on increasing leading to higher energy error for adaptive time step variational integrators. Thus, the magnitude of energy error for adaptive time does not decrease as quickly as it does for fixed time step variational integrators.

We believe the lower order midpoint approximation used for the discrete power term in (3.65) is the reason behind monotonically increasing adaptive time step which leads to inaccurate energy behavior in Figure 3.13. The discrete power terms $g_d^{\pm}$ approximate the total work done due to time variations over an adaptive time step. Since the external forcing (3.62) is linearly proportional to the velocity $\dot{q}$, the integrand in (3.28) will be second order in $\dot{q}$. The discrete power terms $g_d^{\pm}$ in (3.65) approximate the integral by assuming the integrand value is constant over the adaptive time step and is equal to the value of the integrand at the midpoint $\frac{t_k+t_{k+1}}{2}$. For cases where the integrand is linear in $\dot{q}$, like in (3.55), the midpoint approximation works quite well yielding bounded time adaptive time steps. For the dissipative case the midpoint approximation does not capture the work done accurately resulting in increasing adaptive time step. In future, we plan to employ a higher order approximation for discrete power terms and study its effect on the adaptive time step and energy performance.

The trajectory error plots for three cases in Figure 3.14 show the superior trajectory accuracy of adaptive time step variational integrators for dissipative systems. Due to the discretization

error and changing discrete error, the increase in accuracy is not as significant as in Figure 3.3. The comparison in Figure 3.14a shows that both fixed and adaptive algorithms have almost same accuracy with adaptive method being marginally better. With increase in damping ratio, Figure 3.14b and Figure 3.14c exhibit the improved accuracy achieved by adaptive time step variational integrators. But again by the end, the accuracy of fixed time algorithm becomes similar as the adaptive time step increases.

In Figure 3.15 the adaptive time step evolution over time for all three damping parameter values is plotted. For all three cases, the adaptive time step was found to be monotonically increasing. This is not good for a numerical algorithm as eventually it would lead to numerical instability. We have also studied the damped harmonic oscillator system for negative damping parameter values and the results for those systems showed a uniformly decreasing adaptive time step. Thus, there seems to be some inverse relation between the rate of change of energy and the rate of change of the adaptive time step. Again, a higher order approximation of discrete power terms should be investigated to alleviate this adaptation.

3.5 Conclusions

We have presented adaptive time step variational integrators for time-dependent mechanical systems with forcing. We have incorporated forcing into the extended discrete mechanics framework so that the resulting discrete trajectories can be used as numerical integrators for Lagrangian systems with forcing. We first presented the Lagrange-d'Alembert principle in the extended Lagrangian mechanics framework and then derived the extended forced discrete Euler-Lagrange equations from the discrete Lagrange-d'Alembert principle. We demonstrated a general method to construct adaptive time step variational integrators for systems with time-dependent forcing through a forced harmonic oscillator example. The

results from the numerical example showed that the adaptive time step algorithm predicts the change in the energy of the nonautonomus system more accurately than the fixed time step method.

We have also presented results for a nonlinear conservative system by solving the discrete equations exactly, as opposed to the optimization approach suggested in [51]. The energy error results show the advantage of solving discrete equations exactly for adaptive time step variational integrators. We have studied the effect of initial time step on energy error and phase space trajectories and also shown how the discrete equations become more ill-conditioned as the initial time step becomes smaller.

For the damped harmonic oscillator example, contrary to expectation, the fixed time step variational integrator outperforms the adaptive time step variational integrator in energy performance. The adaptive time step for the dissipative system was found to be monotonically increasing which makes the algorithm unsuitable for long-time simulation. We believe the lower order approximation used in discrete power term is the reason behind this unexpected behavior.

Chapter 4

One-step Variational and Galerkin Methods

The purpose of this chapter is twofold. First, we derive Hermite polynomial based $\mathcal{C}^1$–continuous numerical integrators for mechanical systems from two different approaches. For the variational methods, we discretize the variational principle over a single fixed time-step and then use the discrete mechanics framework to develop variational methods. We also use Galerkin's method of weighted residuals of the governing equations over a single fixed time-step to develop one-step Galerkin methods. Second, we study the numerical performance of the developed methods for three different classes of mechanical systems. We also investigate the numerical properties such as symplecticity and energy performance for both methods.

This chapter is organized as follows. In Section 4.1, we review the basic concepts from variational integrators and Galerkin methods used later in this work. In Section 4.2 we present Hermite polynomial based one-step variational and Galerkin methods. First, we introduce cubic Hermite polynomials used for time-discretization in this work. In Section 4.2.2 we utilize the discrete mechanics approach to derive the one-step variational methods for mechanical systems with external forcing. We then use the Galerkin approach to derive one-step Galerkin methods. In Section 4.3 we study three numerical examples to understand the numerical performance of the proposed one-step methods. Finally, in Section 4.4 we provide concluding remarks and suggest future directions for this work.

4.1 Background

The numerical integration of mechanical systems can be approached in different ways. Traditional methods apply time-discretization directly to the governing equations of motion to obtain time-integration algorithms. Unfortunately, this approach does not account for the qualitative properties of the dynamical system. In this section, we review the basic concepts from variational mechanics and Galerkin methods used in the development of our one-step variational and Galerkin methods.

Consider a time-invariant Lagrangian mechanical system with a finite-dimensional, smooth configuration manifold Q, state space TQ, and Lagrangian $L : TQ \to \mathbb{R}$. For such an autonomous Lagrangian system with time-independent external forcing $\mathbf{f}_L(\mathbf{q}(t), \dot{\mathbf{q}}(t))$, the Lagrange-d'Alembert principle characterizes trajectories $\mathbf{q}(t)$ as those satisfying

$$\delta \int_{t_i}^{t_f} L(\mathbf{q}(t), \dot{\mathbf{q}}(t))\ dt + \int_{t_i}^{t_f} \mathbf{f}_L(\mathbf{q}(t), \dot{\mathbf{q}}(t)) \cdot \delta\mathbf{q}\ dt = 0 \tag{4.1}$$

where the first term considers the variation of the action integral and the second term accounts for the virtual work done by the external forces when the path $\mathbf{q}(t)$ is varied by $\delta\mathbf{q}(t)$. Using integration by parts and setting the variations at the endpoints equal to zero gives the forced Euler-Lagrange equations

$$\mathbf{M}_{\text{eq}} = \frac{\partial L(\mathbf{q}(t), \dot{\mathbf{q}}(t))}{\partial \mathbf{q}} - \frac{d}{dt}\left(\frac{\partial L(\mathbf{q}(t), \dot{\mathbf{q}}(t))}{\partial \dot{\mathbf{q}}}\right) + \mathbf{f}_L(\mathbf{q}(t), \dot{\mathbf{q}}(t)) = \mathbf{0} \tag{4.2}$$

where $\mathbf{M}_{\text{eq}}$ denotes equations of motion written in a residual form. For a general mechanical system with a separable Lagrangian of the form $L(\mathbf{q}(t), \dot{\mathbf{q}}(t)) = \frac{1}{2}\dot{\mathbf{q}}(t)^T\mathbb{M}\dot{\mathbf{q}}(t) - U(\mathbf{q})$, the

equations of motion are given by

$$\mathbf{M}_{\text{eq}} = \mathbb{M}\frac{d^2\mathbf{q}}{dt^2} + \frac{\partial U(\mathbf{q})}{\partial \mathbf{q}} - \mathbf{f}_L(\mathbf{q}(t), \dot{\mathbf{q}}(t)) = \mathbf{0} \tag{4.3}$$

where $\mathbb{M}$ is the mass matrix and $U(\mathbf{q})$ is the potential energy of the mechanical system.

Galerkin methods are a class of methods used for converting continuous differential equation problems to discrete problems. The basic idea behind these methods is to seek approximate solutions to the differential equation in a finite-dimensional space spanned by a set of basis functions, i.e. $\mathbf{q} \approx \sum_{i=1}^{N} \mathbf{q}_i \Phi_i(t)$. For a finite number of basis functions, the Galerkin methods lead to a system of equations with finite number of unknowns. Although the Galerkin methods can be used for a wide variety of computational methods, we are only interested in using ideas from Galerkin methods to develop one-step numerical integrators for mechanical systems. For an ODE written in the residual form given by $\mathbf{R}$, the Galerkin method solves the following discrete problem

$$(\mathbf{R}(\mathbf{q}), w_i) = 0, \quad i = 1, 2, ..., N \tag{4.4}$$

where $(\cdot, \cdot)$ is the inner product on the corresponding Hilbert space and w_i are different test functions. Depending on the choice of test functions, these methods can be classified into different methods such as Bubnov-Galerkin, Petrov-Galerkin, collocation methods, least squares method. For this work, we use Petrov-Galerkin method where the test functions are different from the basis functions.

4.2 One-step Time-integration Methods

The structural dynamics community has used time finite elements to derive numerical integrators from the variational principle since the late 1960s. Argryis and Scharpf [175] used cubic Hermite shape functions to formulate time finite elements and discretize Hamilton's principle to obtain numerical integrators for the initial value problems. Unlike the discrete mechanics approach, the finite elements approach only considers the variational principle over one time-step. Using Hermite polynomials for the configuration leads to $\mathcal{C}^1$–continuous trajectories. Recently, Leok and Shingel [176] used Hermite polynomials in the discrete mechanics setting to derive variational integrators that approximate time derivatives of the trajectory with accuracy. Apart from their accuracy and computational stability, discretization using Hermite polynomials also leads to numerical methods that are compliant to control analysis since they naturally yield configuration states and velocities.

4.2.1 Hermite Polynomials

We discretize the continuous trajectory over one time-step using cubic Hermite polynomials

$$\mathbf{q}(t) \approx \mathbf{q}_d(t) = \mathbf{q}_0 N_1(t) + \mathbf{v}_0 N_2(t) + \mathbf{q}_1 N_3(t) + \mathbf{v}_1 N_4(t) \tag{4.5}$$

where $\mathbf{q}_d(t)$ is the discrete approximation and the Hermite polynomials are given by

$$\begin{aligned} N_1(t) &= 2\left(\frac{t}{h}\right)^3 - 3\left(\frac{t}{h}\right)^2 + 1, & N_3(t) &= -2\left(\frac{t}{h}\right)^3 + 3\left(\frac{t}{h}\right)^2, \\ N_2(t) &= h\left[\left(\frac{t}{h}\right)^3 - 2\left(\frac{t}{h}\right)^2 + \left(\frac{t}{h}\right)\right], & N_4(t) &= h\left[\left(\frac{t}{h}\right)^3 - \left(\frac{t}{h}\right)^2\right] \end{aligned} \tag{4.6}$$

where h is the fixed time step. From the above expressions, it is clear that at initial time $t = 0$, we have $N_1(0) = 1$ along with $N_2(0) = N_3(0) = N_4(0) = 0$ which leads to $\mathbf{q}_d(0) = \mathbf{q}_0$. Similarly, we also have $\dot{\mathbf{q}}_d(0) = \mathbf{v}_0$, $\mathbf{q}_d(h) = \mathbf{q}_1$ and $\dot{\mathbf{q}}_d(h) = \mathbf{v}_1$. Using piecewise Hermite polynomials for discretization in the one-step approach leads to numerical solutions that are $\mathcal{C}^1$– continuous.

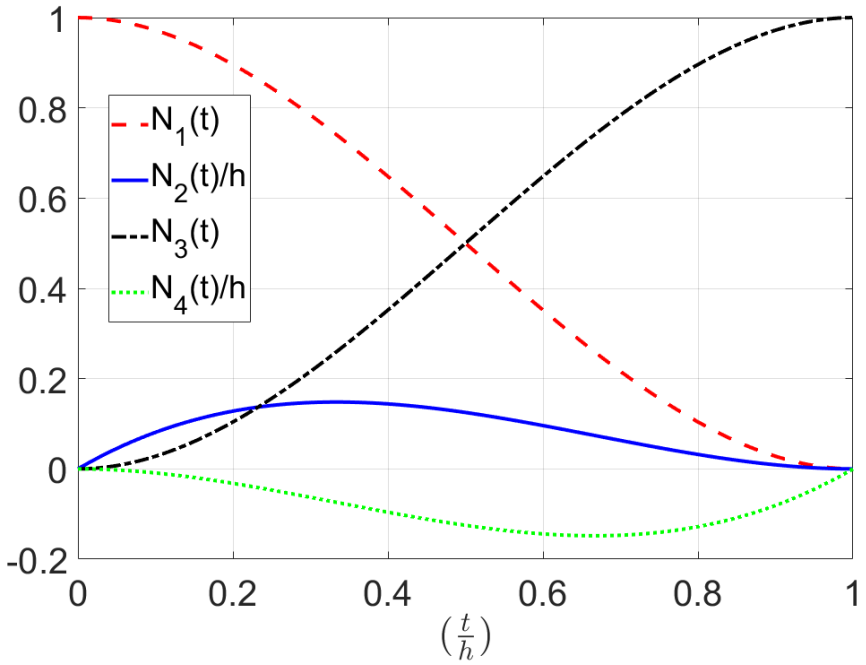

Figure 4.1: Cubic Hermite polynomials plotted over one time-step.

4.2.2 One-step Variational Methods

Unlike the discrete mechanics framework developed by Marsden *et al* [44], we only consider the variational principle over one time-step h and derive one-step numerical integrators from the discretized variational principle.

We use $\mathbf{q}_d(t)$ from (4.5) to obtain a discrete Lagrangian which approximates the action

integral in the following sense

$$L_d(\mathbf{q}_0, \mathbf{v}_0, \mathbf{q}_1, \mathbf{v}_1) = \int_0^h L(\mathbf{q}_d, \dot{\mathbf{q}}_d)\ dt \approx \int_0^h L(\mathbf{q}, \dot{\mathbf{q}})\ dt \tag{4.7}$$

Thus, we have used a cubic polynomial to obtain the discrete Lagrangian in terms of the configuration and velocity at the endpoints. We introduce discrete forces corresponding to displacement and velocity variations to approximate the virtual work

$$\begin{aligned}\int_0^h \mathbf{f}_L(\mathbf{q}(t), \dot{\mathbf{q}}(t)) \cdot \delta\mathbf{q}\ dt &\approx \int_0^h \mathbf{f}_L(\mathbf{q}_d(t), \dot{\mathbf{q}}_d(t)) \cdot \delta\mathbf{q}_d\ dt \\ &= \mathbf{f}_d^+(\mathbf{q}_0, \mathbf{v}_0, \mathbf{q}_1, \mathbf{v}_1) \cdot \delta\mathbf{q}_1 + \mathbf{f}_d^-(\mathbf{q}_0, \mathbf{v}_0, \mathbf{q}_1, \mathbf{v}_1) \cdot \delta\mathbf{q}_0 \\ &\quad + \mathbf{g}_d^+(\mathbf{q}_0, \mathbf{v}_0, \mathbf{q}_1, \mathbf{v}_1) \cdot \delta\mathbf{v}_1 + \mathbf{g}_d^-(\mathbf{q}_0, \mathbf{v}_0, \mathbf{q}_1, \mathbf{v}_1) \cdot \delta\mathbf{v}_0\end{aligned} \tag{4.8}$$

Using $\delta\mathbf{q}_d(t) = \delta\mathbf{q}_0 N_1(t) + \delta\mathbf{v}_0 N_2(t) + \delta\mathbf{q}_1 N_3(t) + \delta\mathbf{v}_1 N_4(t)$, we can obtain the discrete forces $\mathbf{f}_d^{\pm}$ corresponding to displacement variations

$$\mathbf{f}_d^+(\mathbf{q}_0, \mathbf{v}_0, \mathbf{q}_1, \mathbf{v}_1) = \int_0^h \mathbf{f}_L(\mathbf{q}_d(t), \dot{\mathbf{q}}_d(t))\ N_3(t)\ dt \tag{4.9}$$

$$\mathbf{f}_d^-(\mathbf{q}_0, \mathbf{v}_0, \mathbf{q}_1, \mathbf{v}_1) = \int_0^h \mathbf{f}_L(\mathbf{q}_d(t), \dot{\mathbf{q}}_d(t))\ N_1(t)\ dt \tag{4.10}$$

and discrete forces $\mathbf{g}_d^{\pm}$ corresponding to velocity variations

$$\mathbf{g}_d^+(\mathbf{q}_0, \mathbf{v}_0, \mathbf{q}_1, \mathbf{v}_1) = \int_0^h \mathbf{f}_L(\mathbf{q}_d(t), \dot{\mathbf{q}}_d(t))\ N_4(t)\ dt \tag{4.11}$$

$$\mathbf{g}_d^-(\mathbf{q}_0, \mathbf{v}_0, \mathbf{q}_1, \mathbf{v}_1) = \int_0^h \mathbf{f}_L(\mathbf{q}_d(t), \dot{\mathbf{q}}_d(t))\ N_2(t)\ dt \tag{4.12}$$

The discrete Lagrange-d'Alembert principle using one-step variational approach seeks curves

$\mathbf{q}_d(t) = \{\ \mathbf{q}_0, \mathbf{v}_0, \mathbf{q}_1, \mathbf{v}_1\ \}$ that satisfy

$$\delta L_d(\mathbf{q}_0, \mathbf{v}_0, \mathbf{q}_1, \mathbf{v}_1) + [\mathbf{f}_d^+(\mathbf{q}_0, \mathbf{v}_0, \mathbf{q}_1, \mathbf{v}_1) \cdot \delta\mathbf{q}_1 + \mathbf{f}_d^-(\mathbf{q}_0, \mathbf{v}_0, \mathbf{q}_1, \mathbf{v}_1) \cdot \delta\mathbf{q}_0] + [\mathbf{g}_d^+(\mathbf{q}_0, \mathbf{v}_0, \mathbf{q}_1, \mathbf{v}_1) \cdot \delta\mathbf{v}_1 + \mathbf{g}_d^-(\mathbf{q}_0, \mathbf{v}_0, \mathbf{q}_1, \mathbf{v}_1) \cdot \delta\mathbf{v}_0] = 0$$

which gives

$$\left(\frac{\partial L_d}{\partial \mathbf{q}_0} + \mathbf{f}_d^-(\mathbf{q}_0, \mathbf{v}_0, \mathbf{q}_1, \mathbf{v}_1)\right) \cdot \delta\mathbf{q}_0 + \left(\frac{\partial L_d}{\partial \mathbf{v}_0} + \mathbf{g}_d^-(\mathbf{q}_0, \mathbf{v}_0, \mathbf{q}_1, \mathbf{v}_1)\right) \cdot \delta\mathbf{v}_0 + \left(\frac{\partial L_d}{\partial \mathbf{q}_1} + \mathbf{f}_d^+(\mathbf{q}_0, \mathbf{v}_0, \mathbf{q}_1, \mathbf{v}_1)\right) \cdot \delta\mathbf{q}_1 + \left(\frac{\partial L_d}{\partial \mathbf{v}_1} + \mathbf{g}_d^+(\mathbf{q}_0, \mathbf{v}_0, \mathbf{q}_1, \mathbf{v}_1)\right) \cdot \delta\mathbf{v}_1 = 0$$

where $L_d := L_d(\mathbf{q}_0, \mathbf{v}_0, \mathbf{q}_1, \mathbf{v}_1)$. Setting variations at endpoints to zero, i.e. $\delta\mathbf{q}_0 = \delta\mathbf{q}_1 = \mathbf{0}$, gives

$$\frac{\partial L_d}{\partial \mathbf{v}_0}(\mathbf{q}_0, \mathbf{v}_0, \mathbf{q}_1, \mathbf{v}_1) + \mathbf{g}_d^-(\mathbf{q}_0, \mathbf{v}_0, \mathbf{q}_1, \mathbf{v}_1) = \mathbf{0} \tag{4.13}$$

$$\frac{\partial L_d}{\partial \mathbf{v}_1}(\mathbf{q}_0, \mathbf{v}_0, \mathbf{q}_1, \mathbf{v}_1) + \mathbf{g}_d^+(\mathbf{q}_0, \mathbf{v}_0, \mathbf{q}_1, \mathbf{v}_1) = \mathbf{0} \tag{4.14}$$

Given $(\mathbf{q}_0, \mathbf{v}_0)$, these two coupled nonlinear equations can be solved to obtain $(\mathbf{q}_1, \mathbf{v}_1)$. Thus, for Lagrangian systems with external forcing the one-step variational approach can be used to derive numerical integrators that are continuous in both configuration and velocities.

4.2.3 One-step Galerkin Methods

In this subsection, we consider the Galerkin method of weighted residuals to obtain numerical integrators for mechanical systems with external forcing. For a given system of equations we first write it in the residual form $\mathbf{R}(t, q, \frac{d\mathbf{q}}{dt}, ..., \frac{d^n\mathbf{q}}{dt^n})$ and this continuous system of ODEs

is transformed into following discrete equations

$$\left(\mathbf{R}(t, \mathbf{q}_d, \frac{d\mathbf{q}_d}{dt}, ..., \frac{d^n\mathbf{q}_d}{dt^n}), w_i\right) = 0, \quad i = 1, 2, ..., N \tag{4.15}$$

where $\mathbf{q}_d(t)$ is the assumed solution form and w_i are test functions. For our study, we focus on time-integration of mechanical problems with $\mathbf{R} = \mathbf{M}_{eq}(\mathbf{q}, \dot{\mathbf{q}}, \ddot{\mathbf{q}})$ where $\mathbf{M}_{eq}$ are the equations of motion for the mechanical system. Similar to the variational approach discussed in previous section, we use cubic Hermite polynomials as solution functions for approximating the continuous solution over one time-step. Our goal is to use the Petrov-Galerkin approach to derive one-step methods so we consider the following shifted Legendre polynomials as test functions

$$P_0(t) = 1, \quad P_1(t) = \frac{1}{h}(2t - h) \tag{4.16}$$

Given $(\mathbf{q}_0, \mathbf{v}_0)$, the one-step Galerkin method yields

$$\int_0^h \mathbf{M}_{eq}(\mathbf{q}_d)\,(1)\,dt = \mathbf{0}$$

$$\int_0^h \mathbf{M}_{eq}(\mathbf{q}_d)\left(\frac{1}{h}(2t - h)\right)dt = \mathbf{0}$$

Given $(\mathbf{q}_0, \mathbf{v}_0)$, these two coupled nonlinear equations can be solved to obtain the configuration $\mathbf{q}_1$ and velocity $\mathbf{v}_1$ at the next time-step. Just like the variational approach, this system of nonlinear equations can be used as a one-step numerical integrator.

4.2.4 Higher-order One-step Methods

In this subsection, we demonstrate how to derive one-step methods with higher-order Hermite polynomials. The one-step methods presented so far have been based on cubic Hermite polynomials which lead to numerical integrators that are continuous in both configuration and velocities. For discretization using higher-order Hermite polynomials, we consider the following discrete trajectory over one time-step

$$\mathbf{q}_d(t) = \sum_{j=0}^{n-1} \left(\mathbf{q}_0^{(j)} H_{n,j}(t) + \mathbf{q}_1^{(j)} H_{n,j}(h-t) \right) \tag{4.17}$$

where we have written the discrete trajectory in terms of Hermite basis functions and values of $\mathbf{q}(t)$ and its derivatives $\mathbf{q}^{(j)}(t)$ at endpoints. The Hermite basis functions are

$$H_{n,j}(t) = \frac{t^j}{j!} \left(1 - \frac{t}{h}\right)^n \sum_{s=0}^{n-j-1} \binom{n+s-1}{s} \left(\frac{t}{h}\right)^s \tag{4.18}$$

Thus, the discrete trajectory $\mathbf{q}_d$ is represented by $2n-1$ degree polynomial which satisfies

$$\mathbf{q}^{(j)}(0) = \mathbf{q}_d^{(j)}(0) \qquad \mathbf{q}^{(j)}(h) = \mathbf{q}_d^{(j)}(h) \qquad j = 0, ..., n-1 \tag{4.19}$$

It is clear from the above expression that for $n = 1$, the discrete trajectory simply reduces to a linear interpolant between endpoints $\mathbf{q}_0$ and $\mathbf{q}_1$. For $n = 2$, the discrete trajectory is the cubic interpolant discussed in Section 4.2.1. For discretization using higher-order Hermite polynomials with $n \geq 3$, the discrete trajectory $\mathbf{q}_d$ over the fixed time-step is represented by $2n-1$ degree polynomials with $2n$ unknown coefficients. For an initial condition of the form $(\mathbf{q}_0, \mathbf{v}_0)$, the numerical integration problem reduces to solving for the remaining $2n-2$ coefficients. The first $n-2$ coefficients are $\mathbf{q}^j(0)$ for $j = 2, \cdots, n-1$ and the other n coef-

ficients are $\mathbf{q}^j(h)$ for $j = 0, \cdots, n-1$.

Variational Approach: For conservative Lagrangian systems, the discrete Hamilton's principle after setting the configuration variations at the endpoints to zero (i.e. $\delta\mathbf{q}_0 = \delta\mathbf{q}_1 = \mathbf{0}$) leads to the following discrete equations

$$\frac{\partial L_d}{\partial \mathbf{q}^{(j)}(0)} = \frac{\partial L_d}{\partial \mathbf{q}^{(j)}(h)} = \mathbf{0} \qquad j = 1, \cdots, n-1 \tag{4.20}$$

Thus, solving these $2n-2$ coupled nonlinear equations gives the $2n-2$ coefficients and this one-step method can be seen as a numerical integrator from $(\mathbf{q}_0, \mathbf{v}_0)$ to $(\mathbf{q}_1, \mathbf{v}_1)$ with a $2n-1$ degree Hermite piecewise polynomial interpolating the configuration over every fixed time-step. This approach can be extended to Lagrangian systems with forcing by discretizing the Lagrange-d'Alembert principle.

Galerkin Approach: One-step Galerkin methods with discretization using higher-order Hermite polynomials involve the use of shifted Legendre polynomials up to order $2n-2$ as test functions. Given $(\mathbf{q}_0, \mathbf{v}_0)$, the governing discrete equations are given by

$$\int_0^h \mathbf{M}_{eq}(\mathbf{q}_d) P_j(t)\, dt = \mathbf{0} \qquad j = 0, \cdots, 2n-3 \tag{4.21}$$

where $P_j(t)$ are shifted Legendre polynomials of degree j.

4.3 Numerical Results

In this section, we consider three examples to study the numerical performance of the proposed Galerkin and variational one-step methods. We first consider a nonlinear conservative

system to demonstrate the good energy performance of the proposed methods. We also present an order analysis study to understand the convergence behavior of one-step variational and Galerkin methods. We then consider the Duffing oscillator to investigate the numerical behavior of the proposed one-step methods in the presence of dissipative forces. Finally, we consider a nonlinear aeroelastic system to study how the proposed methods perform for a coupled nonlinear dynamical system.

4.3.1 Particle in a Double-well Potential

In this subsection, we apply the proposed methods to a particle in a double-well potential with Lagrangian

$$L(q, \dot{q}) = \frac{1}{2} m \dot{q}^2 - \frac{1}{2} \left(q^4 - q^2 \right) \tag{4.22}$$

The Euler-Lagrange equation for this conservative system is given by

$$m\ddot{q} - q + 2q^3 = 0 \tag{4.23}$$

We have compared the numerical results for $m = 1$ and fixed time-step $h = 0.1$ for two initial conditions. The phase portrait comparisons in Figure 7.3 show how both variational and Galerkin methods agree with the benchmark solution for both initial conditions. The corresponding energy error plots in Figure 4.3 demonstrate the bounded energy error for both one-step methods. For both cases, the energy performance for the Galerkin method is substantially better than for the variational method. The energy error comparison in Figure 4.3a shows that the one-step variational method has energy error magnitude around 10^{-7} whereas the Galerkin method has energy error around 10^{-10}. Similarly, in Figure 4.3b the variational method has energy error magnitude around 10^{-5} and the Galerkin method has energy error around 10^{-8}.

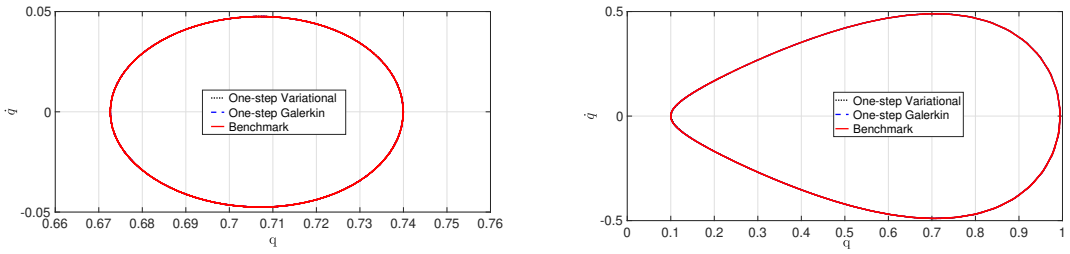

(a) $q(0) = 0.74,\ \dot{q}(0) = 0$ (b) $q(0) = 0.995,\ \dot{q}(0) = 0$

Figure 4.2: Phase space trajectory comparison for fixed time-step $h = 0.1$

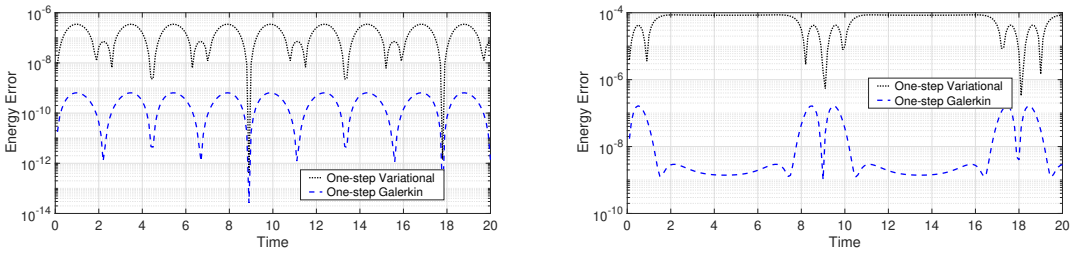

(a) $q(0) = 0.74,\ \dot{q}(0) = 0$ (b) $q(0) = 0.995,\ \dot{q}(0) = 0$

Figure 4.3: The energy error comparison for the two trajectories

In Figure 4.4, we have studied the numerical behavior of these algorithms for different fixed time-step values to understand how the configuration, velocity and energy error values decrease with decrease in the step size. We have also performed the convergence analysis for variational integrators derived from the discrete mechanics framework to understand how they compare to the proposed one-step methods. Since both one-step methods proposed in this work require the solution of two coupled nonlinear equations at each time-step, we have implemented variational integrators that require solving the same number of nonlinear equations. Thus, we have considered a quadratic trajectory over one time-step in the discrete mechanics framework by introducing an interior point and the resulting variational integrator leads to two coupled nonlinear implicit equations at each time-step.

The configuration and velocity convergence plots in Figure 4.8a and Figure 4.8b show that the one-step variational method has second order convergence whereas both the variational

integrator and the one-step Galerkin method have fourth order convergence. For the energy error, both the one-step variational and the variational integrator show second order convergence, and the one-step Galerkin method shows fourth order convergence. Thus, the one-step Galerkin approach gives better trajectory and energy performance than both the one-step variational method and the variational integrator.

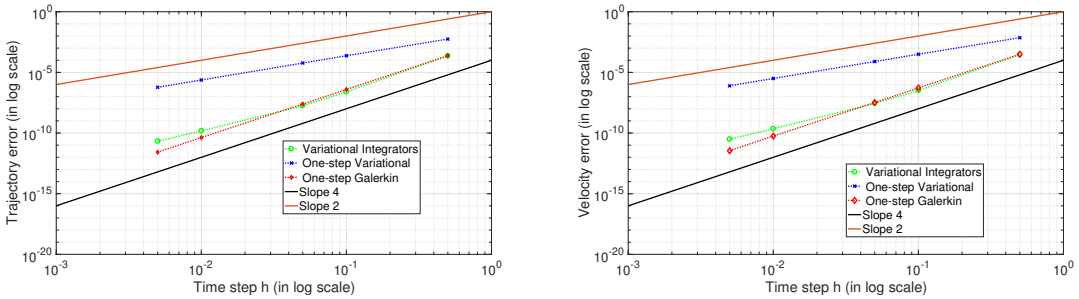

(a) Maximum trajectory error

(b) Maximum velocity error

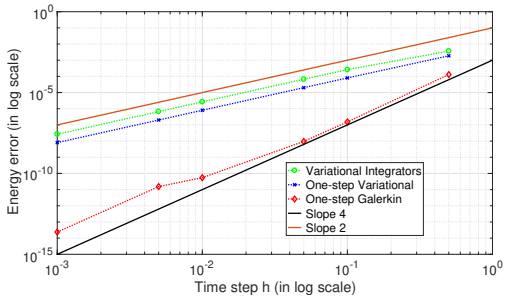

(c) Maximum energy error

Figure 4.4: Convergence analysis of temporal error in configuration, velocity and energy for the nonlinear conservative system.

4.3.2 Duffing Oscillator

In this subsection, we study the numerical performance of these algorithms in the presence of dissipation. The governing second-order, nonlinear differential equation for the Duffing oscillator is given by

$$\ddot{x} + \delta\dot{x} + \alpha x + \beta x^3 = 0 \tag{4.24}$$

where $x(t)$ is the displacement at time t, δ is the linear damping, α is the linear stiffness, and β is the nonlinear stiffness coefficient. The Lagrangian and external forcing for this system are given by

$$L(x, \dot{x}) = \frac{1}{2}\dot{x}^2 - \frac{1}{2}\alpha x^2 - \frac{1}{4}\beta x^4, \qquad f(\dot{x}, t) = -\delta \dot{x} \tag{4.25}$$

We have fixed the stiffness parameters to $\alpha = 1$ and $\beta = 0.5$ and studied this dissipative nonlinear dynamical system for three cases, i.e. $\delta = 0.025, 0.05, 0.1$. With these specific parameter values, the Duffing oscillator can be thought of as the double-well potential system with dissipation. The numerically computed trajectories from both one-step methods are compared with the benchmark solution in Figure 4.5. The plots in Figure 4.5 demonstrate that both methods are able to capture the dissipation effect accurately. In fact, the discrete trajectories are indistinguishable from the benchmark solution for all three cases.

The energy error plots in Figure 4.6 compare the energy performance for both one-step methods and the Galerkin approach outperforms the variational approach in all three cases. For all three cases, the energy error for the one-step variational method starts around 10^{-4} whereas the one-step Galerkin methods exhibit energy error around 10^{-6}. The energy error for both methods decreases over the time due to the presence of dissipative forces and the rate of decrease in energy error increases with increase in the value of the damping parameter δ. This decrease in energy error is seen clearly in Figure 4.6b and Figure 4.6c for higher δ values.

4.3.3 Aeroelastic System

In this subsection, we consider open-loop behavior of the nonlinear aeroelastic system studied by Shukla and Patil [177]. As shown in Figure 4.7, the model contains a flat plate supported by a linear spring in the plunge degree of freedom and cubic nonlinear spring in the pitch

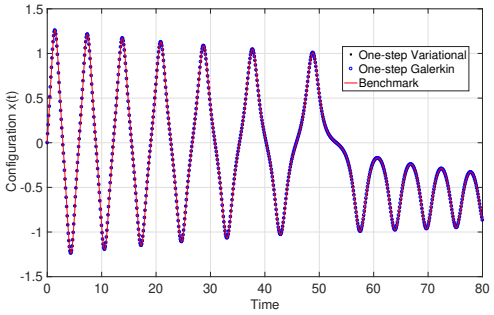

(a) $\delta = 0.025$

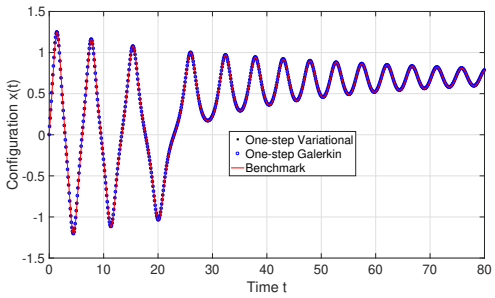

(b) $\delta = 0.05$

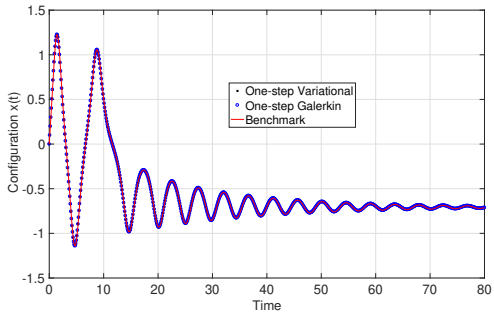

(c) $\delta = 0.1$

Figure 4.5: Duffing oscillator numerical simulation with $\alpha = -1, \beta = 2$ time-step $h = 0.1$

degree of freedom. The flat plate is free to move up and down along the plunge degree of freedom and rotate about the pitch degree of freedom. The Lagrangian for this system is given by

$$L(h, \dot{h}, \alpha, \dot{\alpha}) = m_T \dot{h}^2 + I_\alpha \dot{\alpha}^2 + m_W x_\alpha \dot{h}\dot{\alpha} - \frac{1}{2}k_h h^2 - \frac{1}{2}k_{\alpha_0}\alpha^2 - \frac{1}{3}k_{\alpha_1}\alpha^3 - \frac{1}{4}k_{\alpha_2}\alpha^4 \tag{4.26}$$

where m_W is the mass of the wing and m_T is the total mass of the aeroelastic system. I_α represents the moment of inertia about the elastic axis. The terms k_h and $k_{\alpha_{\{0,1,2\}}}$ are the stiffness functions along the plunge and pitch degrees of freedom respectively. The external nonconservative forces are given by

$$f_h = -c_h \dot{h} + \rho U^2 b C_{L_\alpha} \alpha_{eff} \tag{4.27}$$

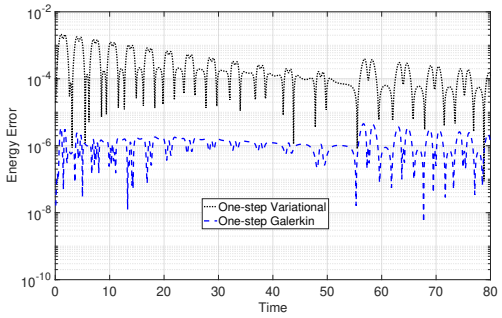

(a) $\delta = 0.025$

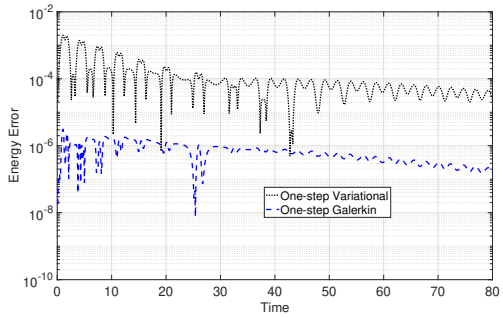

(b) $\delta = 0.05$

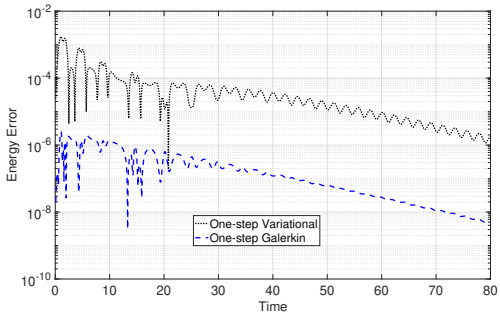

(c) $\delta = 0.1$

Figure 4.6: Duffing oscillator numerical simulation with $\alpha = -1, \beta = 2$ time-step $h = 0.1$

$$f_\alpha = -c_\alpha \dot{\alpha} + \rho U^2 b^2 C_{M_\alpha} \alpha_{eff} \tag{4.28}$$

where c_h and c_α are damping coefficients, C_{L_α} and C_{M_α} are the derivatives of the lift and moment coefficients, and $\alpha_{eff} = \left(\alpha + \frac{\dot{h}}{U} + \left(\frac{1}{2} - a\right) b \frac{\dot{\alpha}}{U}\right)$ is the effective angle of attack. The equations of motion for this aeroelastic system are given by

$$m_T \ddot{h} + m_W x_\alpha b \ddot{\alpha} + c_h \dot{h} + k_h h - \rho U^2 b C_{L_\alpha} \alpha_{eff} = 0 \tag{4.29}$$

$$I_\alpha \ddot{\alpha} + m_W x_\alpha b \ddot{h} + c_\alpha \dot{\alpha} + k_\alpha(\alpha)\alpha + \rho U^2 b^2 C_{M_\alpha} \alpha_{eff} = 0 \tag{4.30}$$

where $k(\alpha) = k_{\alpha_0} + k_{\alpha_1}\alpha + k_{\alpha_2}\alpha^2$.

We have studied the dynamic behavior of the nonlinear aeroelastic system for initial conditions $(h_0, \dot{h}_0, \alpha_0, \dot{\alpha}_0) = (0.01, 0, 0.1, 0)$ at freestream velocity $U = 0.9U_f$ where U_f is the

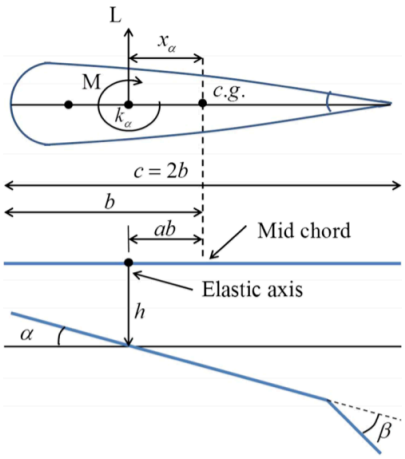

Figure 4.7: Sketch of a two degrees of freedom aeroelastic section model

linear flutter velocity. The phase space plots given in Figure 4.8 clearly demonstrate how both one-step methods capture the subcritical limit cycle oscillations (LCOs) accurately.

The energy plot in Figure 4.9 shows how the total energy of the aeroelastic system evolves over time. Initially there is a sharp decrease in energy followed by an increase, and eventually when the system exhibits periodic motion with constant amplitude the total energy oscillates around a fixed value. As shown in Figure 4.9, both one-step methods track the change in energy accurately for the nonlinear aeroelastic system. The energy error comparison in Figure 4.10 demonstrates how the Galerkin approach has better energy behavior than the one-step variational approach. The one-step variational method has energy error magnitude around 10^{-4} whereas the Galerkin method has energy error around 10^{-6}.

4.3.4 Symplectic Nature

As mentioned in Section 4.2.2, the variational approach to one-step methods only considers the action integral over one time-step whereas the variational integrators consider the action integral over a finite number of fixed time-steps. We know that variational integrators

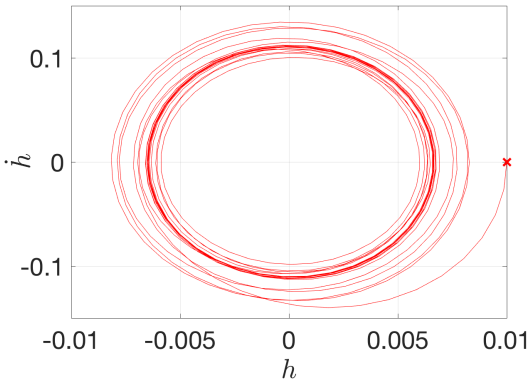

(a) Plunge response (One-step Galerkin)

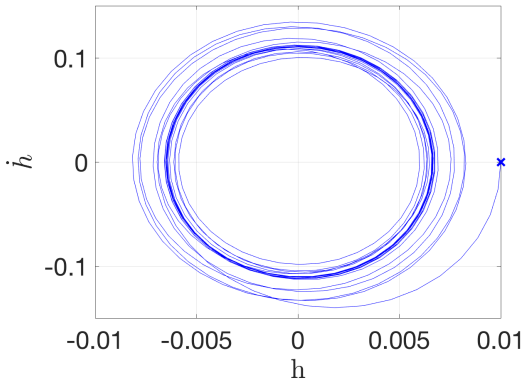

(b) Plunge response (One-step variational)

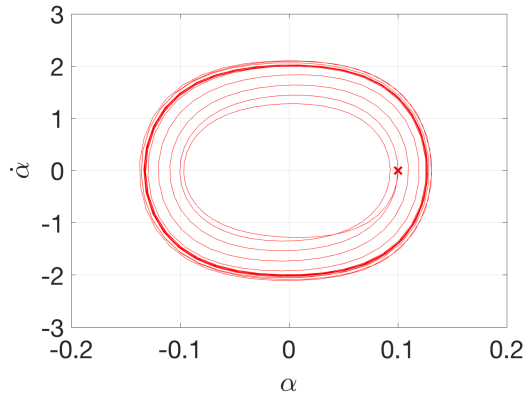

(c) Pitch response (One-step Galerkin)

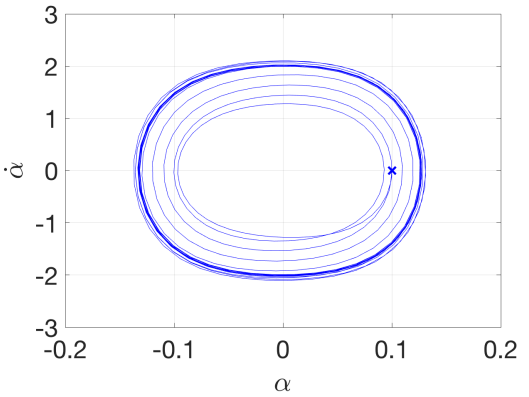

(d) Pitch response (One-step variational)

Figure 4.8: Subcritical LCO simulation using proposed one-step methods

derived from the latter approach yield numerical algorithms that automatically preserve the canonical symplectic form. For a Hamiltonian system with Hamiltonian $H(\mathbf{p}, \mathbf{q})$, the symplectic flow map $\phi_t(\mathbf{p}_0, \mathbf{q}_0) = (\mathbf{p}(t), \mathbf{q}(t))$ satisfies the following condition

$$\left(\frac{\partial \phi_t}{\partial \mathbf{y}_0}\right)^T J \left(\frac{\partial \phi_t}{\partial \mathbf{y}_0}\right) = J \tag{4.31}$$

where $\mathbf{y}_0 = (\mathbf{p}_0, \mathbf{q}_0)$ and $J = \begin{bmatrix} 0 & I \\ -I & 0 \end{bmatrix}$ is the symplectic matrix. Similar to this condition, a given one-step method $\phi_h : (\mathbf{p}_k, \mathbf{q}_k) \to (\mathbf{p}_{k+1}, \mathbf{q}_{k+1})$ is symplectic if it satisfies

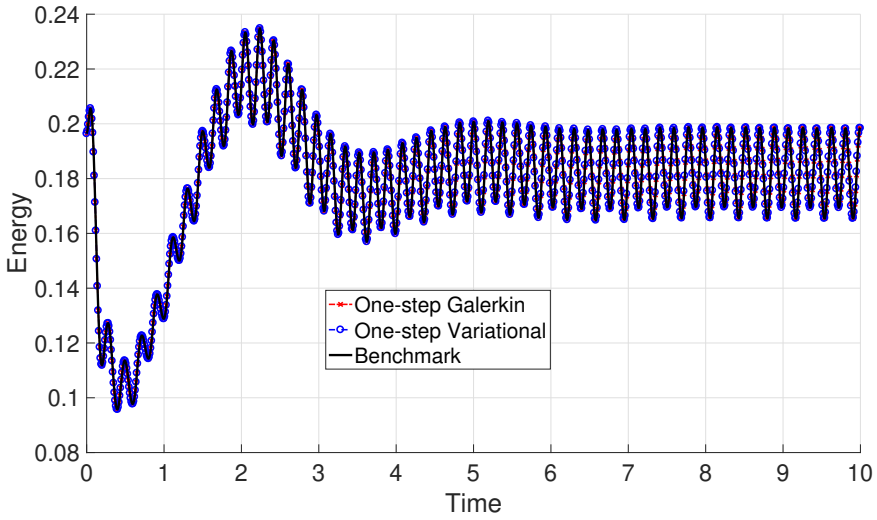

Figure 4.9: Total energy of the aeroelastic system

$\left(\frac{\partial \phi_h}{\partial \mathbf{y}_k}\right)^T J \left(\frac{\partial \phi_h}{\partial \mathbf{y}_k}\right) = J$ for $\mathbf{y}_k = (\mathbf{p}_k, \mathbf{q}_k)$. The key step in this process is to compute the following Jacobian matrix

$$\frac{\partial \phi_h}{\partial \mathbf{y}_k} = \begin{bmatrix} \frac{\partial \mathbf{p}_{k+1}(\mathbf{p}_k,\mathbf{q}_k)}{\partial \mathbf{p}_k} & \frac{\partial \mathbf{p}_{k+1}(\mathbf{p}_k,\mathbf{q}_k)}{\partial \mathbf{q}_k} \\ \frac{\partial \mathbf{q}_{k+1}(\mathbf{p}_k,\mathbf{q}_k)}{\partial \mathbf{p}_k} & \frac{\partial \mathbf{q}_{k+1}(\mathbf{p}_k,\mathbf{q}_k)}{\partial \mathbf{q}_k} \end{bmatrix} \tag{4.32}$$

Since both proposed methods are generally implicit, the computation for the Jacobian matrix involves differentiating the governing discrete equations and then solving a system of linear equations for the entries in the Jacobian matrix. We study the symplectic nature of the one-step algorithms for both linear and nonlinear conservative systems. It is important to note that the one-step methods developed in this chapter are formulated on the state space. In order to check the condition for symplecticity, we need to define $\mathbf{p}_k = m\mathbf{v}_k$ to write these algorithms on phase space. Instead of writing the algorithms on phase space, we pick $m = 1$ to simplify the expressions.

First, we check the condition for the simple harmonic oscillator with $L(q, \dot{q}) = \frac{1}{2}\dot{q}^2 - \frac{1}{2}q^2$

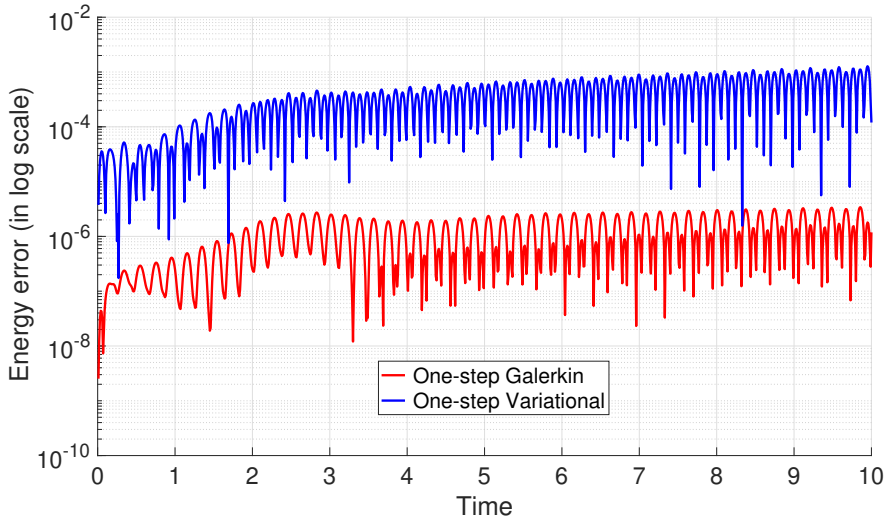

Figure 4.10: Energy error comparison between one-step Galerkin and variational methods

where $q(t)$ is the displacement. For a fixed time-step h, the Jacobians for one-step methods are given by

$$\frac{\partial \phi_{h,V}}{\partial \mathbf{y}_k} = \begin{bmatrix} \frac{(44h^5+143h^4-700h^3+189h^2+1176h-882)}{(7h(h^4+9h^2+210))} & \frac{(8h^5+33h^4-224h^3-217h^2+1568h+294)}{(7(h^4+9h^2+210))} \\ \frac{-(66h^5+169h^4-434h^3+1092h^2+588h+1764)}{(14h(h^4+9h^2+210))} & \frac{-(12h^5+39h^4-224h^3-56h^2+784h-588)}{(14h(h^4+9h^2+210))} \end{bmatrix}$$

$$\frac{\partial \phi_{h,G}}{\partial \mathbf{y}_k} = \begin{bmatrix} \frac{-(2(-h^4+30h^2+22h^2-120))}{h^4+16h^2+240} & \frac{(h(h^4-60h^2-72h^2+720+720))}{6(h^4+16h^2+240)} \\ \frac{-(h(h^4-60h^2-70h^2+600+600))}{5(h^4+16h^2+240)} & \frac{-(h^6-120h^4-120h^4+2640h^2+3600h^2-14400)}{60(h^4+16h^2+240)} \end{bmatrix}$$

For this linear dynamical system, Jacobians from both variational and Galerkin one-step methods satisfy the condition for symplecticity. For a general mechanical system with a nonlinear potential energy $U(q)$ and Lagrangian $L = \frac{1}{2}m\dot{q}^2 - U(q)$, we find that none of the one-step methods satisfy the required condition for symplecticity. It is important to note that the above condition is only to check whether the algorithms preserve the canonical symplectic form. In fact, at present, one can only check whether a given integration scheme exhibits a specific symplectic structure; one cannot determine whether any such symplectic structure

exists, in general. In the past, some of the well-known methods such as Newmark methods have been shown to preserve a noncanonical symplectic form via nonlinear transformations but it is not generally known how to test for the existence of a noncanonical symplectic form for a given algorithm.

4.4 Conclusions

In this chapter we have developed Hermite polynomial based one-step variational and Galerkin methods for mechanical systems with external forcing. We have utilized cubic Hermite polynomials over one time-step for discretization and the resulting numerical algorithms are continuous in both configuration and velocity. We showed that both one-step methods are symplectic for linear dynamical systems but they do not preserve the canonical symplectic form for general nonlinear dynamical systems. We also demonstrated an approach to obtain one-step methods using higher-order Hermite polynomials.

We have studied the numerical behavior of these algorithms through three different numerical examples. The energy performance and convergence analysis results for the conservative example showed how both one-step methods achieve superior numerical performance by obtaining $\mathcal{C}^1$–continuous trajectories. We have also presented results for a dissipative system and the numerical plots show that both one-step methods capture the effect of the dissipative forces accurately over exponentially long time intervals. Finally, numerical studies for the coupled aeroelastic system show how both one-step methods capture the limit cycle oscillations accurately. The numerical results from all three examples showed that the Galerkin approach has significantly better energy behavior. We believe the discrete equation corresponding to the constant test function is the reason behind the superior energy performance of the Galerkin method.

In future work, we would like to investigate the connection between the one-step Galerkin methods and energy-momentum integrators. It would also be desirable to apply these one-step methods to discretizations of infinite-dimensional systems.

Chapter 5

Energy-preserving Lie Group Variational Integrators on SO(3)

The goal of this chapter is to develop energy-preserving Lie group variational integrators for attitude dynamics of a rigid body. First, we derive the equations of motion for a rigid body and then use the extended discrete mechanics framework to construct energy-preserving adaptive time step Lie group variational integrators. This integrator is used to study the dynamics of a 3D pendulum under the influence of gravity and illustrate the advantages of using adaptive time-stepping in Lie group variational integrators.

This chapter is organized as follows. In Section 5.1, we utilize concepts from extended Lagrangian mechanics to derive continuous-time equations of motion for rigid body attitude dynamics. In Section 5.2 we derive energy-preserving, adaptive time step Lie group variational integrator. In Section 5.3 we study the dynamics of an uncontrolled 3D pendulum moving under the effect of gravity. Finally, in Section 5.4 we provide concluding remarks for this work.

5.1 Extended Lagrangian Mechanics on SO(3)

We consider attitude dynamics of a rigid body in presence of attitude dependent potential. We derive the governing equations from Hamilton's principle for a rigid body system with

the following Lagrangian

$$L(R,\omega) = \frac{1}{2}\omega^T J\omega - U(R) = \frac{1}{2}tr\left[S(\omega)J_d S(\omega)^T\right] - U(R), \tag{5.1}$$

where $J_d = \frac{1}{2}\text{tr}[J]I_{3\times 3} - J$ and $S(\cdot) : \mathbb{R}^3 \to \mathbb{R}^{3\times 3}$ maps a vector to a skew-symmetric matrix such that $S(x)y = x \times y$ for $x, y \in \mathbb{R}^3$.

For a Lagrangian system evolving on $Q = \mathsf{SO(3)}$ and time space $\mathbb{R}$, the extended configuration manifold is $\bar{Q} = \mathbb{R} \times \mathsf{SO(3)}$. In the extended Lagrangian mechanics framework, the state space $T\bar{Q} = \mathbb{R} \times T\mathsf{SO(3)}$ is represented by time t, rotation matrix R and angular velocity ω. These three variables are parametrized by an independent variable a. For a given path $c(a)$, the initial time is $t_0 = t(a_0)$ and the final time is $t_f = t(a_f)$. The extended action $\bar{\mathfrak{B}}$ is

$$\bar{\mathfrak{B}} = \int_{t_0}^{t_f} L(t,R,\omega)dt = \int_{a_0}^{a_f} L(t(a),R(a),\omega(a))\ t'(a)\ da, \tag{5.2}$$

where $t'(a) = \frac{dt(a)}{da}$ denotes the derivative with respect to independent variable a. For deriving governing equations we consider the following variation

$$R^\epsilon(a) = R(a)e^{\epsilon\eta(a)}, \qquad t^\epsilon(a) = t(a) + \epsilon\delta t(a), \tag{5.3}$$

where $\epsilon \in \mathbb{R}$ and $\eta(a) \in \mathfrak{so}(3)$ defines a variation in the Lie algebra of skew symmetric rotation matrices that vanishes at the endpoints. Hence,

$$\delta R = \left.\frac{dR^\epsilon}{d\epsilon}\right|_{\epsilon=0} = R(a)\eta(a). \tag{5.4}$$

Using the kinematic relationship $\dot{R}(a) = R(a)S(\omega)$ the variation of the angular velocity ω^ϵ

can be computed by

$$S(\omega^\epsilon) = R^{\epsilon^T}(a)\dot{R}^\epsilon(a) = R^{\epsilon^T}(a)\left(\frac{R^{\epsilon'}(a)}{t^{\epsilon'}(a)}\right) \\ = e^{-\epsilon\eta(a)}R^T(a)\left(\frac{R'(a)e^{\epsilon\eta(a)} + \epsilon R(a)e^{\epsilon\eta(a)}\eta'(a)}{t'(a)+\epsilon\delta t'(a)}\right), \quad (5.5)$$

which after neglecting second order terms simplifies to

$$S(\omega^\epsilon) = \frac{e^{-\epsilon\eta(a)}S(\omega)e^{\epsilon\eta(a)} + \epsilon\eta'(a)}{t'(a)+\epsilon\delta t'(a)} \\ = \left(1-\epsilon\frac{\delta t'(a)}{t'(a)}\right)\left(S(\omega)+\epsilon(\dot{\eta}+S(\omega)\eta-\eta S(\omega))\right). \quad (5.6)$$

Thus, we have

$$S(\omega^\epsilon) = S(\omega) + \epsilon\left(\dot{\eta}+S(\omega)\eta-\eta S(\omega)-S(\omega)\frac{\delta t'(a)}{t'(a)}\right). \quad (5.7)$$

From Hamilton's principle we know that variation of the action integral is zero, i.e. $\delta\bar{\mathfrak{B}} = 0$. Taking variation of (5.2) yields

$$\delta\bar{\mathfrak{B}} = \int_{a_0}^{a_f}\frac{1}{2}\mathrm{tr}\left[-\dot{\eta}S(J\omega)+\eta S(\omega\times J\omega)\right]t'(a)da \\ + \int_{a_0}^{a_f}\left(\left(\frac{1}{2}\omega^T J\omega - U(R)\right) - \mathrm{tr}\left[S(\omega)J_d S(\omega)^T\right]\right)\delta t'(a)\ da \\ + \int_{a_0}^{a_f}\mathrm{tr}\left[\eta R^T\frac{\partial U}{\partial R}\right]t'(a)da, \quad (5.8)$$

which after setting variations at endpoints to zero yields

$$\delta\bar{\mathfrak{B}} = \int_{t_0}^{t_f} \frac{1}{2}\mathrm{tr}\left[\eta\left(S(J\dot{\omega}+\omega\times J\omega)+2R^T\frac{\partial U}{\partial R}\right)\right]\,dt + \int_{t_0}^{t_f}\left[\frac{d}{dt}\left(\omega^T J\omega-\left(\frac{1}{2}\omega^T J\omega-U(R)\right)\right)\right]\delta t\,dt, \quad (5.9)$$

and gives the following governing equations. The first is the equation of motion for a rigid body evolving on SO(3) in Lagrangian form

$$J\dot{\omega}+\omega\times J\omega = \frac{\partial U^T}{\partial R}R - R^T\frac{\partial U}{\partial R}, \quad (5.10)$$

which is the same as the equation obtained using the classical Lagrangian mechanics framework. The second equation is

$$\frac{d}{dt}\left(\frac{1}{2}\omega^T J\omega+U(R)\right)=0, \quad (5.11)$$

which indicates that the total energy of the rigid body system is a constant.

5.2 Adaptive Variational Integrator

Adaptive time step Lie group variational integrators are obtained by discretizing Hamilton's principle in the extended phase space. In this section extended discrete equations of motion for a rigid body are derived using ideas from extended discrete mechanics and Lie group methods.

5.2.1 Extended Discrete Lagrangian Mechanics on SO(3)

In the extended discrete Lagrangian mechanics framework time t_k is treated as a discrete dynamic variable. For the extended discrete mechanics of the rigid body, let $R_k \in \mathsf{SO(3)}$ denote the attitude of the rigid body at time t_k. We define $F_k \in \mathsf{SO(3)}$ such that $R_{k+1} = R_k F_k$. Using the kinematic relationship $\dot{R} = RS(\omega)$ we approximate $S(\omega_k)$ by

$$S(\omega_k) = R_k^T \dot{R}_k \approx R_k^T \left(\frac{R_{k+1} - R_k}{t_{k+1} - t_k} \right) = \frac{1}{h_k}(F_k - I_{3\times 3}), \tag{5.12}$$

where $h_k = t_{k+1} - t_k$ is the k^{th} adaptive time step.

We discretize the continuous time action integral (5.2) using the extended discrete action

$$\bar{\mathfrak{B}}_d = \sum_{k=0}^{N-1} L_d(t_k, R_k, t_{k+1}, R_{k+1}), \tag{5.13}$$

where $L_d : \bar{Q} \times \bar{Q} \to \mathbb{R}$ is the extended discrete Lagrangian function which approximates the action integral between two successive configurations. For the rigid body system we consider the extended discrete Lagrangian L_d

$$\begin{aligned} L_d(t_k, R_k, t_{k+1}, R_{k+1}) &\simeq h_k \left(\frac{L(t_k, R_k, \omega_k) + L(t_{k+1}, R_{k+1}, \omega_k)}{2} \right) \\ &= \frac{1}{h_k} tr\left[(I_{3\times 3} - F_k) J_d \right] - \frac{h_k}{2} U(R_k) - \frac{h_k}{2} U(R_{k+1}). \end{aligned} \tag{5.14}$$

Just like the continuous case, the variations in R_k and t_k can be expressed as follows

$$R_k^\epsilon = R_k e^{\epsilon \eta_k}, \qquad t_k^\epsilon = t_k + \epsilon \delta t_k. \tag{5.15}$$

From $F_k = R_k^T R_{k+1}$ and $h_k = t_{k+1} - t_k$, F_k^ϵ and h_k^ϵ are

$$F_k^\epsilon = R_k^{\epsilon T} R_{k+1}^\epsilon = e^{-\epsilon\eta_k} F_k e^{\epsilon\eta_{k+1}}, \quad h_k^\epsilon = h_k + \epsilon(\delta t_{k+1} - \delta t_k). \tag{5.16}$$

Using above expressions we can write

$$\begin{aligned}\bar{\mathfrak{B}}_d^\epsilon = \sum_{k=0}^{N-1} \frac{1}{h_k^\epsilon} tr\left[(I_{3\times 3} - e^{-\epsilon\eta_k} F_k e^{\epsilon\eta_{k+1}}) J_d\right] \\ - \sum_{k=0}^{N-1} \left\{ \frac{h_k^\epsilon}{2} U(R_k e^{\epsilon\eta_k}) + \frac{h_k^\epsilon}{2} U(R_{k+1} e^{\epsilon\eta_{k+1}}) \right\}.\end{aligned} \tag{5.17}$$

Taking variations of the extended discrete action gives

$$\begin{aligned}\delta\bar{\mathfrak{B}}_d = &\sum_{k=0}^{N-1} \frac{1}{h_k} tr\left[(\eta_k F_k - F_k \eta_{k+1}) J_d\right] \\ &+ \sum_{k=0}^{N-1} \frac{h_k}{2} tr\left[\eta_k R_k^T \frac{\partial U}{\partial R_k} + \eta_{k+1} R_{k+1}^T \frac{\partial U}{\partial R_{k+1}}\right] \\ &- \sum_{k=0}^{N-1} \frac{(\delta t_{k+1} - \delta t_k)}{h_k^2} tr\left[(I_{3\times 3} - F_k) J_d\right] \\ &- \sum_{k=0}^{N-1} \delta t_{k+1} \frac{U(R_k) + U(R_{k+1})}{2} + \sum_{k=0}^{N-1} \delta t_k \frac{U(R_k) + U(R_{k+1})}{2}.\end{aligned} \tag{5.18}$$

Applying discrete Hamilton's principle, i.e. $\delta\bar{\mathfrak{B}}_d = 0$ and setting variations at end points to zero gives

$$\begin{aligned}&\sum_{k=1}^{N-1} \mathrm{tr}\left[\eta_k \left\{ \frac{1}{h_k} F_k J_d - \frac{1}{h_{k-1}} J_d F_{k-1} + \frac{h_k + h_{k-1}}{2} R_k^T \frac{\partial U}{\partial R_k} \right\}\right] \\ &\quad + \sum_{k=1}^{N-1} \left[\frac{1}{h_k^2} tr\left[(I_{3\times 3} - F_k) J_d\right] + \frac{U(R_{k+1}) + U(R_k)}{2} \right] \delta t_k \\ &- \left[\frac{1}{h_{k-1}^2} tr\left[(I_{3\times 3} - F_{k-1}) J_d\right] + \frac{U(R_k) + U(R_{k-1})}{2} \right] \delta t_k = 0,\end{aligned} \tag{5.19}$$

which lead to the extended discrete equations of motion for the rigid body system evolving on $\mathsf{SO(3)}$ in Lagrangian form:

$$\frac{1}{h_k}\left(F_k J_d - J_d F_k^T\right) - \frac{1}{h_{k-1}}\left(J_d F_{k-1} - F_{k-1}^T J_d\right) = \frac{h_k + h_{k-1}}{2}\left(\frac{\partial U}{\partial R_k}^T R_k - R_k^T \frac{\partial U}{\partial R_k}\right), \quad (5.20)$$

$$\frac{1}{h_k^2} tr\left[(I_{3\times 3} - F_k)J_d\right] + \frac{U(R_{k+1}) + U(R_k)}{2} = \frac{1}{h_{k-1}^2} tr\left[(I_{3\times 3} - F_{k-1})J_d\right] + \frac{U(R_k) + U(R_{k-1})}{2}, \quad (5.21)$$

$$R_{k+1} = R_k F_k. \quad (5.22)$$

Given $(h_{k-1}, R_{k-1}, F_{k-1}, R_k)$, the extended discrete equations of motion can be solved to obtain F_k, R_{k+1} and h_k. This extended discrete Lagrangian system can be seen as a numerical integrator of the continuous time rigid body system on $\mathsf{SO(3)}$ with adaptive time steps.

In the extended discrete mechanics framework, we define the discrete momentum Π_k by

$$\Pi_k = D_4 L_d(t_{k-1}, R_{k-1}, t_k, R_k), \quad (5.23)$$

where D_i denotes differentiation with respect to the i^{th} argument of the discrete Lagrangian L_d . We also introduce the discrete energy

$$E_k = D_3 L_d(t_{k-1}, R_{k-1}, t_k, R_k). \quad (5.24)$$

Using the discrete momentum and discrete energy definitions, we can re-write the extended

discrete equations of motion (5.20) and (5.21) in the Hamiltonian form as

$$F_k J_d - J_d F_k^T = h_k S(\Pi_k + \frac{h_k}{2} M_k), \tag{5.25}$$

$$\frac{1}{h_k^2}\text{tr}\left[(I_{3\times 3} - F_k)J_d\right] + \frac{U(R_{k+1}) + U(R_k)}{2} = E_k, \tag{5.26}$$

$$R_{k+1} = R_k F_k, \tag{5.27}$$

$$\Pi_{k+1} = F_k^T \Pi_k + \frac{h_k}{2} F_k^T M_k + \frac{h_k}{2} M_{k+1}, \tag{5.28}$$

$$E_{k+1} = \frac{1}{h_k^2}\text{tr}\left[(I_{3\times 3} - F_k)J_d\right] + \frac{U(R_{k+1}) + U(R_k)}{2}, \tag{5.29}$$

where $M_k \in \mathbb{R}^3$ is defined such that $S(M_k) = \frac{\partial U}{\partial R_k}^T R_k - R_k^T \frac{\partial U}{\partial R_k}$. Given (Π_k, R_k, E_k), the coupled nonlinear equations (5.25),(5.26) and (5.27) are solved implicitly to obtain F_k,R_{k+1} and h_k. The configuration F_k and R_{k+1} along with the time step h_k are then used in (5.28) and (5.29) to obtain (Π_{k+1}, E_{k+1}) explicitly.

5.2.2 Properties of Adaptive Lie Group Variational Integrator

Due to the variational nature of their derivation, adaptive time step variational integrators have been shown to preserve the extended symplectic form and extended discrete Noether's theorem [44]. By choosing an extended discrete Lagrangian (5.14) that inherits all the symmetries of the continuous Lagrangian, all the conserved momenta of the continuous time dynamics are preserved in the discrete dynamics. In fact, since our rigid body system is an autonomous Lagrangian system, the time-symmetry of the discrete Lagrangian leads to conservation of discrete energy (5.24).

At every time step, the rotation matrix R_k is updated by $R_{k+1} = R_k F_k$ where we have defined $F_k \in \mathsf{SO(3)}$. Since the Lie group $\mathsf{SO(3)}$ is closed under matrix multiplication, the updated matrix R_{k+1} remains on $\mathsf{SO(3)}$. Thus, the adaptive time step Lie group variational

integrator (5.25)-(5.29) preserves symplectic form, energy and momentum and also preserves the geometric features of configuration space.

5.2.3 Computational Approach

It is important to note that unlike the fixed time step case the governing discrete nonlinear equations are coupled in F_k and t_{k+1}. Instead of solving both equations simultaneously, we take the sequential approach of first solving the discrete momentum equation (5.25) followed by solving the discrete energy equation (5.26). In order to make sure F_k obtained from the discrete momentum equation lies on $\mathsf{SO(3)}$, we use the Cayley transformation to transform the matrix equation to an equivalent vector equation. The implicit equation (5.25) has the following structure

$$F_k^{(i)} J_d - J_d (F_k^{(i)})^T = S(g_k^{(i)}), \tag{5.30}$$

where $g_k^{(i)} = \Pi_k + \frac{h_k^{(i)}}{2} M_k \in \mathbb{R}^3$ with $(F_k^{(i)}, h_k^{(i)})$ being the solution after i^{th} sequential iteration. We express $F_k^{(i)}$ in terms of a vector $f_k^{(i)}$ using the Cayley transformation

$$F_k^{(i)} = \left(I_{3\times 3} + S(f_k^{(i)}) \right) \left(I_{3\times 3} - S(f_k^{(i)}) \right)^{-1}, \tag{5.31}$$

which transforms the discrete momentum equation to the following vector equation

$$G_{Cay}(f_k^{(i)}) = g_k^{(i)} + g_k^{(i)} \times f_k^{(i)} + ((g_k^{(i)})^T f_k^{(i)}) f_k^{(i)} - 2J f_k^{(i)} = 0. \tag{5.32}$$

The above equation is solved using the Newton method

$$f_{k_{j+1}}^{(i)} = f_{k_j}^{(i)} - \nabla G_{Cay}(f_{k_j}^{(i)})^{-1} G_{Cay}(f_{k_j}^{(i)}), \tag{5.33}$$

where

$$\nabla G_{Cay}(f_{k_j}^{(i)}) = S(g_k^{(i)}) - 2J + ((g_k^{(i)})^T f_k^{(i)}) I_{3\times 3} + (f_k^{(i)}(g_k^{(i)})^T). \tag{5.34}$$

The solution obtained from Newton method is then used to solve (5.26) for $h_k^{(i)}$ using

$$h_k^{(i)} = \sqrt{\frac{tr\left[(I_{3\times 3} - F_k^{(i)})J_d\right]}{E_k - \left(\frac{U(R_{k+1}^{(i)}) + U(R_k)}{2}\right)}}, \tag{5.35}$$

where $F_k^{(i)}$ is the F_k solution obtained after i^{th} sequential iteration and $R_{k+1}^{(i)} = R_k F_k^{(i)}$.

5.3 Numerical Example of a 3D Pendulum

We apply the adaptive time step Lie group variational integrator developed in this chapter to study the dynamics of an uncontrolled 3D pendulum, a rigid asymmetric body supported by a frictionless pivot acting under the influence of gravity [100]. The potential due to the gravitational force, acting in the vertical or e_3 direction, is given by

$$U = -mge_3^T R\rho, \tag{5.36}$$

where $\rho \in \mathbb{R}^3$ is the vector from the pivot to the center of mass of the body expressed in the body fixed frame.

5.3.1 Adaptive Variational Integrator

For the motion of 3D pendulum under the influence of gravity, the governing discrete equations are given by

$$F_k J_d - J_d F_k^T = h_k S(\Pi_k) + \frac{h_k^2}{2} mg \left(R_k^T e_3 \rho^T - \rho e_3^T R_k \right), \tag{5.37}$$

$$\frac{1}{h_k^2} tr\left[(I_{3\times 3} - F_k) J_d \right] - mg e_3^T \frac{R_{k+1} + R_k}{2} \rho = E_k, \tag{5.38}$$

$$R_{k+1} = R_k F_k, \tag{5.39}$$

$$\Pi_{k+1} = F_k^T \Pi_k + \frac{h_k}{2} F_k^T mg \left(\rho \times R_k^T e_3 \right) + \frac{h_k}{2} mg \left(\rho \times R_{k+1}^T e_3 \right), \tag{5.40}$$

$$E_{k+1} = \frac{1}{h_k^2} tr\left[(I_{3\times 3} - F_k) J_d \right] - mg e_3^T \frac{R_{k+1} + R_k}{2} \rho. \tag{5.41}$$

Left multiplying both sides of (5.40) by R_{k+1} and using the definition of $F_k = R_{k+1}^T R_k$

$$R_{k+1}\Pi_k - R_k \Pi_k = \frac{h_k}{2} mg \left[R_k \left(\rho \times R_k^T e_3 \right) + R_{k+1} \left(\rho \times R_{k+1}^T e_3 \right) \right] \tag{5.42}$$

If we take dot product of the above equation with e_3, the right hand side of the goes to zero, which means that our integrator conserves $e_3^T R_k \Pi_k$ which is the discrete analogue of the vertical component of the angular momentum. In fact, the left hand side of (5.38) and right hand side of (5.41) are same i.e. $E_{k+1} = E_k$, which means that at every time step our integrator conserves the discrete energy E_k.

5.3.2 Numerical Results

In this subsection, we implement adaptive Lie group variational integrator for the 3D pendulum to study the uncontrolled dynamics. We consider the 3D pendulum parameters and initial conditions first studied in [100] and compare the fixed time step Lie group variational

integrator results with the results from the adaptive time step Lie group variational integrator to demonstrate the superior numerical performance of the adaptive algorithm. The mass properties of the 3D pendulum are

$$J = \text{diag}[1, 2.8, 2]\text{kgm}^2, \quad m = 1\text{kg}, \quad \rho = [0, 0, 1]\text{m}. \tag{5.43}$$

We present results for the following two initial conditions.

1. Small perturbation from the hanging equilibrium

$$R_0 = I_{3\times 3}, \quad \omega_0 = [0.5, -0.5, 0.4]\text{rad/s}. \tag{5.44}$$

2. Small perturbation from the inverted equilibrium

$$R_0 = \text{diag}[-1, 1, -1], \quad \omega_0 = [0.5, -0.5, 0.4]\text{rad/s}. \tag{5.45}$$

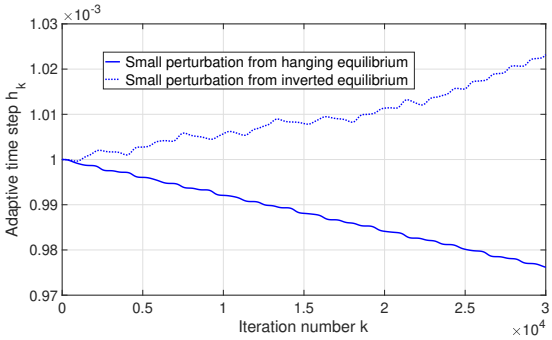

Figure 5.1: Adaptive time step behavior for both cases

For both cases, results from the adaptive algorithm for an initial time step of $h_0 = 0.001$ are compared with results from the fixed algorithm for a fixed step size of $h = 0.001$. Numerical results for the first case are presented in Fig. 5.2, where Fig. 5.2a shows that time history of the angular velocity for both algorithms are indistinguishable, and Fig. 5.2b compares

the error in conserved quantities for both algorithms. The discrete energy error plot for the first case shows that the adaptive time step algorithm has nearly exact energy preservation whereas the fixed time step method has energy error around 10^{-7}. The other two plots in the Fig. 5.2b show that adaptive time step variational integrator preserves the first integrals and the structure of the configuration space with the same accuracy as the fixed time step variational integrator.

For the second case, the angular velocities in Fig. 5.3a are irregular, with the time histories not matching for both algorithms. In Fig. 5.3b, energy error for the fixed time step algorithm increases to 10^{-4} for the fixed time step algorithm as compared to 10^{-12} for the adaptive time step algorithm. The angular momentum and orthogonality error plots for the second case show a numerical performance similar to the first case.

Fig. 5.1 shows how the adaptive time step behaves differently for both cases. The adaptive time step h_k doesn't decrease or increase substantially from the initial time step of $h_0 = 0.001$ over the 3000 iterations. For the case with dynamics around the hanging equilibrium, the adaptive time step is found to be decreasing whereas it increases irregularly for the second case with chaotic behavior.

We have done an order analysis comparison between the fixed and adaptive time step variational integrators for different time step values to understand the effect of the time step on the mean energy error and computational time. For the first case, in Fig. 5.4 we have varied the time step from 0.001 to 0.1 to understand how the mean energy error and CPU time change. Fig. 5.4a shows a second order convergence for the mean energy error for decreasing time step whereas the mean energy error remains at the machine level accuracy for the adaptive algorithm due to its energy-preserving nature. In Fig. 5.4b CPU time for both algorithms converge with the same order with adaptive algorithm being 2-5 times more expensive due to the additional discrete energy equation solved at every iteration.

Table 5.1: Fixed and Adaptive Algorithm Comparison for the 3D Pendulum

Method	Time step	Mean $\|\Delta E\|$	CPU time	Mean $\|\|I - R^T R\|\|$
Adaptive	10^{-4}	2.3×10^{-13}	72.5	1.2×10^{-12}
Algorithm	4×10^{-3}	1.6×10^{-13}	18.0	6.7×10^{-14}
	10^{-3}	1.7×10^{-13}	7.5	2.6×10^{-14}
Fixed	10^{-4}	1.7×10^{-7}	48.8	4.1×10^{-13}
Algorithm	4×10^{-3}	3.1×10^{-6}	12.1	3.9×10^{-14}
	10^{-3}	1.7×10^{-5}	5.2	2.0×10^{-14}

In Table 5.1 we have compared numerical performance of fixed and adaptive algorithms for the second case to demonstrate that adaptive algorithms are able to achieve orders of magnitude better energy behavior with less CPU time. For example, the adaptive algorithm achieves mean energy error around 10^{-13} with an initial step size of 0.001 and CPU time of 7.5. On the other hand, the fixed time step algorithm with a smaller step size of 0.0001 and CPU time of 48.8 is only able to achieve mean energy error of around 10^{-7}. Thus, the adaptive algorithm gives orders of magnitude better energy performance with only 1/6th of CPU time.

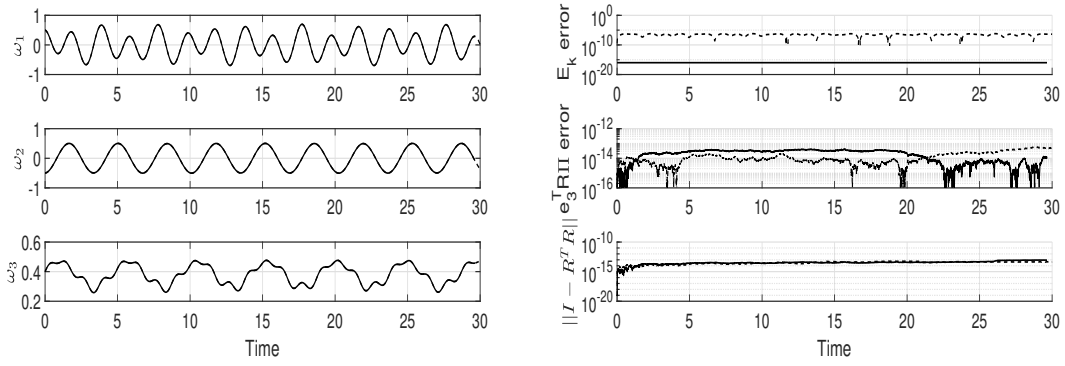

(a) Angular velocity comparison

(b) Error in conserved quantities

Figure 5.2: Small perturbation from the hanging equilibrium. (Adaptive algorithm: solid. Fixed algorithm: dashed)

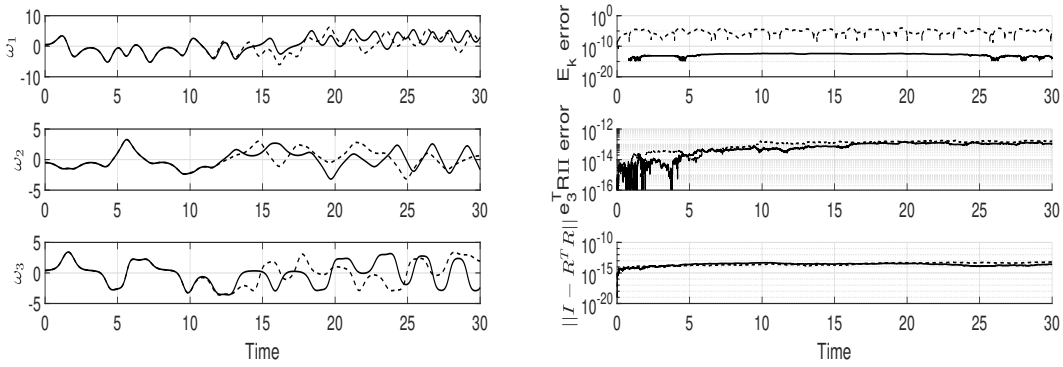

(a) Angular velocity comparison (b) Error in conserved quantities

Figure 5.3: Small perturbation from the inverted equilibrium. (Adaptive algorithm: solid. Fixed algorithm: dashed)

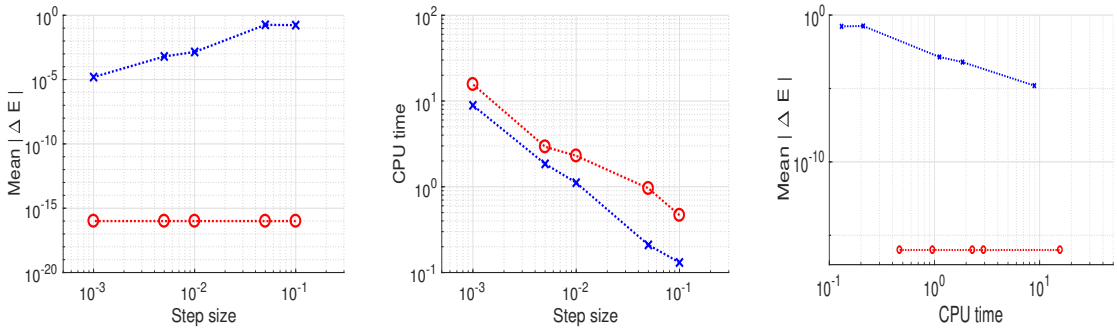

(a) Mean energy error (b) Computational cost (c) Energy error vs CPU time

Figure 5.4: Order with respect to energy and computational cost(Adaptive algorithm: red, circle. Fixed algorithm: blue, cross)

5.4 Conclusions

In this chapter, we present adaptive time step variational integrators for attitude dynamics of a rigid body under the influence of attitude dependent potential. By developing the extended Lagrangian mechanics framework on $\mathsf{SO(3)}$, we derive extended equations of motion for the rigid body system in continuous time. To derive energy-preserving variational integrators, we use concepts from extended discrete mechanics, where in addition to the configuration variables time is also considered a discrete dynamic variable. The govern-

ing discrete equations are obtained from the discrete Hamilton's principle in the extended phase space, and resulting adaptive algorithm preserves the discrete energy in addition to the symplectic and momentum preservation properties characteristic of the fixed time step variational integrators.

The resulting adaptive time step Lie group variational integrator is used to study the dynamics of uncontrolled 3D pendulum in presence of gravity. The adaptive time step algorithm exhibits superior energy performance in both cases compared to the fixed time step algorithm while maintaining the same level of accuracy for orthogonality error and angular momentum conservation. The order analysis results show that, despite solving an additional nonlinear equation at each time step, the adaptive algorithm takes - due to its superior energy performance- less computation time than the fixed time step Lie group variational integrator to achieve same level of energy accuracy.

Chapter 6

Energy-preserving Lie Group Variational Integrators on $\mathsf{SE}(3)$

The goal of this chapter is to develop adaptive time step Lie group variational integrators for simultaneously rotating and translating rigid body motion. First, we derive the continuous time equations of motion for a rigid body in $\mathsf{SE}(3)$ using extended Lagrangian mechanics. We then use the extended discrete mechanics framework to construct adaptive time step variational integrators from the discretized variational principle. This integrator is used to study the dynamics of an underwater vehicle. The results demonstrate the superior energy performance of adaptive time step Lie group variational integrators compared to their fixed time step counterpart.

This chapter is organized as follows. In Section 6.1, we utilize concepts from extended Lagrangian mechanics to derive continuous-time equations of motion for rigid body motion in $\mathsf{SE}(3)$. In Section 6.2 we derive energy-preserving, adaptive time step Lie group variational integrator. In Section 6.3 we study the dynamics of a neutrally buoyant conservative underwater. Finally, in Section 6.4 we provide concluding remarks and suggest future directions for this work.

6.1 Continuous Time Model

A rigid body that is simultaneously translating and rotating is said to undergo Euclidean motion. For describing this Euclidean motion, we arbitrarily select an inertial frame and a body fixed frame in the rigid body such that the origin is at the center of mass of the rigid body. The configuration space of a rotating and translating rigid body in three dimensions is the Lie group $\mathsf{SE}(3)$ and we represent the configuration $(R, x) \in \mathsf{SE}(3)$ by the homogeneous matrix $G = \begin{bmatrix} R & x \\ 0 & 1 \end{bmatrix}$ where $R \in \mathsf{SO}(3)$ is the rotation matrix and $x \in \mathbb{R}^3$ is the position of the center of mass in inertial frame. The rotational and translational kinematics for a rigid body are described by $(R, x, \dot{R}, \dot{x}) \in \mathsf{TSE}(3)$. The rotational and translational kinematics equations can be written as

$$\dot{G} = \begin{bmatrix} \dot{R} & \dot{x} \\ 0 & 0 \end{bmatrix} = \begin{bmatrix} R & x \\ 0 & 1 \end{bmatrix} \begin{bmatrix} S(\omega) & v \\ 0 & 0 \end{bmatrix} = GV, \tag{6.1}$$

where $\omega, v \in \mathbb{R}^3$ are the angular and translational velocity vectors in the body-fixed frame and V is an element of the Lie algebra $\mathfrak{se}(3)$. $S(\cdot) : \mathbb{R}^3 \to \mathbb{R}^{3\times 3}$ maps a vector to a skew-symmetric matrix such that $S(x)y = x \times y$ for $x, y \in \mathbb{R}^3$.

6.1.1 Extended Lagrangian Mechanics on $\mathsf{SE}(3)$

Consider a time-dependent Lagrangian system evolving on $Q = \mathsf{SE}(3)$ and time space $\mathbb{R}$. In the extended Lagrangian mechanics framework, time t, configuration G and velocity V are parameterized by an independent variable a. For a given path $c(a)$, the initial time is

$t_0 = t(a_0)$ and the final time is $t_f = t(a_f)$. The extended action $\bar{\mathfrak{B}}$ is

$$\bar{\mathfrak{B}} = \int_{t_0}^{t_f} L(t, G, V)dt = \int_{a_0}^{a_f} L(t(a), G(a), V(a))\ t'(a)\ da, \tag{6.2}$$

where $(\cdot)' = \frac{d}{da}(\cdot)$ denotes the derivative with respect to independent variable a. We consider the following admissible variations

$$G^\epsilon(a) = G(a)e^{\epsilon\Gamma(a)}, \qquad t^\epsilon(a) = t(a) + \epsilon\delta t(a), \tag{6.3}$$

where Γ is an admissible differentiable curve on $\mathfrak{se}(3)$. Using the isomorphism $\mathcal{S} : \mathbb{R}^3 \times \mathbb{R}^3 \to \mathfrak{se}(3)$ we define $\Gamma = \mathcal{S}(\eta, \chi) = \begin{bmatrix} S(\eta) & \chi \\ 0 & 0 \end{bmatrix}$ with the variations $\eta, \chi \in \mathbb{R}^3$ vanishing at t_0 and t_f. Using the G^ϵ definition, we get

$$\delta G = \left.\frac{dG^\epsilon}{d\epsilon}\right|_{\epsilon=0} = G(a)\Gamma(a) = \begin{bmatrix} RS(\eta) & R\chi \\ 0 & 0 \end{bmatrix}. \tag{6.4}$$

We obtain $\dot{G}^\epsilon$ from the G^ϵ and t^ϵ definitions (6.3)

$$\dot{G}^\epsilon = \frac{\frac{dG^\epsilon}{da}}{\frac{dt^\epsilon}{da}} = \frac{G'(a)e^{\epsilon\Gamma(a)} + \epsilon G(a)e^{\epsilon\Gamma(a)}\Gamma'(a)}{t'(a)\left(1 + \epsilon\frac{\delta t'(a)}{t'(a)}\right)}. \tag{6.5}$$

Using the binomial expansion for the denominator gives

$$\begin{aligned}
\dot{G}^\epsilon = \frac{\frac{dG^\epsilon}{da}}{\frac{dt^\epsilon}{da}} &= \frac{G'(a)e^{\epsilon\Gamma(a)} + \epsilon G(a)e^{\epsilon\Gamma(a)}\Gamma'(a)}{t'(a)\left(1 + \epsilon\frac{\delta t'(a)}{t'(a)}\right)} \\
&= \left(\dot{G}(a)e^{\epsilon\Gamma(a)} + \epsilon G(a)e^{\epsilon\Gamma(a)}\dot{\Gamma}(a)\right)\left(1 - \epsilon\frac{\delta t'(a)}{t'(a)} + O(\epsilon^2)\right) \\
&= \dot{G}e^{\epsilon\Gamma} + \epsilon G e^{\epsilon\Gamma}\dot{\Gamma} - \epsilon\dot{G}e^{\epsilon\Gamma}\frac{\delta t'}{t'} + O(\epsilon^2).
\end{aligned} \tag{6.6}$$

From $\dot{G}^\epsilon$ and kinematic equation (6.1), we obtain $\delta\dot{G}$

$$\delta\dot{G} = \frac{d\dot{G}^\epsilon}{d\epsilon}\bigg|_{\epsilon=0} = \dot{G}\Gamma + G\dot{\Gamma} - \dot{G}\frac{\delta t'}{t'} = G\left(V\Gamma + \dot{\Gamma} - V\frac{\delta t'}{t'}\right). \tag{6.7}$$

Taking variations of the kinematic equation (6.1)

$$\delta\dot{G} = \delta G V + G\delta V = G\Gamma V + G\delta V, \tag{6.8}$$

and equating it with $\delta\dot{G}$ from (6.7) gives δV

$$\delta V = V\Gamma - \Gamma V + \dot{\Gamma} - V\frac{\delta t'(a)}{t'(a)}. \tag{6.9}$$

Using $S(a \times b) = S(a)S(b) - S(b)S(a)$, we simplify

$$\begin{aligned} V\Gamma - \Gamma V &= \begin{bmatrix} S(\omega \times \eta) & S(\omega)\chi - S(\eta)v \\ 0 & 0 \end{bmatrix} \\ &= \mathcal{S}\left(\begin{bmatrix} S(\omega) & 0 \\ S(v) & S(\omega) \end{bmatrix}\begin{bmatrix} \eta \\ \chi \end{bmatrix}\right), \end{aligned} \tag{6.10}$$

which gives

$$\delta V = \mathcal{S}\left(\begin{bmatrix} S(\omega) & 0 \\ S(v) & S(\omega) \end{bmatrix}\begin{bmatrix} \eta \\ \chi \end{bmatrix}\right) + \dot{\Gamma} - V\frac{\delta t'(a)}{t'(a)}. \tag{6.11}$$

Taking variations of the extended action

$$\begin{aligned} \delta\bar{\mathfrak{B}} = \int_{a_0}^{a_f}\left[\frac{\partial L}{\partial G}\cdot\delta G + \frac{\partial L}{\partial V}\cdot\delta V + \frac{\partial L}{\partial t}\cdot\delta t\right]t'(a)da \\ + \int_{a_0}^{a_f} L\ \delta t'(a)\ da. \end{aligned} \tag{6.12}$$

Using $(\delta R, \delta x) = R(S(\eta), \chi)$, we compute

$$\frac{\partial L}{\partial R} \cdot \delta R = \sum_{i=1}^{3} \frac{\partial L}{\partial r_i} \cdot \delta r_i = -\sum_{i=1}^{3} S(r_i) \frac{\partial L}{\partial r_i} \cdot \eta, \tag{6.13}$$

where r_i is the i-th column of R^T for $i = 1, 2, 3$. Thus,

$$\begin{aligned} \int_{a_0}^{a_f} \left(\frac{\partial L}{\partial G} \cdot \delta G \right) t'(a)\, da &= \int_{t_0}^{t_f} \left(\frac{\partial L}{\partial R} \cdot \delta R + \frac{\partial L}{\partial x} \cdot R\chi \right) dt \\ &= \int_{t_0}^{t_f} \mathcal{S} \left(\begin{bmatrix} -\sum_{i=1}^{3} S(r_i) \frac{\partial L}{\partial r_i} \\ R^T \frac{\partial L}{\partial x} \end{bmatrix} \right) \cdot \Gamma \, dt. \end{aligned} \tag{6.14}$$

Similarly

$$\begin{aligned} \frac{\partial L}{\partial V} \cdot \delta V &= \mathcal{S} \left(\frac{\partial L}{\partial \omega}, \frac{\partial L}{\partial v} \right) \cdot \left(V\Gamma - \Gamma V + \dot{\Gamma} - V \frac{\delta t'(a)}{t'(a)} \right) \\ &= \mathcal{S} \left(\begin{bmatrix} -S(\omega) & -S(v) \\ 0 & -S(\omega) \end{bmatrix} \begin{bmatrix} \frac{\partial L}{\partial \omega} \\ \frac{\partial L}{\partial v} \end{bmatrix} \right) \cdot \Gamma \\ &\quad + \frac{\partial L}{\partial V} \cdot \left(\dot{\Gamma} - V \frac{\delta t'(a)}{t'(a)} \right). \end{aligned} \tag{6.15}$$

From Hamilton's principle we know that for the actual path of the motion $\delta \bar{\mathfrak{B}} = 0$. Substituting all the computed terms in (6.12) and using integration by parts gives

$$\begin{aligned} &\int_{t_0}^{t_f} S \left(\begin{bmatrix} -S(\omega) & -S(v) \\ 0 & -S(\omega) \end{bmatrix} \begin{bmatrix} \frac{\partial L}{\partial \omega} \\ \frac{\partial L}{\partial v} \end{bmatrix} + \begin{bmatrix} -\sum_{i=1}^{3} S(r_i) \frac{\partial L}{\partial r_i} \\ R^T \frac{\partial L}{\partial x} \end{bmatrix} \right) \cdot \Gamma dt \\ &\qquad \left[\frac{\partial L}{\partial V} \cdot \Gamma - \frac{\partial L}{\partial V} \cdot V \delta t \right]_{t_0}^{t_f} + \int_{t_0}^{t_f} -\frac{d}{dt} \begin{bmatrix} \frac{\partial L}{\partial \omega} \\ \frac{\partial L}{\partial v} \end{bmatrix} \cdot \Gamma dt \\ &\qquad + \int_{t_0}^{t_f} \left(\frac{\partial L}{\partial t} + \frac{d}{dt} \left(\frac{\partial L}{\partial \omega} \cdot \omega + \frac{\partial L}{\partial v} \cdot v - L \right) \right) \delta t dt = 0. \end{aligned} \tag{6.16}$$

Setting the variations at endpoints to zero leads us to the governing equations in the extended mechanics framework. Equations of motion for a rigid body evolving on SE(3) are

$$\frac{d}{dt}\begin{bmatrix}\frac{\partial L}{\partial \omega}\\ \frac{\partial L}{\partial v}\end{bmatrix}+\begin{bmatrix}S(\omega) & S(v)\\ 0 & S(\omega)\end{bmatrix}\begin{bmatrix}\frac{\partial L}{\partial \omega}\\ \frac{\partial L}{\partial v}\end{bmatrix}-\begin{bmatrix}-\sum_{i=1}^{3} S(r_i)\frac{\partial L}{\partial r_i}\\ R^T\frac{\partial L}{\partial x}\end{bmatrix}=0. \tag{6.17}$$

The second equation is the energy evolution equation

$$\frac{\partial L}{\partial t}+\frac{d}{dt}\left(\frac{\partial L}{\partial \omega}\cdot\omega+\frac{\partial L}{\partial v}\cdot v-L\right)=0, \tag{6.18}$$

which describes how the energy of the rigid body system evolves with time.

6.1.2 Equations of Motion

We consider the special case with the following Lagrangian for the motion of a rigid body in $SE(3)$

$$\begin{aligned}L(x,v,R,\omega)&=\frac{1}{2}v^TMv+\frac{1}{2}\omega^TJ\omega-U(x,R)\\ &=\frac{1}{2}v^TMv+\frac{1}{2}tr\left[S(\omega)J_dS(\omega)^T\right]-U(x,R),\end{aligned} \tag{6.19}$$

where J is the standard inertia matrix, $J_d=\frac{1}{2}tr[J]I_{3\times3}-J$ is the nonstandard inertia matrix and M is the mass matrix for the body. The governing extended equations of motion are

$$M\dot{v}+\omega\times Mv+R^T\frac{\partial U(G)}{\partial x}=0, \tag{6.20}$$

$$J\dot{\omega}+\omega\times J\omega+v\times Mv+R^T\frac{\partial U(G)}{\partial R}-\frac{\partial U(G)}{\partial R}^T R=0, \tag{6.21}$$

$$\frac{d}{dt}\left(\frac{1}{2}v^T M v + \frac{1}{2}\omega^T J\omega + U(x,R)\right) = 0. \tag{6.22}$$

We know that the linear and angular momenta of the rigid body are given by $\gamma = Mv \in \mathbb{R}^3$ and $\Pi = J\omega \in \mathbb{R}^3$ in the body fixed frame. The extended equations of motion in the Hamiltonian form are

$$\dot{\gamma} + R\omega \times R^T\gamma + \frac{\partial U(G)}{\partial x} = 0, \tag{6.23}$$

$$\dot{\Pi} + \omega \times \Pi + v \times R^T\gamma + R^T\frac{\partial U(G)}{\partial R} - \frac{\partial U(G)}{\partial R}^T R = 0, \tag{6.24}$$

$$\frac{d}{dt}\left(\frac{1}{2}\gamma^T R M^{-1} R^T\gamma + \frac{1}{2}\Pi^T J^{-1}\Pi + U(x,R)\right) = 0. \tag{6.25}$$

These linear and angular momenta are related to the momenta conjugate to $\dot{x}$ and R, $P_{\dot{x}} \in \mathbb{R}^3$ and $P_{\dot{R}} \in \mathbb{R}^{3\times 3}$, by

$$P_{\dot{x}} = R\gamma, \qquad P_{\dot{R}} - P_{\dot{R}}^T = S(\Pi). \tag{6.26}$$

6.2 Adaptive Variational Integrator

In this section adaptive time step Lie group variational integrators for rigid body motion in $\mathsf{SE(3)}$ are obtained by discretizing Hamilton's principle. Using ideas from extended discrete mechanics and Lie group methods, extended discrete equations of motion are derived in both Lagrangian and Hamiltonian form.

6.2.1 Extended Discrete Lagrangian Mechanics on SE(3)

In the discrete domain, we treat the time t_k as a discrete dynamic variable. By discretizing the kinematic relation $\dot{R} = RS(\omega)$, we obtain

$$\frac{R_{k+1} - R_k}{h_k} = R_k S(\omega_k), \tag{6.27}$$

where $h_k = t_{k+1} - t_k$. We define $F_k \in \mathsf{SO(3)}$ such that $R_{k+1} = R_k F_k$. This gives the following approximation to $S(\omega_k)$

$$S(\omega_k) \approx \frac{1}{h_k} \left(F_k - I_{3\times 3} \right). \tag{6.28}$$

Similarly discretizing the kinematic relation $\dot{x} = Rv$ gives

$$x_{k+1} = h_k R_k v_k + x_k. \tag{6.29}$$

We define the extended discrete Lagrangian $L_d : \bar{Q} \times \bar{Q} \to \mathbb{R}$ and discretize the extended action

$$\bar{\mathfrak{B}}_d = \sum_{k=0}^{N-1} L_d(t_k, x_k, R_k, t_{k+1}, x_{k+1}, R_{k+1}). \tag{6.30}$$

For the rigid body system, we consider

$$\begin{aligned} L_d \simeq h_k \left(\frac{L(t_k, R_k, x_k, v_k, \omega_k) + L(t_{k+1}, R_{k+1}, x_{k+1}, v_k, \omega_k)}{2} \right) \\ = \frac{1}{h_k} tr\left[(I_{3\times 3} - F_k) J_d \right] + \frac{h_k}{2} v_k^T M v_k - \frac{h_k}{2} \left(U_k + U_{k+1} \right), \end{aligned} \tag{6.31}$$

where $U_k := U(x_k, R_k)$. We consider the following variations

$$G_k^\epsilon = G_k e^{\epsilon \Gamma_k}, \qquad t_k^\epsilon = t_k + \epsilon \delta t_k. \tag{6.32}$$

The variation of $F_k = R_k^T R_{k+1}$ using $\delta R_k = R_k S(\eta_k)$ yields

$$\delta F_k = -S(\eta_k)F_k + F_k S(\eta_{k+1}). \tag{6.33}$$

Similarly variation of $v_k = \frac{R_k^T}{h_k}(x_{k+1} - x_k)$ gives

$$\delta v_k = \frac{R_k^T}{h_k}(\delta x_{k+1} - \delta x_k) - S(\eta_k)v_k - \frac{R_k^T}{h_k^2}(x_{k+1} - x_k)\delta h_k. \tag{6.34}$$

If we consider the variation of the kinetic energy term we get

$$\begin{aligned}\delta\left(\frac{1}{h_k}tr\left[(I_{3\times3} - F_k)J_d\right] + \frac{h_k}{2}v_k^T M v_k\right) = \frac{\delta h_k}{2}v_k^T M v_k + \\ \frac{1}{h_k}tr\left[(S(\eta_k)F_k - F_k S(\eta_{k+1}))J_d\right] - \frac{\delta h_k}{h_k^2}tr\left[(I_{3\times3} - F_k)J_d\right] \\ + v_k^T M\left(R_k^T(\delta x_{k+1} - \delta x_k) - h_k S(\eta_k)v_k - v_k\delta h_k\right).\end{aligned} \tag{6.35}$$

Similarly variation of the potential energy term gives

$$\begin{aligned}\delta\left(-\frac{h_k}{2}\left(U_k + U_{k+1}\right)\right) = -\frac{\delta h_k}{2}\left(U_k + U_{k+1}\right) \\ - \frac{h_k}{2}\sum_{j=k}^{k+1}\left(\frac{\partial U_j}{\partial R_j}\cdot\delta R_j + \frac{\partial U_j}{\partial x_j}^T\delta x_j\right),\end{aligned} \tag{6.36}$$

where $\frac{\partial U}{\partial R}\cdot\delta R = \frac{\partial U}{\partial R_{[ij]}}\delta R_{[ij]}$. Using $\delta R = RS(\eta)$ and the identity $\frac{\partial U}{\partial R}RS(\eta) = -tr\left[S(\eta)R^T\frac{\partial U}{\partial R}\right]$ we get

$$\begin{aligned}\delta\left(-\frac{h_k}{2}\left(U_k + U_{k+1}\right)\right) = -\frac{\delta t_{k+1} - \delta t_k}{2}\sum_{j=k}^{k+1}(U_j) \\ - \frac{h_k}{2}\sum_{j=k}^{k+1}\left(-tr\left[S(\eta_j)R_j^T\frac{\partial U_j}{\partial R_j}\right] + \frac{\partial U_j}{\partial x_j}^T\delta x_j\right).\end{aligned} \tag{6.37}$$

Setting $\delta\bar{\mathfrak{B}}_d$ and variations at endpoints to zero gives

$$\begin{aligned}0 = \sum_{k=1}^{N-1} \left[v_{k-1}^T M R_{k-1}^T - v_k^T M R_k^T - \frac{h_k + h_{k-1}}{2} \frac{\partial U_k}{\partial x_k}^T \right] \delta x_k \\ + \sum_{k=1}^{N-1} tr \left[S(\eta_k) \left\{ \frac{1}{h_k} F_k J_d - \frac{1}{h_{k-1}} J_d F_{k-1} \right\} \right] \\ - \sum_{k=1}^{N-1} tr \left[S(\eta_k) \left\{ h_k v_k v_k^T M - \frac{h_k + h_{k-1}}{2} R_k^T \frac{\partial U_k}{\partial R_k} \right\} \right] \\ + \sum_{k=1}^{N-1} \left[\frac{tr[(I_{3\times 3} - F_k) J_d]}{h_k^2} + \frac{v_k^T M v_k}{2} + \frac{U_k + U_{k+1}}{2} \right] \delta t_k \\ - \sum_{k=1}^{N-1} \left[\frac{tr[(I_{3\times 3} - F_{k-1}) J_d]}{h_{k-1}^2} - \frac{v_{k-1}^T M v_{k-1}}{2} - \frac{U_k + U_{k-1}}{2} \right] \delta t_k. \quad (6.38)\end{aligned}$$

The above equation should be satisfied for all admissible variations $\eta_k, \delta x_k$ and δt_k, and since $S(\eta_k)$ is skew-symmetric, the governing extended discrete equations on SE(3) in Lagrangian form are

$$\begin{aligned}\frac{1}{h_k} \left(F_k J_d - J_d F_k^T \right) - \frac{1}{h_{k-1}} \left(J_d F_{k-1} - F_{k-1}^T J_d \right) \\ = h_k \left(v_k v_k^T M - M v_k v_k^T \right) + \frac{h_k + h_{k-1}}{2} \left(\frac{\partial U_k}{\partial R_k}^T R_k - R_k^T \frac{\partial U_k}{\partial R_k} \right), \quad (6.39)\end{aligned}$$

$$M v_k + \frac{h_k + h_{k-1}}{2} R_k^T \frac{\partial U_k}{\partial x_k} = F_{k-1}^T M v_{k-1}, \quad (6.40)$$

$$\begin{aligned}\frac{1}{h_k^2} tr[(I_{3\times 3} - F_k) J_d] + \frac{v_k^T M v_k}{2} + \frac{U_k + U_{k+1}}{2} = \\ \frac{1}{h_{k-1}^2} tr[(I_{3\times 3} - F_{k-1}) J_d] + \frac{v_{k-1}^T M v_{k-1}}{2} + \frac{U_k + U_{k-1}}{2}, \quad (6.41)\end{aligned}$$

$$x_{k+1} = x_k + (h_k R_k v_k), \quad (6.42)$$

$$R_{k+1} = R_k F_k. \tag{6.43}$$

Given $(h_{k-1}, x_k, v_{k-1}, R_k, F_{k-1})$, above equations can be solved to obtain $(h_k, x_{k+1}, v_k, R_{k+1}, F_k)$. Using the discrete Legendre transform, we can re-write the governing discrete equations in the Hamiltonian form

$$\frac{1}{h_k}(F_k J_d - J_d F_k^T) - \frac{h_k}{2} S(M_k) - h_k(v_k v_k^T M - M v_k v_k^T) = S(\Pi_k), \tag{6.44}$$

$$M v_k + \frac{h_k}{2} R_k^T \frac{\partial U_k}{\partial x_k} = R_k^T \gamma_k, \tag{6.45}$$

$$R_{k+1} = R_k F_k, \tag{6.46}$$

$$x_{k+1} = x_k + (h_k R_k v_k), \tag{6.47}$$

$$\frac{1}{h_k^2} tr[(I_{3\times 3} - F_k) J_d] + \frac{v_k^T M v_k}{2} + \frac{U_k + U_{k+1}}{2} = E_k, \tag{6.48}$$

$$\gamma_{k+1} = R_k M v_k - \frac{h_k}{2} \frac{\partial U_{k+1}}{\partial x_{k+1}}, \tag{6.49}$$

$$S(\Pi_{k+1}) = \frac{1}{h_k}(J_d F_k - F_k^T J_d) + \frac{h_k}{2} S(M_{k+1}), \tag{6.50}$$

$$E_{k+1} = \frac{1}{h_k^2} tr[(I_{3\times 3} - F_k) J_d] + \frac{v_k^T M v_k}{2} + \frac{U_k + U_{k+1}}{2}, \tag{6.51}$$

where $M_k \in \mathbb{R}^3$ is defined such that $S(M_k) = \frac{\partial U}{\partial R_k}^T R_k - R_k^T \frac{\partial U}{\partial R_k}$. Given $(h_{k-1}, x_k, R_k, \gamma_k, \Pi_k, E_k)$, the coupled implicit equations (6.44)-(6.48) are solved to obtain $(F_k, v_k, h_k, x_{k+1}, R_{k+1})$ which are used in the explicit equations (6.49)-(6.51) to obtain discrete momenta $(\gamma_{k+1}, \Pi_{k+1})$ and discrete energy E_{k+1}.

6.2.2 Numerical properties of the adaptive algorithm

Adaptive time step variational integrators preserve the extended symplectic form and exhibit a discrete analogue of Noether's theorem [44] that leads to conservation of the discrete momentum in presence of symmetries. Our choice of the discrete Lagrangian (6.31) inherits all the symmetries of the continuous Lagrangian, therefore the adaptive algorithm preserves all the conserved momenta of the continuous time system in the numerical simulation. The discrete energy equation (6.41) ensures that the adaptive time step is chosen such that the energy is conserved in the discrete dynamics.

Since we have defined $F_k \in \mathsf{SO(3)}$ and the Lie group $\mathsf{SO(3)}$ is closed under matrix multiplication, the rotational configuration at the next time lies on $\mathsf{SO(3)}$ i.e. $R_{k+1} = R_k F_k \in \mathsf{SO(3)}$. This way the configuration of the rigid body (R_k, x_k) automatically remains on $\mathsf{SE(3)}$. Thus, in addition to being symplectic as well as energy and momentum-conserving, the adaptive time step Lie group variational integrator also preserves the geometry of the nonlinear configuration space.

6.2.3 Computational Approach

Based on the structure of the coupled implicit discrete equations (6.44)-(6.48), we suggest a computational approach for solving these equations sequentially instead of solving all equations simultaneously. Given $(h_{k-1}, x_k, R_k, \gamma_k, \Pi_k, E_k)$ and an initial guess $h_k^{(0)} = h_{k-1}$ for the adaptive time step h_k, we start by solving the explicit discrete equation (6.45) to obtain $v_k^{(i)}$ which is used to solve (6.44) for $F_k^{(i)}$. The implicit discrete equation (6.44) can be re-written as

$$F_k^{(i)} J_d - J_d (F_k^{(i)})^T = S(g_k^{(i)}), \tag{6.52}$$

where $S(g_k^{(i)}) = S(\Pi_k + \frac{h_k^{(i)}}{2} M_k) + h_k^{(i)}(v_k^{(i)}(v_k^{(i)})^T M - M v_k^{(i)}(v_k^{(i)})^T)$. To make sure F_k lies on $\mathsf{SO(3)}$, we express it as the exponential of an element of its Lie algebra $S(f) \in \mathfrak{so}(3)$ for some $f \in \mathbb{R}^3$. We use the Cayley transformation

$$F_k^{(i)} = \left(I_{3\times 3} + S(f_k^{(i)})\right)\left(I_{3\times 3} - S(f_k^{(i)})\right)^{-1}, \tag{6.53}$$

to transform the matrix equation (6.52) to the following equivalent vector equation

$$G_{Cay}(f_k^{(i)}) = g_k^{(i)} + g_k^{(i)} \times f_k^{(i)} + ((g_k^{(i)})^T f_k^{(i)}) f_k^{(i)} - 2J f_k^{(i)} = 0. \tag{6.54}$$

This vector equation is solved using the Newton method to obtain $f_k^{(i)}$ which yields $F_k^{(i)}$. This $F_k^{(i)}$ along with $v_k^{(i)}$ is substituted in the discrete kinematic relations (6.46) and (6.47) to obtain $(x_{k+1}^{(i)}, R_{k+1}^{(i)})$. Finally, we solve the discrete energy equation (6.48) for $h_k^{(i)}$ using

$$h_k^{(i)} = \sqrt{\frac{tr[(I_{3\times 3} - F_k^{(i)}) J_d]}{E_k - \frac{v_k^{(i)T} M v_k^{(i)}}{2} - \frac{U_k + U_{(k+1)}^{(i)}}{2}}}. \tag{6.55}$$

6.3 Numerical Results

This section presents numerical simulation results for a conservative underwater vehicle. We assume that dissipative forces are negligible and the mass is uniformly distributed. Under these assumptions, the underwater vehicle can be modeled as a rigid body immersed in an infinite volume of ideal fluid. In this numerical study, we use the mass and inertia parameters first studied in [178]. Since the center of buoyancy and center of gravity are coincident for a uniform rigid body, the kinetic energy is given by

$$T = \frac{1}{2} v^T M v + \frac{1}{2} \omega^T J \omega. \tag{6.56}$$

The mass is $m = 123.8$ kg whereas the mass and inertia matrices are

$$M = m\ I + \text{diag}[65, 70, 75]\ \text{kg},\ \ J = \text{diag}[5.46, 5.29, 5.72]\ \text{kgm}^2, \tag{6.57}$$

where the added masses are included in the mass matrix. The potential energy due to the gravity, acting in the vertical or e_3 direction (same as the positive b_3 body axis), is given by

$$U = -(m - \rho\mathcal{V})gx_3, \tag{6.58}$$

where m is the mass of the vehicle, ρ is the density of water, g is the gravitational acceleration, $\mathcal{V}$ is the volume occupied by the vehicle. The weight of displaced water is $\rho\mathcal{V}g = 1215.8$ N. We have considered the following three initial conditions

1. $R_0 = \exp(S([1, 2, 3]^T))$
   $x_0 = (0, 0, 10)^T \text{m}$
   $\omega_0 = (1.5, 1.0, 0.5)^T \text{s}^{-1}$
   $v_0 = R_0^T(0.1, -0.2, 0.1)^T \text{ms}^{-1}$,

2. $R_0 = \exp(S([1, 2, 3]^T))$
   $x_0 = (0, 0, 10)^T \text{m}$
   $\omega_0 = (1.5, 1.0, 0.5)^T \text{s}^{-1}$
   $v_0 = R_0^T(0.1, 0.15, 0.1)^T \text{ms}^{-1}$,

3. $R_0 = \exp(S([3, 2, 3]^T))$
   $x_0 = (0, 0, 10)^T \text{m}$
   $\omega_0 = (1.0, 1.5, 0.5)^T \text{s}^{-1}$
   $v_0 = R_0^T(0.1, 0.15, 0.1)^T \text{ms}^{-1}$.

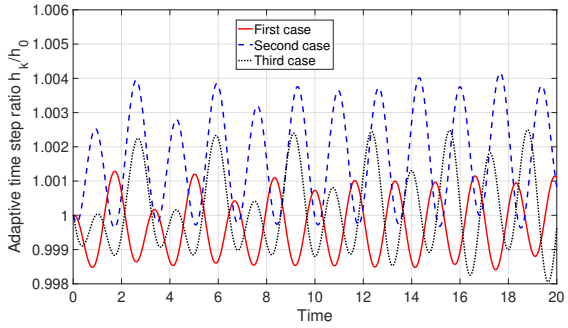

Figure 6.1: Adaptive time step behavior for all cases

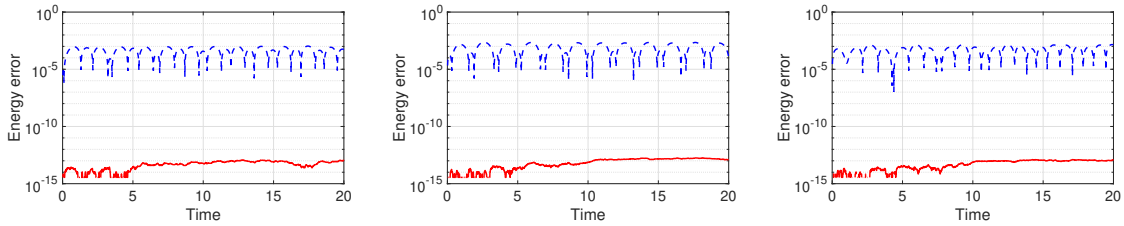

(a) First case (b) Second case (c) Third case

Figure 6.2: Energy behavior comparison (Adaptive algorithm: red, solid. Fixed algorithm: blue, dotted)

For all the cases, results from the adaptive algorithm for an initial time step of $h_0 = 0.01$ are compared with results from the fixed algorithm for a fixed step size of $h = 0.01$. Energy error comparison between fixed and adaptive time step Lie group variational integrator for the three cases are presented in Fig. 6.2. The discrete energy error plot comparison for all cases show that the adaptive time step algorithm has energy error around 10^{-13} whereas the fixed time step method has energy error around 10^{-3}. As expected, the fixed time step integrator does not conserve energy exactly but because of its symplecticity the energy error remains bounded. On the other hand, adaptive time-stepping allows our method to conserve momentum, energy and symplectic structure while staying on the configuration manifold.

In Fig. 6.1, we have plotted the ratio of the adaptive time step h_k and the initial time step h_0 for all three cases. The adaptive time step h_k behavior for this numerical example suggests that adaptive time step h_k remains bounded and doesn't decrease or increase substantially

from the initial time step of h_0. This implies that our approximations of v_k and ω_k, which depend on h_k, remain sufficiently accurate. Since time is treated as a dynamic variable in this framework, we know the adaptive time step h_k is intimately connected with the dynamics. Unlike the one or two degree of freedom examples considered in [51] and [55], the state space for our numerical example is 12 dimensional and this multi-dimensional nature of the problem makes it difficult to relate increase or decrease in adaptive time step to the dynamics.

We have also studied the mean energy error and the CPU time for the first case for three different initial time steps. As shown in Table 6.1, for all three initial time steps, the mean energy error for adaptive algorithm remains around 10^{-13} whereas for fixed time step algorithm the mean energy error increases with increase in the step size. The CPU time for for adaptive algorithm is 2-4 times more than the fixed time step algorithm. Though it is clear that if energy conservation is critical, we can use the adaptive algorithm to get energy preserving solutions for high initial step size and low computational effort.

Table 6.1: Fixed and Adaptive Algorithm Comparison for the Underwater Vehicle

Method	Time step	Mean $\lvert\Delta E\rvert$	CPU time
Adaptive	10^{-4}	8.2×10^{-13}	54.8
Algorithm	10^{-3}	1.5×10^{-13}	7.05
	10^{-2}	3.1×10^{-14}	3.08
Fixed	10^{-4}	4.0×10^{-6}	25.7
Algorithm	10^{-3}	4.7×10^{-5}	2.88
	10^{-2}	4.8×10^{-4}	0.86

6.4 Conclusions

We have derived adaptive time step variational integrators for rigid body undergoing Euclidean motion. By developing the extended Lagrangian mechanics framework for mechanical systems evolving on $\mathsf{SE}(3)$, we derive extended equations of motion for the rigid body system in continuous time. Using concepts from extended discrete mechanics, we discretize Hamilton's principle and derive the extended discrete equations of motion. The adaptive time step Lie group variational integrators are derived in both Lagrangian and Hamiltonian forms. The presented adaptive method is symplectic as well as energy and momentum-preserving while also preserving the geometry of the configuration space.

The resulting adaptive time step Lie group variational integrator is used to numerically study the motion of a conservative underwater vehicle in the presence of an attitude and position dependent potential. The simulation results demonstrate that adaptive time step algorithm exhibits superior energy performance for all three cases as compared to the fixed time step algorithm. The numerical study for different time steps show that, for smaller time step values adaptive algorithms are able to achieve significantly better energy behavior compared to their fixed time step algorithms for a similar computational cost. These adaptive time step Lie group variational integrators can be useful for applications where accurate energy prediction is essential to the dynamics or for simulating the dynamics at a lower computational cost using relatively large time steps without violating the geometric structure and invariants of motion.

Chapter 7

Symplectic Accelerated Optimization on $\mathsf{SO}(3)$

A lot of problems in the field of machine learning, robotics or statistics can be formulated as an optimization problem

$$x^* = \arg\min_{x \in X} f(x), \tag{7.1}$$

where $f : X \to \mathbb{R}$ is a differentiable function. In most of these optimization problems, the unknown parameter x is assumed to lie in a vector space, i.e., $X \subseteq \mathbb{R}^d$. However, a lot of interesting problems in robotics or computer vision involve optimizing a scalar function defined on set of rigid rotations. For example, robotic mapping problems [179] often require finding the optimal rotation matrices on the special orthogonal group $\mathsf{SO}(3)$ for solving the non-convex optimization problem in simultaneous localization and mapping.

For optimization on $\mathbb{R}^n$, one of the most popular algorithms is the gradient descent technique. This algorithm is easy to implement and it scales well to large problem sizes. However, the convergence rate can be low. The gradient descent method achieves $O(\frac{1}{n})$ convergence for general convex functions, where n is the number of iterations. Polyak [180] achieved faster convergence by introducing momentum terms at each iteration. Later, Nesterov [181] used successive gradients to achieve $O(\frac{1}{n^2})$ convergence for general convex functions. Both of these accelerated gradient methods have gained popularity because of their ability to attain best

worst-case complexity bounds. For optimization on non-Euclidean manifolds, the traditional optimization methods often employ projection or Lagrange multipliers after each iteration to ensure that the trajectories lie on the correct manifold.

Taylor and Kriegman [182] used local parametrizations instead of single global parametrizations for minimization on $\mathsf{SO}(3)$. Plumbley [183] incorporated ideas from Lie group methods to develop optimization algorithms for problems with orthogonality constraints. Abrudan *et al* [184] utilized Riemannian geometry to develop optimization algorithms on the Lie group of unitary matrices. Recently, Zhang and Sra [185] developed accelerated gradient methods on Riemannian manifolds.

Recently, a promising research direction has emerged by relating continuous dynamical systems and their governing differential equations to optimization algorithms. Using well-established results from the theory of ordinary differential equations (ODE), this approach provides a clear interpretation of optimization algorithms and their continuous approximations. Su *et al* [186] developed a framework for continuous approximation analysis of optimization algorithms and derived a second-order ODE corresponding to Nesterov's accelerated gradient method under the limit of infinitesimal time step. Building on this work, Wibisono *et al* [187] studied a more general class of ODE and corresponding accelerated gradient methods by the Bregman Lagrangian framework. Yang et el. [188] developed a unified framework to understand these optimization algorithms and provided a link to the physical systems behind these methods. Instead of starting with an optimization algorithm to derive an ODE via vanishing step size arguments, Muehlebach and Jordan [189] provided a different perspective by deriving Nesterov's accelerated gradient method by discretizing a second-order ODE with curvature dependent damping. Recently, Franca *et al* [190] developed conformal symplectic optimization algorithms which preserve the underlying symplectic geometry.

In this chapter, we present an accelerated gradient method for optimization on the special orthogonal group $\mathsf{SO}(3)$. First, we show that the classical momentum method on the Euclidean space can be constructed by utilizing the variational integrator [44] to the continuous approximation analysis of [186]. Next, in parallel to these results, it is shown that the gradient descent flow on $\mathsf{SO}(3)$ is also represented by the attitude dynamics of a rigid body. We discretize it with a Lie group variational integrator [100, 191], which preserves the symplecticity of Hamiltonian mechanics and Lie group structures of the configuration manifold, to construct a symplectic accelerated gradient method for optimization on $\mathsf{SO}(3)$. Finally, we apply the proposed accelerated gradient methods for two optimization problems on $\mathsf{SO}(3)$ to illustrate the acceleration achieved by our methods compared to the conventional gradient descent.

7.1 Optimization on $\mathbb{R}^n$

We first formulate the optimization problem on $\mathbb{R}^n$ and review the existing gradient-based optimization methods. We then use ideas from unified continuous approximation analysis to connect the optimization algorithms to continuous physical systems. Finally, we show how discrete mechanics and variational integrators framework can be used to derive the classical momentum method from a nonlinear generalization of a damped harmonic oscillator.

7.1.1 Gradient-Based Optimization Techniques

Consider the following minimization problem

$$q^* = \arg\min_{q \in \mathbb{R}^n} f(q), \tag{7.2}$$

for a real valued scalar function $f : \mathbb{R}^n \to \mathbb{R}$.

We present a brief review of existing gradient-based optimization techniques for the minimization problem on $\mathbb{R}^n$ formulated above.

1. **Gradient descent method**: a gradient descent method is a first order optimization algorithm used for searching the minimum of a objective function. For objective function $f : \mathbb{R}^n \to \mathbb{R}$, this algorithm searches for the local minimum by taking steps along the negative of the gradient direction. The gradient descent method is given by

$$q_{k+1} = q_k - \epsilon \nabla f(q_k), \tag{7.3}$$

   for $\epsilon > 0$.

2. **Classical momentum method**: a gradient descent with additional momentum terms, also known as classical momentum method, is given by

$$p_{k+1} = \mu p_k - \epsilon \nabla f(q_k), \tag{7.4}$$

$$q_{k+1} = q_k + p_{k+1}, \tag{7.5}$$

   where $\mu \in (0, 1)$ is the momentum factor, $\epsilon > 0$ is the stepsize or the learning rate. This reduces to the above gradient descent when $\mu = 0$.

3. **Nesterov's accelerated gradient**: the Nesterov's accelerated gradient method is constructed by evaluating the gradient of the above momentum method at a predicted

point as follows.

$$p_{k+1} = \mu p_k - \epsilon \nabla f(q_k + \mu p_k), \tag{7.6}$$

$$q_{k+1} = q_k + p_{k+1}. \tag{7.7}$$

7.1.2 Dynamic System Interpretation

We now use the continuous approximation analysis approach [186], to derive a continuous dynamical system corresponding to the classical momentum method. First we eliminate the momentum variables by substituting p_{k+1} from (7.5) into (7.4) to obtain

$$(q_{k+1} - q_k) - \mu(q_k - q_{k-1}) + \epsilon \nabla f(q_k) = 0. \tag{7.8}$$

Let $t = kh$ for a stepsize h. Using the following Taylor series expansions

$$q_{k+1} - q_k = h\dot{q}(t) + \frac{h^2}{2}\ddot{q}(t) + o(h^3),$$
$$q_k - q_{k-1} = h\dot{q}(t) - \frac{h^2}{2}\ddot{q}(t) + o(h^3),$$

equation (7.8) is converted into the following continuous differential equation:

$$\frac{(1+\mu)h^2}{2\epsilon}\ddot{q}(t) + \frac{(1-\mu)h}{\epsilon}\dot{q}(t) + \nabla f(q(t)) + O(h) = 0. \tag{7.9}$$

If we consider the limit of $h \to 0$, then the above equation can be seen as the equation of motion for a spring-mass-damper system,

$$m\ddot{q}(t) + c\dot{q}(t) + \nabla f(q(t)) = 0, \tag{7.10}$$

with the mass parameter $m = \frac{(1+\mu)h^2}{2\epsilon}$ and the damping parameter $c = \frac{(1-\mu)h}{\epsilon}$. Both of these parameters are finite for $h, \epsilon \to 0$.

Gradient descent method The above reduces to the gradient descent method by taking $\mu = 0$ and $h = o(\epsilon)$, which lead to $m = 0$ and $c = c_0$. Thus, the continuous dynamical system corresponding to the gradient descent method is the following first order ODE,

$$\dot{q}(t) + \frac{1}{c}\nabla f(q(t)) = 0. \tag{7.11}$$

Nesterov's accelerated gradient method For Nesterov's method, take $\mu = o(\sqrt{\epsilon})$ and $h = o(\epsilon)$ to yield $m = m_0$ and $c = \frac{c_0}{t}$. Thus, the continuous dynamical system corresponding to the Nesterov's method is

$$\ddot{q}(t) + \frac{c_0}{m_0}\frac{\dot{q}(t)}{t} + \frac{1}{m_0}\nabla f(q(t)) = 0, \tag{7.12}$$

which shows that the damping coefficient is reduced over time.

7.1.3 Momentum Method as a Variational Integrator

Now we show that the classical momentum method can be constructed as a variational integrator. Motivated by (7.10), we consider a Lagrangian system with the following Lagrangian and the forcing term:

$$L(q, \dot{q}) = \frac{\dot{q}^2}{2} - \eta f(q), \tag{7.13}$$

$$f_L(q, \dot{q}) = -\gamma \dot{q} \tag{7.14}$$

for $\eta, \gamma > 0$.

We derive a variational integrators for the Lagrangian system described above. Use the rectangle rule for the discrete Lagrangian to obtain

$$L_d(q_k, q_{k+1}) = h\left[\frac{1}{2}\left(\frac{q_{k+1} - q_k}{h}\right)^2 - \eta f(q_k)\right], \tag{7.15}$$

along with the following discrete forces

$$f_d^+(q_k, q_{k+1}) = 0, \quad f_d^-(q_k, q_{k+1}) = -\gamma(q_{k+1} - q_k). \tag{7.16}$$

Substituting these into forced discrete Euler-Lagrange equations

$$\begin{aligned} p_k &= \frac{q_{k+1} - q_k}{h} + h\eta\nabla f(q_k) + \gamma(q_{k+1} - q_k), \\ p_{k+1} &= \frac{q_{k+1} - q_k}{h}. \end{aligned}$$

Rearranging these,

$$p_{k+1} = \frac{1}{1+\gamma h}p_k - \frac{\eta}{1+\gamma h}\nabla f(q_k), \tag{7.17}$$

$$q_{k+1} = q_k + hp_{k+1}. \tag{7.18}$$

Setting $h = 1$, the above variational integrator is equivalent to the classical momentum method, (7.4)–(7.5), with the momentum factor $\mu = \frac{1}{1+\gamma} \in (0, 1)$ and the step size $\epsilon = \frac{\eta}{1+\gamma} > 0$.

7.2 Optimization on $\mathsf{SO}(3)$

In this section, we present a gradient-based optimization method on $\mathsf{SO}(3)$. Similar to the previous section, we first formulate the optimization problem on $\mathsf{SO}(3)$ and review a gradient descent method on $\mathsf{SO}(3)$. We use the continuous approximation analysis to derive the continuous ODE on $\mathsf{SO}(3)$ corresponding to this gradient descent. This is discretized by a Lie group variational integrator to construct a symplectic accelerated optimization scheme on $\mathsf{SO}(3)$.

7.2.1 Mathematical Preliminaries

The special orthogonal group is defined by

$$\mathsf{SO}(3) = \{R \in \mathbb{R}^{3\times 3} | R^T R = I_{3\times 3},\ \det(R) = +1\}.$$

The Lie algebra of $\mathsf{SO}(3)$, denoted by $\mathfrak{so}(3)$, is the set of all 3×3 skew-symmetric matrices, i.e.,

$$\mathfrak{so}(3) = \{\xi \in \mathbb{R}^{3\times 3} | \xi^T = -\xi\}.$$

The hat map $\wedge : \mathbb{R}^3 \to \mathbb{R}^3$ is defined such that $\hat{x}y = x \times y$ for any $x, y \in \mathbb{R}^3$. The inverse of the hat map is denoted by the vee map $\vee : \mathfrak{so}(3) \to \mathbb{R}^3$.

The tangent space of $\mathsf{SO}(3)$ at $R \in \mathsf{SO}(3)$ is given by $\mathsf{T}_R\mathsf{SO}(3) = \{V \in \mathbb{R}^{3\times 3} | R^T V + V^T R = 0\}$. It is isomorphic to $\mathbb{R}^3$ via left trivialization by setting $V_i = R\hat{v}_i$ for $i \in \{1, 2\}$ and $\langle V_1, V_2 \rangle = v_1^T v_2$ for any $V_1, V_2 \in \mathsf{T}_R\mathsf{SO}(3)$. Also, $\mathsf{SO}(3)$ is locally diffeomorphic to $\mathbb{R}^3$ from

the exponential map:

$$\exp \hat{\eta} = I_{3\times 3} + \sin \|\eta\| \hat{a} + (1 - \cos \|\eta\|)\hat{a}^2,$$

for the unit vector defined as $a = \frac{\eta}{\|\eta\|} \in \mathbb{R}^3$.

7.2.2 Gradient-Based Optimization on $\mathsf{SO}(3)$

For a scalar function defined on the special orthogonal group $\mathsf{SO}(3)$, i.e. $f : \mathsf{SO}(3) \to \mathbb{R}$, the optimization problem is formulated as

$$R^* = \underset{R\in\mathsf{SO}(3)}{\arg\min}\, f(R). \tag{7.19}$$

The gradient descent method on $\mathsf{SO}(3)$ is constructed as follows. Using the left trivialization, the infinitesimal variation of f at R along $\delta R = R\hat{\eta}$ for $\eta \in \mathbb{R}^3$ is given by

$$\delta f(R) = \left.\frac{d}{d\epsilon}\right|_{\epsilon=0} f(R \exp(\epsilon\hat{\eta})). \tag{7.20}$$

Let $\frac{\partial f}{\partial R} \in \mathbb{R}^{3\times 3}$ be defined such that

$$\left[\frac{\partial f(R)}{\partial R}\right]_{ij} = \frac{\partial f(R)}{\partial [R]_{ij}},$$

for $i, j \in \{1, \dots 3\}$, where $[\cdot]_{ij}$ denotes the i, j-th element of a matrix. Since $\exp(\epsilon\hat{\eta}) = I_{3\times 3} + \epsilon\hat{\eta} + \mathcal{O}(\epsilon^2)$, (7.20) can be rewritten as

$$\delta f(R) = \mathrm{tr}\left[\frac{\partial f(R)}{\partial R}^T R\hat{\eta}\right].$$

Using the identity, $\mathrm{tr}[A\hat{x}] = x^T(A^T - A)^\vee$ for any $x \in \mathbb{R}^3$ and $A \in \mathbb{R}^{3\times 3}$, it is rewritten as

$$\delta f(R) = \eta^T \nabla_L f(R), \tag{7.21}$$

where $\nabla_L f(R) \in \mathbb{R}^3$ is defined as

$$\nabla_L f(R) = \left(R^T \frac{\partial f(R)}{\partial R} - \frac{\partial f(R)}{\partial R}^T R \right)^\vee, \tag{7.22}$$

which is defined as the left trivialized gradient of $f(R)$.

Consequently, the gradient descent algorithm on $\mathsf{SO}(3)$ is given by

$$R_{k+1} = R_k \exp(-\alpha \nabla_L f(R)), \tag{7.23}$$

for $\alpha > 0$, which is comparable to (7.3).

Analogous to (7.4)–(7.5), an accelerated, momentum method on $\mathsf{SO}(3)$ can be written as

$$R_{k+1} = R_k \exp(\hat{\Omega}_{k+1}), \tag{7.24}$$

$$\Omega_{k+1} = \mu \Omega_k - \epsilon \nabla_L f(R_k). \tag{7.25}$$

Similar to the classical momentum method (7.4)-(7.5), this accelerated gradient method on $\mathsf{SO}(3)$ also uses momentum terms to update the rotation matrix R_k with acceleration. The key difference between these methods is how the variable is updated. In contrast to the optimization on $\mathbb{R}^n$, here the rotation matrix is updated by the group operation, i.e., the matrix multiplication with the exponential map, to ensure that the updated matrix, namely R_{k+1} also lie on $\mathsf{SO}(3)$.

7.2.3 Dynamic System Interpretation

We apply continuous approximation analysis to derive the continuous ODE corresponding to the above accelerated gradient method. Using Taylor series expansions for R_{k+1}, Ω_{k+1} and $\exp(\hat{\Omega}_{k+1})$ in (7.24)-(7.25) along with $t = kh$,

$$R_k + h\dot{R}(t) + o(h^2) = R_k(I + h\hat{\Omega}_k) + o(h^2),$$
$$\Omega_k + h\dot{\Omega}(t) + o(h^2) = \mu\Omega_k - \epsilon\nabla_L f(R_k).$$

Substituting these back to (7.24)–(7.25),

$$\dot{R} = R\hat{\Omega}, \tag{7.26}$$
$$\dot{\Omega} = \left(\frac{\mu - 1}{h}\right)\Omega - \left(\frac{\epsilon}{h}\right)\nabla_L f(R). \tag{7.27}$$

The first equation is the same as the kinematic equation for rigid body dynamics. The next equation describes how the angular momentum changes over time.

Gradient descent Next, by setting $\mu = 0$, (7.27) reduces to

$$h\dot{\Omega} = -\Omega - \epsilon\nabla f(R). \tag{7.28}$$

Further, $h \to 0$ gives $\Omega = -\epsilon\nabla_L f(R)$. Substituting, we obtain

$$\dot{R} = R(-\epsilon\nabla_L f(R))^\wedge, \tag{7.29}$$

which is the continuous ODE corresponding to the gradient descent method on SO(3).

Similar with the spring-mass-damper case discussed in Section 7.1.2, we study the connection

between the continuous system of (7.27) and the attitude dynamics of a rigid body. We consider the Lagrangian formulation for the attitude dynamics of a rigid body under the influence of a potential energy $f(R)$ and a linear dissipation. The Lagrangian and the external moment from dissipation for such a system are chosen as

$$L(R,\Omega) = \frac{1}{2}\Omega^T J\Omega - \eta f(R), \tag{7.30}$$

$$\tau(R,\Omega) = -\gamma\Omega, \tag{7.31}$$

for a symmetric, positive-definite inertia matrix $J \in \mathbb{R}^{3\times3}$ and $\eta > 0$. From the Lagrange-d'Alembert principle, the corresponding Euler-Lagrange equation is given by

$$J\dot{\Omega} + \Omega \times J\Omega = -\eta\nabla_L f(R) - \gamma\Omega, \tag{7.32}$$

which along with the rotational kinematic equations $\dot{R} = R\hat{\Omega}$.

If $J = hI_{3\times3}$, the cross term vanishes, i.e., $\Omega \times J\Omega = 0$. Therefore, the above equation reduces to (7.27), with $\eta = \epsilon$ and $\gamma = 1 - \mu$. Thus, the continuous system corresponding to the accelerated gradient method (7.24)–(7.25) is a Lagrangian system with linear dissipation and it can be interpreted as the attitude dynamics of a rigid body evolving on SO(3).

7.2.4 Symplectic Accelerated Optimization on SO(3)

In this subsection we discretize the continuous Lagrangian system (7.30) using Lie group variational integrators to derive a symplectic, accelerated gradient methods on SO(3).

In geometric numerical integration, Lie group methods [95] are a class of structure-preserving numerical methods that conserve the Lie group structures. This is achieved by utilizing the group operation to update group elements. These Lie group methods were first adopted in

the variational integrators framework in [192] to integrate the structure-preserving aspects of Lie-group methods and variational integrators. This is applied to the rigid body dynamics in [191]. They exhibit the desirable symplectic, momentum-preserving features of variational integrators, while preserving the group structures. The basics of variational integrators and Lie group methods can be reviewed in [193].

Similar with [191], let the discrete Lagrangian corresponding to (7.30) be

$$L_d(R_k, F_k) = \frac{1}{h}\text{tr}[(I_{3\times 3} - F_k)J_d] - h\eta f(R_{k+1}),$$

with the discrete toques

$$\tau_d^+ = 0, \quad \tau_d^- = h\tau(R_k, \Omega_k),$$

Here, $F_k \in \mathsf{SO(3)}$ is defined as the relative attitude change between two steps, i.e., $F_k = R_k^T R_{k+1}$.

The corresponding discrete Euler-Lagrange equations are given by

$$h(J\Omega_k + h\tau_k)^\wedge = F_k J_d - J_d F_k^T, \tag{7.33}$$

$$R_{k+1} = R_k F_k, \tag{7.34}$$

$$J\Omega_{k+1} = F_k^T(J\Omega_k + h\tau_k) - h\eta\nabla_L f(R_{k+1}). \tag{7.35}$$

where $J_d = \frac{1}{2}\text{tr}[J]I_{3\times 3} - J \in \mathbb{R}^{3\times 3}$.

Given (R_k, Ω_k), the implicit equation (7.33) is solved for F_k, and then the updated position R_{k+1} and the angular velocity Ω_{k+1} are obtained from the explicit equations (7.34) and (7.35), respectively. Thees yield a discrete flow $(R_k, \Omega_k) \to (R_{k+1}, \Omega_{k+1})$ for accelerated optimization. At (7.34), R_{k+1} is constructed by the product of two rotation matrices. As such, R_{k+1} is guaranteed to be on $\mathsf{SO(3)}$ up to round-off errors.

The implicit equation (7.33) can be solved by a numerical iteration on $\mathbb{R}^3$. However, as discussed above, we can set the inertia matrix as a diagonal matrix $J = jI_{3\times 3}$ for any $j \in \mathbb{R}$. Then, (7.33) reduces to

$$h(j\Omega_k + h\tau_k)^\wedge = \frac{j}{2}(F_k - F_k^T),$$

which yields an explicit solution of

$$F_k = \exp(\frac{\sin^{-1}\|hg_k\|}{\|g_k\|}g_k), \tag{7.36}$$

with $g_k = \Omega_k + \frac{h}{j}\tau_k = (1 - \frac{\gamma h}{j})\Omega_k$.

Also, (7.35) is rewritten as

$$\Omega_{k+1} = (1 - \frac{\gamma h}{j})F_k^T\Omega_k - \frac{h\eta}{j}\nabla_L f(R_{k+1}). \tag{7.37}$$

In short, the proposed symplectic accelerated gradient descent scheme on $\mathsf{SO(3)}$ is composed of (7.34), (7.36), and (7.37). As constructed as a Lie group variational integrator, this preserves the symplectic structure underlying the Lagrangian system evolving on $\mathsf{SO(3)}$, and it ensures that the optimized rotation matrix remains on $\mathsf{SO(3)}$.

7.3 Numerical Examples

In this section, we consider two numerical examples to evaluate the numerical performance of the proposed accelerated gradient methods. We have compared gradient descent (GD) (7.23), accelerated gradient descent (AGD) (7.24)-(7.25) and symplectic accelerated gradient descent (SAGD) (7.34)-(7.37).

7.3.1 Trace Function

In this subsection, we study the numerical performance of our proposed accelerated gradient methods for minimization of $f(R) = -\text{tr}[X^T R]$ for a given matrix $X \in \mathbb{R}^{3\times 3}$. This appears in the attitude determination from vector measurements, and it has the following analytic solution. The optimal rotation matrix is given by $R^* = UV^T$ where $U, V \in \mathsf{SO(3)}$ are obtained from the proper singular value decomposition of X given by $X = USV^T$ with a diagonal matrix $S \in \mathbb{R}^{3\times 3}$ [194].

We choose

$$X = \begin{bmatrix} 45 & 1 & 0 \\ 0 & 20 & 0 \\ 0 & 0 & 2 \end{bmatrix}. \tag{7.38}$$

The corresponding optimization results are illustrated at Figure 7.1, which shows that the proposed SAGD algorithm achieves faster convergence than both AGD and GD algorithms on $\mathsf{SO(3)}$. The step size α for GD has been tuned to find the optimal $\alpha = 0.024$. Based on that α, we set $h = \epsilon = \sqrt{0.024}$ along with $\mu = 0.05$ for AGD algorithm which leads to faster convergence compared to GD. Finally, using $j = h = \sqrt{0.125}, \epsilon = 2h$ and $\gamma = 0.9090$ we achieve faster convergence than both AGD and GD algorithms.

We have studied the numerical performance of this choice of accelerated optimization parameters for a variety of X and SAGD performs better than AGD and GD for all those cases. Depending on the particular case, these parameters can be tuned slightly to improve the convergence even further but that may introduce oscillations.

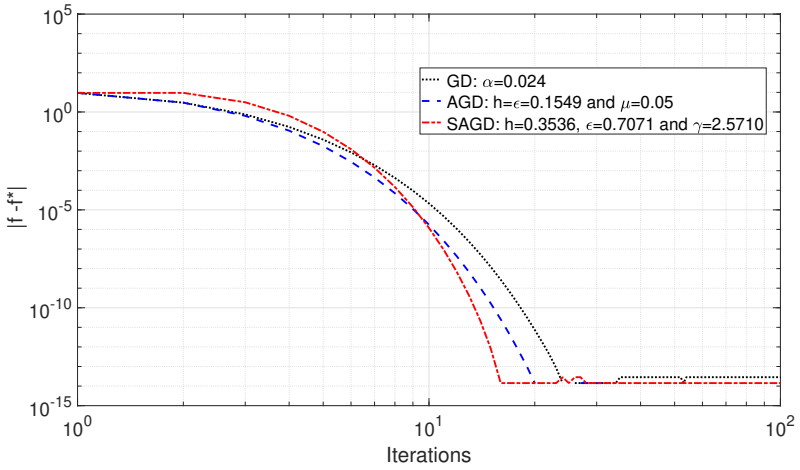

Figure 7.1: Convergence comparison between gradient descent (GD), accelerated gradient descent (AGD) and symplectic accelerated gradient descent (SAGD) on $\mathsf{SO}(3)$ for minimization of $f(R) = -\mathrm{tr}[X^T R]$

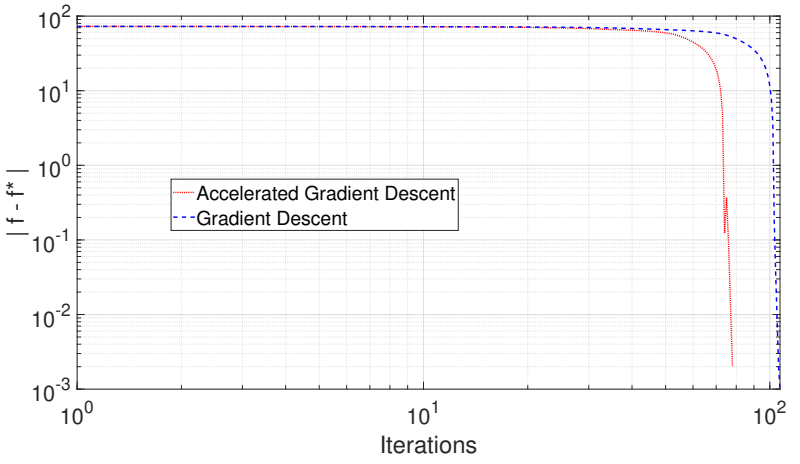

Figure 7.2: Convergence comparison between AGD and GD on $\mathsf{SO}(3)$ for spherical shape matching problem

7.3.2 Spherical Shape Matching

In this subsection, we apply GD and AGD for spherical shape correlation and matching considered in [195]. We consider an object (without holes) embedded in $\mathbb{R}^3$ whose shape can be described by deforming the sphere. Specifically, let $f(x) : \mathsf{S}^2 \to \mathbb{R}$ represent the shape, as the elevation for each direction x on the unit-sphere $\mathsf{S}^2 = \{x \in \mathbb{R}^3 \,|\, \|x\| = 1\}$. Also, let $g(x) : \mathsf{S}^2 \to \mathbb{R}$ denote the shape function when the object is rotated.

The spherical shape matching problem involves finding the rotation matrix $R \in \mathsf{SO(3)}$ that minimizes the discrepancy between $g(x)$ and $f(x)$ rotated by R, i.e.

$$\mathcal{J}(R) = \frac{1}{2}\|g(x) - f(R^T x)\|_{\mathsf{S}^2}^2,$$

where $\|\cdot\|_{\mathsf{S}^2}$ denote the norm for the functions defined on S^2. By expanding the norm,

$$\mathcal{J}(R) = \frac{1}{2}\|g(x)\|_{\mathsf{S}^2}^2 + \frac{1}{2}\|f(x)\|_{\mathsf{S}^2}^2 - \left\langle g(x), f(R^T x)\right\rangle_{\mathsf{S}^2},$$

The objective is to find the true rotation matrix R that minimizes the cost function $\mathcal{J}(R)$, or equivalently, maximizes the measure of correlation function $\mathcal{C}(R) = \left\langle g(x), f(R^T x)\right\rangle_{\mathsf{S}^2}$. A computational approach to evaluate the correlation function has been proposed in [195] using harmonic analysis on $\mathsf{SO(3)}$, with a numerical example for an Earth elevation map.

Here, we adopt the same numerical example for spherical shape matching of the Earth elevation map. But, we implement the presented AGD. For the numerical comparison, we have used $\alpha = 0.0002$ for GD and $\mu = 0.15$ along with $h = \sqrt{(\alpha_{optimal})}$ and $\epsilon = 1.2\sqrt{(\alpha_{optimal})}$ for AGD algorithm. The comparison between the gradient descent and accelerated gradient method in Figure 7.2 demonstrates how the AGD converges in fewer iterations. In Figure 7.2, we have shown how the correlation function and its gradient evolve over the iterations.

Both plots show how for the first few iterations both methods give similar updates but as the number of iterations increases, effects of the additional momentum term become visible which results in faster convergence.

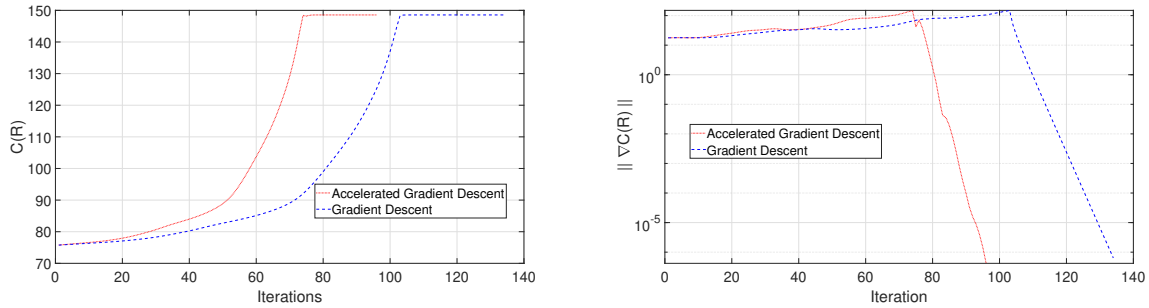

(a) Function value (b) Gradient

Figure 7.3: Comparison of function and gradient value plots over iterations

7.4 Conclusions

We have presented accelerated gradient methods for optimization on $\mathsf{SO(3)}$. Similar to the classical momentum method on $\mathbb{R}^n$, we include additional momentum term in the standard gradient descent on $\mathsf{SO(3)}$ to achieve faster convergence. Using continuous approximation analysis tools, first we derived the continuous system corresponding to classical momentum on $\mathbb{R}^n$ and then discretized the continuous system using variational integrators to show that classical momentum method on $\mathbb{R}^n$ is a structure-preserving method. We also derived the continuous systems corresponding to both gradient descent and proposed accelerated gradient method on $\mathsf{SO(3)}$ and demonstrated that the continuous system is a Lagrangian rigid body system evolving on $\mathsf{SO(3)}$ under the influence of potential forcing and dissipation. We discretized the continuous time system on $\mathsf{SO(3)}$ using the Lie group variational integrator framework and presented the symplectic accelerated gradient method.

The proposed algorithms are used to numerically study two optimization problems on $\mathsf{SO}(3)$. First, we have applied these methods to solve the benchmark problem of a trace function to demonstrate that the symplectic accelerated gradient method converges faster than both accelerated gradient descent and gradient descent on $\mathsf{SO}(3)$. We have also applied accelerated gradient descent to the spherical shape matching of earth elevation map and the numerical results show that the accelerated gradient method outperforms the gradient descent method. For future works, we plan to study how the different choice of the discrete Lagrangian yield a different form of optimization schemes.

Chapter 8

Performance Assessment of Energy-preserving, Adaptive Time Step Variational Integrators

The main goal of this chapter is to understand the numerical performance of energy-preserving, adaptive time step variational integrators. First, we focus on the discrete energy error behavior from a computational perspective. We obtain a conservative bound on the discrete energy error based on the error propagation from the residual of the discrete energy equation and compare the energy performance of the adaptive algorithm with fixed time-step variational integrators. We then use variable precision arithmetic in the adaptive algorithm to show how the energy performance can be further improved by using more significant digits in the computation. Motivated by this improvement in energy performance, we approach the problem from a theoretical perspective by investigating the stability of the adaptive algorithm. We first use time-transformation to represent the adaptive algorithm as the fixed time-step algorithm and then apply backward error analysis tools in the transformed setting.

The early development of backward error analysis in 1960s was motivated by numerical linear algebra applications and it was mainly used as a tool for evaluating the propagation of rounding errors in matrix algorithms. Although Wilkinson [196] first used it in the context of eigenvalue problems, the underlying idea of backward error analysis has been also

applied to numerical integrators for dynamical systems. Truncation errors introduced by the numerical integrator play the same role as rounding errors do in the numerical linear algebra setting. The focus in the backward error analysis of a numerical integrator is the question: what dynamical system does the numerical integrator solve? Thus, instead of studying the difference between the trajectories obtained using the numerical integrator and the exact solution, we look for a nearby dynamical system which would be solved exactly by the numerical integrator. For dynamical systems with underlying geometric structure, we would like the modified system to also possess similar features. The existence of such a nearby dynamical system has direct implications for the accurate long-time behavior of the long-time simulation.

Sanz-Serna [197] first applied tools from backward error analysis to symplectic integrators and showed that numerical trajectories from symplectic integrators can be interpreted as the exact solution of a perturbed Hamiltonian system. Reich [37] used a recursive definition of modified vector fields to provide a unifying framework for the backward error analysis of GNI methods. Hairer [198] developed variable time-step symplectic integrators and proved backward stability of the adaptive algorithm by using time transformations. Recently, Vermeeran [199] studied the backward stability of variational integrators from the Lagrangian perspective.

This chapter is organized as follows. In Section 8.1, we study the energy behavior of the adaptive algorithm and the effect of variable precision arithmetic on the conservation properties. In Section 8.2, we present a time transformation to interpret the adaptive algorithm as a fixed time-step variational integrator in the transformed setting. Finally, in Section 8.3, we provide concluding remarks and discuss remaining challenges in the backward error analysis of adaptive algorithms.

8.1 Energy Behavior

As shown in Section 3.1.2, the extended discrete equations for the adaptive time step variational integrators conserve the discrete energy E_k exactly. Unfortunately, numerically the discrete energy equation is not solved exactly and the residual from this equation builds up as the iterations increase. Such a build up of discrete energy error might lead to a substantial enough energy error and that can defeat the purpose of the adaptive time-stepping algorithm. Thus, we need to investigate the long-term behavior of energy error.

For a given initial configuration $(t_0, \mathbf{q}_0, \mathbf{p}_0, E_0)$, the discrete energy E_k after k adaptive time steps can be written as

$$E_k = E_0 + \sum_{i=1}^{k} (E_i - E_{i-1}) \tag{8.1}$$

We can use this expression to obtain a conservative bound on the discrete energy error

$$|E_k - E_0| \leq \sum_{i=1}^{k} |E_k - E_{k-1}| \leq k \max_i |E_i - E_{i-1}| \tag{8.2}$$

where $\max_i |E_i - E_{i-1}|$ is the maximum discrete energy error introduced in one iteration during the whole numerical simulation. Using this conservative bound, we can compare the energy behavior of fixed time-step variational integrators with the worst case scenario for the adaptive algorithm. For example, if we consider an example where the fixed time-step algorithm exhibits discrete energy error around 10^{-6} then the adaptive algorithm, with 10^{-18} accuracy in solving discrete energy equation, will exhibit better energy performance for 10^{12} steps

$$k = \frac{10^{-6}}{\max_i |E_i - E_{i-1}|} = \frac{10^{-6}}{10^{-18}} = 10^{12} \ steps \tag{8.3}$$

It is important to note that the discrete energy error bound in (8.2) is very conservative because it assumes the worst case scenario where at each time-step the energy error is of the

same sign and maximum magnitude. The numerical results for a particle in a double-well potential example shows how using Variable Precision Arithmetic (VPA) with 32 significant digits results in exactly zero discrete energy error. The adaptive time step behavior also matches with previous results. Based on these results, we have shown how increasing the precision can lead to nearly exact energy behavior. It is important to note that using VPA makes the adaptive algorithm computationally prohibitive. The key takeaway from these results obtained using VPA is that, if solved with enough precision, the adaptive algorithm can conserve the discrete energy. This also points to the importance of studying the numerical stability of the adaptive algorithm.

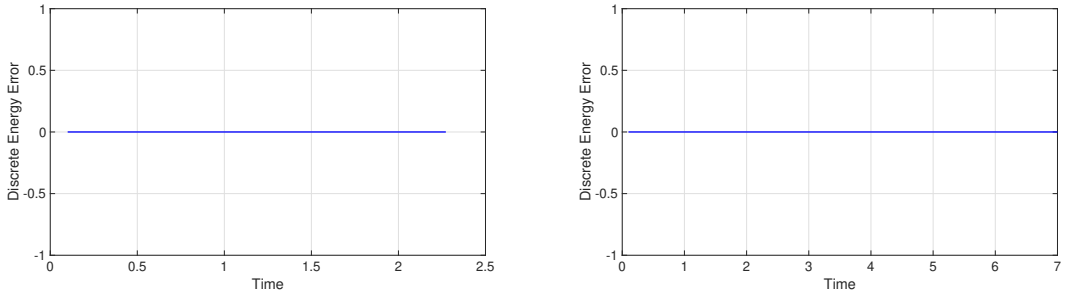

(a) $q(0) = 0.74,\ \dot{q}(0) = 0$ (b) $q(0) = 0.995,\ \dot{q}(0) = 0$

Figure 8.1: Discrete energy error results using VPA

8.2 Time Transformation

In this section, we introduce a time-transformation from the physical time t to a fictitious time a and represent the energy-preserving, adaptive time step variational integrator as a fixed time-step variational integrator in the transformed setting. Using ideas from the extended Lagrangian mechanics, we interpret the parameterization of $t = t(a)$ in terms of the independent variable a as a time transformation. For such a time transformation, i.e. $t \to a$, the configuration in the transformed setting is given by $\bar{q}(a) = (q(a), t(a))$. For this

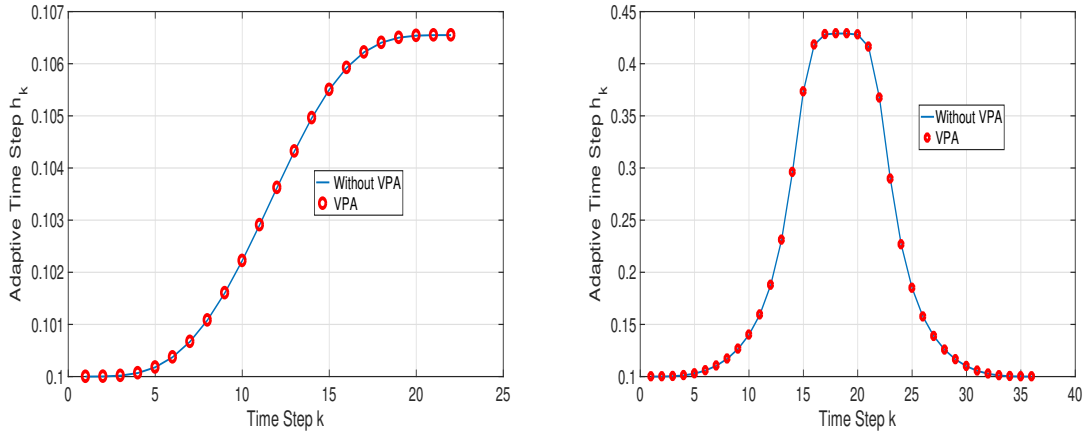

(a) $q(0) = 0.74,\ \dot{q}(0) = 0$ (b) $q(0) = 0.995,\ \dot{q}(0) = 0$

Figure 8.2: adaptive time step behavior using VPA

transformation, we introduce

$$\bar{L}((\bar{q}(a), \bar{q}'(a))) = t'(a)L(q(t), \dot{q}(t)) = t'(a)L\left(q(a), \frac{q'(a)}{t'(a)}\right) \tag{8.4}$$

where we have used $\dot{q}(t) = \frac{q'(a)}{t'(a)}$. The Euler-Lagrange equations in the transformed setting are

$$\frac{\partial \bar{L}}{\partial q} - \frac{d}{da}\left(\frac{\partial \bar{L}}{\partial q'}\right) = t'(a)\frac{\partial L}{\partial q} - \frac{d}{da}\left(t'(a)\frac{\partial L}{\partial \dot{q}}\frac{1}{t'(a)}\right) = t'(a)\left(\frac{\partial L}{\partial \dot{q}} - \frac{d}{dt}\left(\frac{\partial L}{\partial \dot{q}}\right)\right) = 0 \tag{8.5}$$

$$\frac{\partial \bar{L}}{\partial t} - \frac{d}{da}\left(\frac{\partial \bar{L}}{\partial t'}\right) = -\frac{d}{da}\left(L\left(q(a), \frac{q'(a)}{t'(a)}\right) + t'(a)\frac{\partial L}{\partial \dot{q}}(-\frac{\dot{q}}{t'(a)})\right) = t'(a)\frac{d}{dt}\left(\frac{\partial L}{\partial \dot{q}} \cdot \dot{q} - L\right) = 0 \tag{8.6}$$

Thus, the Euler-Lagrange equations in the transformed setting lead to the original Euler-Lagrange equation along with the redundant energy equation. Although, these equations are the same as the extended Euler-Lagrange equations, it is important to understand the above equations as Euler-Lagrange equations in the transformed setting. This interpretation will play a key role in the following Lemma about the equivalence of trajectories of the original

Lagrangian system and the transformed system.

Lemma 1: Let $(q(t), \dot{q}(t))$ and $(\bar{q}(a), \dot{\bar{q}}(a))$ be the solutions to the Euler-Lagrange equations corresponding to the physical Lagrangian L and the extended Lagrangian $\bar{L}$ respectively. Then,

$$\bar{q}(T) = q(\alpha(T))$$

where $\alpha(T) = \int_0^T t'(a)da$.

Proof: This follows from the fact that $\bar{q}(T)$ and $q(\alpha(T))$ satisfy the original Euler-Lagrange equation with same initial conditions.

Consider a discrete trajectory on the extended space with $\Delta a = a_{k+1} - a_k$. The discrete extended action $\bar{S}_d$ approximates the action integral

$$\bar{S}_d = \sum_{i=1}^{N} \bar{L}_d(\bar{q}_k, \bar{q}_{k+1}) \approx \int_{a_0}^{a_f} \bar{L}(\bar{q}(a), \dot{\bar{q}}(a))da \tag{8.7}$$

where $\bar{q}_k = (q_k, t_k)$ and the extended discrete Lagrangian is given by

$$\bar{L}_d = \Delta a \left[\bar{L}\left(\frac{\bar{q}_k + \bar{q}_{k+1}}{2}, \frac{\bar{q}_{k+1} - \bar{q}_k}{\Delta a}\right)\right] \approx \int_{a_k}^{a_{k+1}} \bar{L}(\bar{q}(a), \bar{q}'(a))\ da \tag{8.8}$$

The resulting discrete Euler-Lagrange equations are given by

$$\frac{\partial \bar{L}_d(\bar{q}_{k-1}, \bar{q}_k)}{\partial q_k} + \frac{\partial \bar{L}_d(\bar{q}_k, \bar{q}_{k+1})}{\partial q_k} = 0 \tag{8.9}$$

$$\frac{\partial \bar{L}_d(\bar{q}_{k-1}, \bar{q}_k)}{\partial t_k} + \frac{\partial \bar{L}_d(\bar{q}_k, \bar{q}_{k+1})}{\partial t_k} = 0 \tag{8.10}$$

These variational integrators with a fixed time-step Δa in the transformed setting are equivalent to the energy-preserving, adaptive time step variational integrators. This equivalence

will allow us to apply established results from backward error analysis of fixed time-step variational integrators.

8.3 Conclusions

We have presented a performance assessment of energy-preserving, adaptive time step variational integrators in this chapter. From the extended discrete Euler-Lagrange equations, we obtained a conservative bound on the discrete energy error. We also implemented adaptive algorithm using VPA to demonstrate exact discrete energy conservation. Motivated by these numerical results, we proposed a time transformation approach to investigate the numerical stability of the adaptive algorithm. Using equivalence of trajectories, we derived the energy-preserving, adaptive time step variational integrators as fixed time-step variational integrators in the transformed setting.

The interpretation of the adaptive algorithm as a fixed time-step algorithm in a transfomed setting will allow us to use results from backward error analysis results from Vermeeren [199]. Apart from the adaptive nature of the algorithm, backward error analysis of energy-preserving, adaptive time step variational integrators has two challenges. First, these algorithms are derived from Lagrangian perspective and hence, the governing Euler-Lagrange equations are second-order. The second challenge is the unique nature of the adaptive algorithm where the time transformation map $t(a)$ is not explicitly given. In future work, we plan to build on the work presented in this chapter to tackle these two challenges and investigate the backward stability of the adaptive algorithm.

Chapter 9

Conclusions

9.1 Summary

In summary, this dissertation develops a variety of structure-preserving algorithms for mechanical systems. The key idea is to derive energy-preserving, adaptive time step variational integrators from discretized variational principles in the extended Lagrangian mechanics framework. These methods are applied to a variety of Lagrangian/Hamiltonian dynamical systems.

A review of structure-preserving methods and their engineering applications has been presented in Chapter 2. We have provided an overview of existing GNI methods and their capabilities in an accessible way, while adding perspectives and application examples from the literature. This survey is intended to provide a gateway into the field for practitioners.

Energy-preserving variational integrators for forced Lagrangian systems are presented in Chapter 3. We presented the Lagrange-d'Alembert principle in the extended phase space and derived adaptive time step, energy-preserving variational integrators for time-dependent Lagrangian systems with non-conservative forcing. In Chapter 4, we have used Hermite polynomials to derive one-step variational and Galerkin methods. In addition to their excellent energy behavior, these one-step methods are continuous in both configuration and velocity which makes them compliant to control analysis.

The energy-preserving, adaptive time step variational integrators have been extended to rigid body systems evolving on $\mathsf{SO}(3)$ and $\mathsf{SE}(3)$ in Chapter 5 and Chapter 6, respectively. These adaptive algorithms are symplectic as well as energy and momentum-preserving while also preserving the geometry of the configuration space. The numerical studies from these chapters demonstrate that, for smaller time step values adaptive algorithms are able to achieve significantly better energy behavior compared to their fixed time step algorithms for a similar computational cost.

In Chapter 7, discrete mechanics and Lie group variational integrators are used to develop accelerated gradient methods on $\mathsf{SO}(3)$. Using continuous approximation analysis, we have shown the connection between accelerated gradient methods and continuous dynamical systems and demonstrated that the classical momentum method on $\mathbb{R}^n$ is a variational integrator. We also derived the continuous systems corresponding to both gradient descent and the proposed accelerated gradient method on $\mathsf{SO}(3)$ and demonstrated that the continuous system is a Lagrangian rigid body system evolving on $\mathsf{SO}(3)$ under the influence of potential forcing and dissipation. We discretized the continuous time system on $\mathsf{SO}(3)$ using the Lie group variational integrator framework and presented the symplectic accelerated gradient method on $\mathsf{SO}(3)$.

In Chapter 8, the numerical performance of energy-preserving, adaptive time step variational integrators is studied from both numerical and theoretical point of views. Using the residual from discrete energy equation, a conservative bound on the discrete energy error was obtained. By considering variable precision arithmetic (VPA) in computations, almost exact energy conservation was achieved. The numerical stability of the adaptive algorithm was studied by representing it as a fixed time step algorithm in a transformed setting.

9.2 Future Work

Based on the work presented in this dissertation, we have divided the future work section in two categories. Based on our literature review in Chapter 2, we first discuss key future thrust areas for broader use of structure-preserving methods in engineering applications. We then talk about specific future research directions related to our original research work.

9.2.1 Key Thrust Areas for Broader Use

Based on the literature review, we find that prior research efforts in the field of geometric numerical integration have demonstrated the advantage of structure-preserving integration methods largely through comparison with traditional integrators (e.g., the non-structure-preserving Runge-Kutta method) for "toy" problems. While this approach is useful to demonstrate the advantages of structure-preservation, it does not provide a fair assessment for practitioners.

We believe more work is needed on the applications of structure-preserving methods with a focus on large-scale systems from specific engineering applications. Furthermore, it is of interest to know how these methods compare with traditional methods in terms of the computational cost. Recently, Johnson and Murphey [200] utilized the tree-based structure to develop scalable variational integrators. Using ideas from the recursive Newton-Euler algorithm and articulated body algorithm, Lee *et al* [201] developed a linear-time variational integrator for multibody systems, and Fan *et al* [202] developed linear-time higher order variational integrators. A key topic related to this is the issue of solvability of geometric methods as most of these methods for nonlinear systems are implicit and require the solution of a system of nonlinear equations at every iteration. The connection between time step selection and solvability of implicit methods has not received enough attention in the

context of structure-preserving methods. Kobilarov [203] studied the solvability of geometric integrators and developed bounds on the fixed time step which guarantee convergence of the root-finding problem of the system of nonlinear equations. Future work along these directions will play a key role in broader use of structure-preserving methods for engineering applications.

From the reviewed literature, we also find that the majority of research published in the field of geometric numerical integration compares the results of proposed/developed structure-preserving methods with traditional methods that are not designed to respect the underlying geometric structure. In the growing literature on structure-preserving methods, apart from few exceptions [77, 204, 205], there is very little work focusing on comparison between different classes of structure-preserving methods. For example, both variational (symplectic-momentum) and energy-momentum integrators respect the qualitative features of mechanical systems. On one hand, energy conservation guarantees, a priori, that the numerical solution is restricted to a codimension 1 submanifold of the configuration manifold whereas variational integrators through symplectic structure preservation, ensure a more global and multi-dimensional behavior. From an engineering perspective, this points to a very important question: For a given mechanical system, should one use variational (symplectic-momentum) or energy-momentum methods to numerically simulate it? In order to answer this question, a detailed comparison of the numerical performance of both methods for benchmark problems from various types of mechanical systems is required. We believe research work in this direction will help practitioners understand which class of structure-preserving numerical methods is best suited to a given mechanical system.

Finally, most of the mechanical systems in engineering applications are subject to non-conservative external forcing. It is of interest to understand which class of methods performs better for non-conservative systems where the external forcing drives the dynamics such

as highly oscillatory systems found in biolocomotion or aeroelasticity applications. Also of interest is the extent to which the long-time stability advantages of structure preservation for conservative dynamical systems can carry over to mechanical systems with external forcing.

Most of the research so far has been done for PDEs with variational structure [25, 49]. Going further the research challenge is to consider nonvariational PDEs [30] and develop/extend structure-preserving algorithms for a wider class of PDEs.

9.3 Specific Future Research Directions

- **Energy-preserving, adaptive time step variational integrator** Despite their excellent conservation properties, the utility of energy-preserving, adaptive time step variational integrators for engineering applications is still an open question due to the difficulties associated with their numerical implementation. These adaptive algorithms require solving a coupled nonlinear implicit system of equations at every time step to update the configuration variables and time variable. Unlike traditional adaptive algorithms, the adaptive time step computation in these methods is inherently coupled with the discrete dynamics. In fact, existence of solutions for these discrete trajectories is not always guaranteed. Shibberu [53] has discussed the well-posedness of these adaptive algorithms and identified points in the extended state space where the adaptive algorithm has no solutions. Even for the points with existence of solution, the governing update equations are ill-conditioned. Due to the ill-conditioned nature, discrete energy error is introduced at every iteration which can lead to inaccurate numerical behavior in long-time simulations. Due to these various challenges involved with numerical simulation using energy-preserving, adaptive time step variational integrators, the numerical properties of these algorithms needs to be investigated from

an analysis point of view. Backward error analysis of these algorithms will be helpful in understanding the long-time behavior of energy error. Apart from the numerical stability, it would also be interesting to develop variational order analysis framework for these algorithms.

- **Optimal control:** Based on the discrete variational principles, the Discrete Mechanics and Optimal Control (DMOC) framework is used for optimal control of mechanical systems. It would be natural to utilize the energy-preserving, adaptive time step variational integrators developed in the DMOC setting for path following problems. Since a lot of these problems evolve on Lie groups, this would also involve extending the energy-preserving, adaptive time step Lie group variational integrators to mechanical systems with external control forcing. These algorithms can be derived by discretizing the Lagrange-d'Alembert principle on Lie groups in the extended Lagrangian mechanics setting.

- **Optimization:** With growing interest in machine learning and robotics applications, there is a need to develop understanding about optimization algorithms. Apart from the classical momentum method studied in Chapter 7, it would be interesting to study the Nesterov's accelerated gradient method from a dynamical systems perspective. Better understanding of Nesterov's accelerated gradient method from this approach can be particularly useful for developing Nesterov-like accelerated gradient methods on nonlinear manifolds.

Bibliography

[1] Asteroid 2002 AJ129 to fly safely past earth february 4. https://www.jpl.nasa.gov/news/news.php?feature=7042. Accessed: 2018-01-21.

[2] Dennis Overbye. Yearning for new physics at cern, in a post-higgs way. *The New York Times*, June 2017.

[3] Jerrold E Marsden and Tudor S Ratiu. *Introduction to Mechanics and Symmetry: A Basic Exposition of Classical Mechanical Systems*, volume 17. Springer Science & Business Media, 2013.

[4] Darryl D Holm, Tanya Schmah, and Cristina Stoica. *Geometric Mechanics and Symmetry: From Finite to Infinite Dimensions*, volume 12. Oxford University Press, 2009.

[5] Taeyoung Lee, Melvin Leok, and N Harris McClamroch. *Global Formulations of Lagrangian and Hamiltonian Dynamics on Manifolds*. Springer, 2017.

[6] Brian F Doolin and Clyde F Martin. *Introduction to Differential Geometry for Engineers*. Courier Corporation, 2013.

[7] William M Boothby. *An Introduction to Differentiable Manifolds and Riemannian Geometry*, volume 120. Academic press, 1986.

[8] Isaac Newton. *Philosophiae Naturalis Principia Mathematica*, volume 1. G. Brookman, 1833.

[9] J L Lagrange. Application de la méthode exposée dans le mémoire précédent à la solution des problèmes de dynamique différents. *Œuvres de Lagrange (1867–1892)*, 1:151–316, 1762.

[10] Joseph Louis Lagrange. *Mécanique Analytique*, volume 1. Mallet-Bachelier, 1853.

[11] Sir William Rowan Hamilton. *On a General Method in Dynamics*. Richard Taylor, 1834.

[12] William Rowan Hamilton. Vii. second essay on a general method in dynamics. *Philosophical Transactions of the Royal Society of London*, 125:95–144, 1835.

[13] Jerrold E Marsden, Sergey Pekarsky, Steve Shkoller, and Matthew West. Variational methods, multisymplectic geometry and continuum mechanics. *Journal of Geometry and Physics*, 38(3-4):253–284, 2001.

[14] H. Goldstein. *Classical Mechanics*. Reading, MA: Addison-Wesley, 1980. 672 pages.

[15] Emmy Noether. Invariante variations probleme, nachr. ges. wiss. *Gottingen Math.-Phys. Kl.*, pages 235–257, 1918.

[16] Paul K Newton. *The N-vortex Problem: Analytical Techniques*, volume 145. Springer Science & Business Media, 2013.

[17] Ralph Abraham and Jerrold E Marsden. *Foundations of Mechanics*, volume 36. Benjamin/Cummings Publishing Company Reading, Massachusetts, 1978.

[18] Anthony M Bloch, P S Krishnaprasad, Jerrold E Marsden, and Richard M Murray. Nonholonomic mechanical systems with symmetry. *Archive for Rational Mechanics and Analysis*, 136(1):21–99, 1996.

[19] Jerrold E Marsden, Richard Montgomery, and Tudor S Ratiu. *Reduction, Symmetry, and Phases in Mechanics*, volume 436. American Mathematical Soc., 1990.

[20] Razvan C Fetecau, Jerrold E Marsden, Michael Ortiz, and Matthew West. Nonsmooth Lagrangian mechanics and variational collision integrators. *SIAM Journal on Applied Dynamical Systems*, 2(3):381–416, 2003.

[21] Joan-Andreu Lázaro-Camí and Juan-Pablo Ortega. Stochastic Hamiltonian dynamical systems. *arXiv preprint math/0702787*, 2007.

[22] Jean-Michel Bismut. Mécanique aléatoire. In *Ecole d'Eté de Probabilités de Saint-Flour X-1980*, pages 1–100. Springer, 1982.

[23] Nawaf Bou-Rabee and Houman Owhadi. Stochastic variational integrators. *IMA Journal of Numerical Analysis*, 29(2):421–443, 2009.

[24] MJ Gotay, J Isenberg, JE Marsden, and R Montgomery. Momentum maps and classical fields, part i, covariant field theory (2004). *arXiv preprint physics/9801019*.

[25] Jerrold E Marsden, George W Patrick, and Steve Shkoller. Multisymplectic geometry, variational integrators, and nonlinear pdes. *Communications in Mathematical Physics*, 199(2):351–395, 1998.

[26] Kang Feng and Mengzhao Qin. *Symplectic Geometric Algorithms for Hamiltonian Systems*. Springer, 2010.

[27] Robert W Atherton and George M Homsy. On the existence and formulation of variational principles for nonlinear differential equations. *Studies in Applied Mathematics*, 54:31–60, 1975.

[28] Nail H Ibragimov. Integrating factors, adjoint equations and Lagrangians. *Journal of Mathematical Analysis and Applications*, 318(2):742–757, 2006.

[29] Nail H Ibragimov. A new conservation theorem. *Journal of Mathematical Analysis and Applications*, 333(1):311–328, 2007.

[30] Michael Kraus and Omar Maj. Variational integrators for nonvariational partial differential equations. *Physica D: Nonlinear Phenomena*, 310:37–71, 2015.

[31] Rene De Vogelaere. Methods of integration which preserve the contact transformation property of the Hamilton equations. *Technical report (University of Notre Dame. Dept. of Mathematics)*, 1956.

[32] Ronald D Ruth. A canonical integration technique. *IEEE Trans. Nucl. Sci.*, 30(CERN-LEP-TH-83-14):2669–2671, 1983.

[33] FM Lasagni. Canonical runge-kutta methods. *Zeitschrift für Angewandte Mathematik und Physik (ZAMP)*, 39(6):952–953, 1988.

[34] JM Sanz-Serna. Runge-Kutta schemes for Hamiltonian systems. *BIT Numerical Mathematics*, 28(4):877–883, 1988.

[35] Yu B Suris. On the conservation of the symplectic structure in the numerical solution of Hamiltonian systems. *Numerical Solution of Ordinary Differential Equations*, pages 148–160, 1988.

[36] Sebastian Reich. Momentum conserving symplectic integrators. *Physica D: Nonlinear Phenomena*, 76(4):375–383, 1994.

[37] Sebastian Reich. Backward error analysis for numerical integrators. *SIAM Journal on Numerical Analysis*, 36(5):1549–1570, 1999.

[38] Zhong Ge and Jerrold E Marsden. Lie–Poisson integrators and Lie–Poisson Hamilton–jacobi theory. *Phys. Lett. A*, 133:134–139, 1988.

[39] Shigeru Maeda. Lagrangian formulation of discrete systems and concept of difference space. *Math. Japonica*, 27:345–356, 1982.

[40] Shigeru Maeda. Extension of discrete noether theorem. *Math. Japonica*, 26(1):85–90, 1981.

[41] Alexander P Veselov. Integrable discrete-time systems and difference operators. *Functional Analysis and its Applications*, 22(2):83–93, 1988.

[42] Alexander P Veselov. Integrable Lagrangian correspondences and the factorization of matrix polynomials. *Functional Analysis and Its Applications*, 25(2):112–122, 1991.

[43] Jürgen Moser and Alexander P Veselov. Discrete versions of some classical integrable systems and factorization of matrix polynomials. *Communications in Mathematical Physics*, 139(2):217–243, 1991.

[44] Jerrold E Marsden and Matthew West. Discrete mechanics and variational integrators. *Acta Numerica*, 10:357–514, 2001.

[45] Jeffrey M Wendlandt and Jerrold E Marsden. Mechanical integrators derived from a discrete variational principle. *Physica D: Nonlinear Phenomena*, 106(3-4):223–246, 1997.

[46] Ernst Hairer, Christian Lubich, and Gerhard Wanner. *Geometric Numerical Integration: Structure-preserving Algorithms for Ordinary Differential Equations*, volume 31. Springer Science & Business Media, 2006.

[47] A J Lew, J E Marsden, M Ortiz, and M West. Variational time integrators. *International Journal for Numerical Methods in Engineering*, 60(1):153–212, 2004.

[48] Ernst Hairer and Christian Lubich. The life-span of backward error analysis for numerical integrators. *Numerische Mathematik*, 76(4):441–462, 1997.

[49] Benedict Leimkuhler and Sebastian Reich. *Simulating Hamiltonian Dynamics*, volume 14. Cambridge university press, 2004.

[50] Couro Kane, Jerrold E Marsden, Michael Ortiz, and Matthew West. Variational integrators and the Newmark algorithm for conservative and dissipative mechanical systems. *International Journal for Numerical Methods in Engineering*, 49(10):1295–1325, 2000.

[51] C Kane, Jerrold E Marsden, and Michael Ortiz. Symplectic-energy-momentum preserving variational integrators. *Journal of mathematical physics*, 40(7):3353–3371, 1999.

[52] Tsung-Dao Lee. Can time be a discrete dynamical variable? *Physics Letters B*, 122(3-4):217–220, 1983.

[53] Y. Shibberu. *Is symplectic-energy-momentum integration well-posed?* 2006. arXiv:math-ph/0608016.

[54] Yosi Shibberu. How to regularize a symplectic-energy-momentum integrator. *arXiv preprint math/0507483*, 2005.

[55] Harsh Sharma, Mayuresh Patil, and Craig Woolsey. Energy-preserving variational integrators for forced Lagrangian systems. *Communications in Nonlinear Science and Numerical Simulation*, 64:159–177, 2018.

[56] Anthony M Bloch, John Baillieul, Peter E Crouch, Jerrold E Marsden, Dmitry Zenkov, Perinkulam Sambamurthy Krishnaprasad, and Richard M Murray. *Nonholonomic Mechanics and Control*, volume 24. Springer, 2003.

[57] Jorge Cortés. Energy conserving nonholonomic integrators. *arXiv preprint math/0209314*, 2002.

[58] Marin Kobilarov, Jerrold E Marsden, and Gaurav S Sukhatme. Geometric discretiza-

tion of nonholonomic systems with symmetries. *Discrete and Continuous Dynamical Systems Series S*, 3(1):61–84, 2010.

[59] Grigori N Milstein, Yu M Repin, and Michael V Tretyakov. Numerical methods for stochastic systems preserving symplectic structure. *SIAM Journal on Numerical Analysis*, 40(4):1583–1604, 2002.

[60] Grigori N Milstein, Yu M Repin, and Michael V Tretyakov. Symplectic integration of Hamiltonian systems with additive noise. *SIAM Journal on Numerical Analysis*, 39(6):2066–2088, 2002.

[61] Nawaf Bou-Rabee and Houman Owhadi. Stochastic variational partitioned Runge-Kutta integrators for constrained systems. *arXiv preprint arXiv:0709.2222*, 2007.

[62] Darryl D Holm and Tomasz M Tyranowski. Stochastic discrete Hamiltonian variational integrators. *BIT Numerical Mathematics*, 58(4):1009–1048, 2018.

[63] R C Fetecau, Jerrold E Marsden, and M West. Variational multisymplectic formulations of nonsmooth continuum mechanics. In *Perspectives and problems in nolinear science*, pages 229–261. Springer, 2003.

[64] Gwen Johnson, Sigrid Leyendecker, and Michael Ortiz. Discontinuous variational time integrators for complex multibody collisions. *International Journal for Numerical Methods in Engineering*, 100(12):871–913, 2014.

[65] S Lall and Matthew West. Discrete variational Hamiltonian mechanics. *Journal of Physics A: Mathematical and general*, 39(19):5509, 2006.

[66] Melvin Leok and Jingjing Zhang. Discrete Hamiltonian variational integrators. *IMA Journal of Numerical Analysis*, 31(4):1497–1532, 2010.

[67] Jeremy M Schmitt and Melvin Leok. Properties of Hamiltonian variational integrators. *IMA Journal of Numerical Analysis*, 38(1):377–398, 2017.

[68] Mark J Gotay, James Isenberg, Jerrold E Marsden, and Richard Montgomery. Momentum maps and classical relativistic fields. part i: Covariant field theory. *arXiv preprint physics/9801019*, 1998.

[69] Adrian J Lew, Jerrold E Marsden, Michael Ortiz, and Matthew West. Asynchronous variational integrators. *Archive for Rational Mechanics and Analysis*, 167(2):85–146, 2003.

[70] T Belytschko and DF Schoeberle. On the unconditional stability of an implicit algorithm for nonlinear structural dynamics. *Journal of Applied Mechanics*, 42(4):865–869, 1975.

[71] O Gonzalez and Juan C Simo. On the stability of symplectic and energy-momentum algorithms for non-linear Hamiltonian systems with symmetry. *Computer Methods in Applied Mechanics and Engineering*, 134(3-4):197–222, 1996.

[72] Robert A LaBudde and Donald Greenspan. Discrete mechanics—a general treatment. *Journal of Computational Physics*, 15(2):134–167, 1974.

[73] Robert A LaBudde and Donald Greenspan. Energy and momentum conserving methods of arbitrary order for the numerical integration of equations of motion. *Numerische Mathematik*, 25(4):323–346, 1975.

[74] Robert A LaBudde and Donald Greenspan. Energy and momentum conserving methods of arbitrary order for the numerical integration of equations of motion. *Numerische Mathematik*, 26(1):1–16, 1976.

[75] J C Simo and Nils Tarnow. The discrete energy-momentum method. conserving algorithms for nonlinear elastodynamics. *Zeitschrift für angewandte Mathematik und Physik (ZAMP)*, 43(5):757–792, 1992.

[76] Juan C Simo, N Tarnow, and K K Wong. Exact energy-momentum conserving algorithms and symplectic schemes for nonlinear dynamics. *Computer Methods in Applied Mechanics and Engineering*, 100(1):63–116, 1992.

[77] J C Simo and O Gonzalez. Assessment of energy-momentum and symplectic schemes for stiff dynamical systems. In *American Society of Mechanical Engineers, ASME Winter Annual Meeting, New Orleans, Louisiana*, 1993.

[78] P Betsch and P Steinmann. Conservation properties of a time FE method. part i: time-stepping schemes for N-body problems. *International Journal for Numerical Methods in Engineering*, 49(5):599–638, 2000.

[79] P Betsch and P Steinmann. Conservation properties of a time FE method—part ii: Time-stepping schemes for non-linear elastodynamics. *International Journal for Numerical Methods in Engineering*, 50(8):1931–1955, 2001.

[80] P Betsch and P Steinmann. Conservation properties of a time FE method—part iii: mechanical systems with holonomic constraints. *International Journal for Numerical Methods in Engineering*, 53(10):2271–2304, 2002.

[81] M Groß, P Betsch, and P Steinmann. Conservation properties of a time FE method. part iv: Higher order energy and momentum conserving schemes. *International Journal for Numerical Methods in Engineering*, 63(13):1849–1897, 2005.

[82] Francisco Armero and Eva Petőcz. A new dissipative time-stepping algorithm for

frictional contact problems: formulation and analysis. *Computer Methods in Applied Mechanics and Engineering*, 179(1-2):151–178, 1999.

[83] Thomas JR Hughes. Analysis of transient algorithms with particular reference to stability behavior. In *Comput Methods for Transient Anal*, pages 67–155. North-Holland Comput Methods in Mech. v 1 Amsterdam, Neth and, 1983.

[84] Detlef Kuhl and Ekkehard Ramm. Generalized energy–momentum method for non-linear adaptive shell dynamics. *Computer Methods in Applied Mechanics and Engineering*, 178(3-4):343–366, 1999.

[85] Oscar Gonzalez. Time integration and discrete Hamiltonian systems. *Journal of Nonlinear Science*, 6(5):449, 1996.

[86] Robert I McLachlan, GRW Quispel, and Nicolas Robidoux. Geometric integration using discrete gradients. *Philosophical Transactions of the Royal Society of London. Series A: Mathematical, Physical and Engineering Sciences*, 357(1754):1021–1045, 1999.

[87] Oscar Gonzalez. Mechanical systems subject to holonomic constraints: Differential–algebraic formulations and conservative integration. *Physica D: Nonlinear Phenomena*, 132(1-2):165–174, 1999.

[88] Elena Celledoni, Marta Farré Puiggalí, Eirik Hoel Høiseth, and David Martín de Diego. Energy-preserving integrators applied to nonholonomic systems. *Journal of Nonlinear Science*, pages 1–40, 2016.

[89] Robert I McLachlan and GRW Quispel. Discrete gradient methods have an energy conservation law. *arXiv preprint arXiv:1302.4513*, 2013.

[90] Elena Celledoni, Volker Grimm, Robert I McLachlan, DI McLaren, D O'Neale, Brynjulf Owren, and GRW Quispel. Preserving energy resp. dissipation in numerical pdes using

the "average vector field" method. *Journal of Computational Physics*, 231(20):6770–6789, 2012.

[91] A Iserles and GRW Quispel. Why geometric numerical integration? *arXiv preprint arXiv:1602.07755*, 2015.

[92] Peter E Crouch and R Grossman. Numerical integration of ordinary differential equations on manifolds. *Journal of Nonlinear Science*, 3(1):1–33, 1993.

[93] Hans Z Munthe-Kaas. Runge-kutta methods on Lie groups. *BIT Numerical Mathematics*, 38(1):92–111, 1998.

[94] Hans Z Munthe-Kaas. High order runge-kutta methods on manifolds. *Applied Numerical Mathematics*, 29(1):115–127, 1999.

[95] Arieh Iserles, Hans Z Munthe-Kaas, Syvert P Nørsett, and Antonella Zanna. Lie-group methods. *Acta numerica*, 9:215–365, 2000.

[96] Elena Celledoni, Håkon Marthinsen, and Brynjulf Owren. An introduction to Lie group integrators–basics, new developments and applications. *Journal of Computational Physics*, 257:1040–1061, 2014.

[97] Debra Lewis and Juan Carlos Simo. Conserving algorithms for the dynamics of Hamiltonian systems on Lie groups. *Journal of Nonlinear Science*, 4(1):253–299, 1994.

[98] Aleksandr I Bobenko and Yu B Suris. Discrete time Lagrangian mechanics on Lie groups, with an application to the Lagrange top. *Communications in mathematical physics*, 204(1):147–188, 1999.

[99] Jerrold E Marsden, Sergey Pekarsky, and Steve Shkoller. Discrete Euler-Poincaré and Lie-Poisson equations. *Nonlinearity*, 12(6):1647, 1999.

[100] Taeyoung Lee, N Harris McClamroch, and Melvin Leok. A Lie group variational integrator for the attitude dynamics of a rigid body with applications to the 3d pendulum. In *Proceedings of 2005 IEEE Conference on Control Applications*, pages 962–967, Aug. 2005.

[101] Taeyoung Lee, Melvin Leok, and N Harris McClamroch. Lie group variational integrators for the full body problem. *Computer Methods in Applied Mechanics and Engineering*, 196(29):2907–2924, 2007.

[102] Taeyoung Lee, Melvin Leok, and N Harris McClamroch. Lagrangian mechanics and variational integrators on two-spheres. *International Journal for Numerical Methods in Engineering*, 79(9):1147–1174, 2009.

[103] François Demoures. *Lie group and Lie algebra variational integrators for flexible beam and plate in* $\mathbb{R}^3$ *[Ph.D.thesis]*. PhD thesis, École Polytechnique Fédéralge de Lausanne, 2012.

[104] François Demoures, François Gay-Balmaz, Marin Kobilarov, and Tudor S Ratiu. Multisymplectic Lie group variational integrator for a geometrically exact beam in $\mathbb{R}^3$. *Communications in Nonlinear Science and Numerical Simulation*, 19(10):3492–3512, 2014.

[105] François Demoures, François Gay-Balmaz, Sigrid Leyendecker, Sina Ober-Blöbaum, Tudor S Ratiu, and Yves Weinand. Discrete variational Lie group formulation of geometrically exact beam dynamics. *Numerische Mathematik*, 130(1):73–123, 2015.

[106] Harsh Sharma and Taeyoung Lee. Energy-preserving, adaptive time-step Lie group variational integrators for the attitude dynamics of a rigid body. In *2019 American Control Conference (ACC)*, pages 5487–5492. IEEE, 2019.

[107] Harsh Sharma, Mayuresh Patil, and Craig Woolsey. Energy-preserving, adaptive time-step Lie group variational integrators for rigid body motion in SE(3). In *2019 58th IEEE Conference on Decision and Control (accepted)*. IEEE, 2019.

[108] Kang Feng and Meng-zhao Qin. The symplectic methods for the computation of Hamiltonian equations. In *Numerical methods for partial differential equations*, pages 1–37. Springer, 1987.

[109] Paul J Channell and Clint Scovel. Symplectic integration of Hamiltonian systems. *Nonlinearity*, 3(2):231, 1990.

[110] Etienne Forest and Ronald D Ruth. Fourth-order symplectic integration. *Physica D: Nonlinear Phenomena*, 43(1):105–117, 1990.

[111] Jack Wisdom and Matthew Holman. Symplectic maps for the n-body problem. *The Astronomical Journal*, 102:1528–1538, 1991.

[112] Jack Wisdom. The origin of the Kirkwood gaps-a mapping for asteroidal motion near the 3/1 commensurability. *The Astronomical Journal*, 87:577–593, 1982.

[113] Jack Wisdom. Chaotic behavior and the origin of the 3/1 Kirkwood gap. *Icarus*, 56(1):51–74, 1983.

[114] Haruo Yoshida. Recent progress in the theory and application of symplectic integrators. In *Qualitative and Quantitative Behaviour of Planetary Systems*, pages 27–43. Springer, 1993.

[115] Brett Gladman, Martin Duncan, and Jeff Candy. Symplectic integrators for long-term integrations in celestial mechanics. *Celestial Mechanics and Dynamical Astronomy*, 52(3):221–240, 1991.

[116] Hiroshi Kinoshita, Haruo Yoshida, and Hiroshi Nakai. Symplectic integrators and their application to dynamical astronomy. *Celestial Mechanics and Dynamical Astronomy*, 50(1):59–71, 1990.

[117] E Imre and PL Palmer. High-precision, symplectic numerical, relative orbit propagation. *Journal of guidance, control, and dynamics*, 30(4):965–973, 2007.

[118] John E Chambers. A hybrid symplectic integrator that permits close encounters between massive bodies. *Monthly Notices of the Royal Astronomical Society*, 304(4):793–799, 1999.

[119] F Varadi, CM De la Barre, WM Kaula, and M Ghil. Singularly weighted symplectic forms and applications to asteroid motion. *Celestial Mechanics and Dynamical Astronomy*, 62(1):23–41, 1995.

[120] Lin Liu, Jiang-hui Ji, and Xin-hao Liao. A numerical study of the orbits of near earth asteroids with symplectic algorithm. *Chinese Astronomy and Astrophysics*, 23(1):108–119, 1999.

[121] Harold F Levison and Martin J Duncan. The long-term dynamical behavior of short-period comets. *Icarus*, 108(1):18–36, 1994.

[122] Vacheslav Emel'yanenko. An explicit symplectic integrator for cometary orbits. *Celestial Mechanics and Dynamical Astronomy*, 84(4):331–341, 2002.

[123] Yuichi Tsuda and Daniel J Scheeres. Computation and applications of an orbital dynamics symplectic state transition matrix. *Journal of guidance, control, and dynamics*, 32(4):1111–1123, 2009.

[124] J Wisdom, M Holman, and J Touma. Symplectic correctors. *Integration Algorithms and Classical Mechanics*, 10:217–244, 1996.

[125] Will M Farr and Edmund Bertschinger. Variational integrators for the gravitational N-body problem. *The Astrophysical Journal*, 663(2):1420, 2007.

[126] Taeyoung Lee, Melvin Leok, and N Harris McClamroch. High-fidelity numerical simulation of complex dynamics of tethered spacecraft. *Acta Astronautica*, 99:215–230, 2014.

[127] Taeyoung Lee and Frederick Leve. Lagrangian mechanics and Lie group variational integrators for spacecraft with imbalanced reaction wheels. In *2014 American Control Conference*, pages 3122–3127. IEEE, 2014.

[128] James Hall and Melvin Leok. Spectral variational integrators. *Numerische Mathematik*, 130(4):681–740, 2015.

[129] Leonel Palacios and Pini Gurfil. Variational and symplectic integrators for satellite relative orbit propagation including drag. *Celestial Mechanics and Dynamical Astronomy*, 130(4):31, 2018.

[130] JC Simo and O Gonzalez. Recent results on the numerical integration of infinite-dimensional Hamiltonian systems. *Recent Developments in Finite Element Analysis. CIMNE, Barcelona, Spain*, pages 255–271, 1994.

[131] Oscar Gonzalez. Exact energy and momentum conserving algorithms for general models in nonlinear elasticity. *Computer Methods in Applied Mechanics and Engineering*, 190(13-14):1763–1783, 2000.

[132] S Leyendecker, P Betsch, and P Steinmann. Objective energy–momentum conserving integration for the constrained dynamics of geometrically exact beams. *Computer Methods in Applied Mechanics and Engineering*, 195(19-22):2313–2333, 2006.

[133] Mirza Muhammad Irfan Baig and Klaus-Jürgen Bathe. On direct time integration in large deformation dynamic analysis. In *Third MIT Conference on Computational Fluid and Solid Mechanics, Boston, MA, June*, pages 14–17, 2005.

[134] C Sansour, P Wriggers, and J Sansour. Nonlinear dynamics of shells: theory, finite element formulation, and integration schemes. *Nonlinear Dynamics*, 13(3):279–305, 1997.

[135] Adrian Jose Lew. *Variational time integrators in computational solid mechanics [Ph.D. thesis]*. PhD thesis, California Institute of Technology, 2003.

[136] Kedar G Kale and Adrian J Lew. Parallel asynchronous variational integrators. *International Journal for Numerical Methods in Engineering*, 70(3):291–321, 2007.

[137] Juan C GarcÍa Orden and José M Goicolea. Conserving properties in constrained dynamics of flexible multibody systems. *Multibody System Dynamics*, 4(2-3):225–244, 2000.

[138] Peter Betsch and Sigrid Leyendecker. The discrete null space method for the energy consistent integration of constrained mechanical systems. part ii: Multibody dynamics. *International journal for numerical methods in engineering*, 67(4):499–552, 2006.

[139] Sigrid Leyendecker, Peter Betsch, and Paul Steinmann. The discrete null space method for the energy-consistent integration of constrained mechanical systems. part iii: Flexible multibody dynamics. *Multibody System Dynamics*, 19(1-2):45–72, 2008.

[140] P Betsch and P Steinmann. Constrained integration of rigid body dynamics. *Computer Methods in Applied Mechanics and Engineering*, 191(3-5):467–488, 2001.

[141] Peter Betsch and Stefan Uhlar. Energy-momentum conserving integration of multibody dynamics. *Multibody System Dynamics*, 17(4):243–289, 2007.

[142] Stefan Uhlar and Peter Betsch. On the derivation of energy consistent time stepping schemes for friction afflicted multibody systems. *Computers & Structures*, 88(11-12):737–754, 2010.

[143] Sigrid Leyendecker, Jerrold E Marsden, and Michael Ortiz. Variational integrators for constrained dynamical systems. *ZAMM-Journal of Applied Mathematics and Mechanics*, 88(9):677–708, 2008.

[144] Sigrid Leyendecker and Sina Ober-Blöbaum. A variational approach to multirate integration for constrained systems. In *Multibody dynamics*, pages 97–121. Springer, 2013.

[145] Olivier Brüls and Alberto Cardona. On the use of Lie group time integrators in multibody dynamics. *Journal of Computational and Nonlinear Dynamics*, 5(3):031002, 2010.

[146] Olivier Brüls, Alberto Cardona, and Martin Arnold. Lie group generalized-α time integration of constrained flexible multibody systems. *Mechanism and Machine Theory*, 48:121–137, 2012.

[147] Jonghoon Park and Wan-Kyun Chung. Geometric integration on euclidean group with application to articulated multibody systems. *IEEE Transactions on Robotics*, 21(5):850–863, 2005.

[148] Zdravko Terze, Andreas Müller, and Dario Zlatar. Lie-group integration method for constrained multibody systems in state space. *Multibody system dynamics*, 34(3):275–305, 2015.

[149] Blair Perot. Conservation properties of unstructured staggered mesh schemes. *Journal of Computational Physics*, 159(1):58–89, 2000.

[150] Sharif Elcott, Yiying Tong, Eva Kanso, Peter Schröder, and Mathieu Desbrun. Stable, circulation-preserving, simplicial fluids. *ACM Transactions on Graphics (TOG)*, 26(1):4, 2007.

[151] Vladimir Arnold. Sur la géométrie différentielle des groupes de Lie de dimension infinie et ses applications à l'hydrodynamique des fluides parfaits. In *Annales de l'institut Fourier*, volume 16, pages 319–361, 1966.

[152] Colin J Cotter, Darryl D Holm, and Peter E Hydon. Multisymplectic formulation of fluid dynamics using the inverse map. *Proceedings of the Royal Society A: Mathematical, Physical and Engineering Sciences*, 463(2086):2671–2687, 2007.

[153] Jerrold E Marsden, David G Ebin, and Arthur E Fischer. Diffeomorphism groups, hydrodynamics and relativity. Canadian Mathematical Congress, 1972.

[154] Patrick Mullen, Keenan Crane, Dmitry Pavlov, Yiying Tong, and Mathieu Desbrun. Energy-preserving integrators for fluid animation. *ACM Transactions on Graphics (TOG)*, 28(3):38, 2009.

[155] Dmitry Pavlov, Patrick Mullen, Yiying Tong, Eva Kanso, Jerrold E Marsden, and Mathieu Desbrun. Structure-preserving discretization of incompressible fluids. *Physica D: Nonlinear Phenomena*, 240(6):443–458, 2011.

[156] Evans S Gawlik, Patrick Mullen, Dmitry Pavlov, Jerrold E Marsden, and Mathieu Desbrun. Geometric, variational discretization of continuum theories. *Physica D: Nonlinear Phenomena*, 240(21):1724–1760, 2011.

[157] Mathieu Desbrun, Evan S Gawlik, François Gay-Balmaz, and Vladimir Zeitlin. Variational discretization for rotating stratified fluids. *Discrete and Continuous Dynamical Systems*, 34(2):477–509, 2013.

[158] Werner Bauer and François Gay-Balmaz. Towards a geometric variational discretization of compressible fluids: the rotating shallow water equations. *arXiv preprint arXiv:1711.10617*, 2017.

[159] Zachary Manchester, Neel Doshi, Robert J Wood, and Scott Kuindersma. Contact-implicit trajectory optimization using variational integrators. *The International Journal of Robotics Research*, page 0278364919849235, 2019.

[160] Oliver Junge, Jerrold E Marsden, and Sina Ober-Blöbaum. Discrete mechanics and optimal control. *IFAC Proceedings Volumes*, 38(1):538–543, 2005.

[161] Sina Ober-Blöbaum, Oliver Junge, and Jerrold E Marsden. Discrete mechanics and optimal control: an analysis. *ESAIM: Control, Optimisation and Calculus of Variations*, 17(2):322–352, 2011.

[162] Sigrid Leyendecker, Sina Ober-Blöbaum, Jerrold E Marsden, and Michael Ortiz. Discrete mechanics and optimal control for constrained systems. *Optimal Control Applications and Methods*, 31(6):505–528, 2010.

[163] Marin Kobilarov and Gaurav Sukhatme. Optimal control using nonholonomic integrators. In *Proceedings 2007 IEEE International Conference on Robotics and Automation*, pages 1832–1837. IEEE, 2007.

[164] Paul Manns and Katja Mombaur. Towards discrete mechanics and optimal control for complex models. *IFAC-PapersOnLine*, 50(1):4812–4818, 2017.

[165] Oliver Junge, Jerrold E Marsden, and Sina Ober-Blobaum. Optimal reconfiguration of formation flying spacecraft—a decentralized approach. In *Proceedings of the 45th IEEE Conference on Decision and Control*, pages 5210–5215. IEEE, 2006.

[166] Taeyoung Lee, N Harris McClamroch, and Melvin Leok. Attitude maneuvers of a rigid spacecraft in a circular orbit. In *2006 American Control Conference*, pages 1742–1747. IEEE, 2006.

[167] Zeeshan Shareef and Ansgar Trächtler. Simultaneous path planning and trajectory optimization for robotic manipulators using discrete mechanics and optimal control. *Robotica*, 34(6):1322–1334, 2016.

[168] David Pekarek, Aaron D Ames, and Jerrold E Marsden. Discrete mechanics and optimal control applied to the compass gait biped. In *2007 46th IEEE Conference on Decision and Control*, pages 5376–5382. IEEE, 2007.

[169] Tatsuya Kai and Kouhei Yamaki. Development of discrete mechanics for 2-dimensional distributed parameter mechanical systems and its application to vibration suppression control of a film. In *Proc. International Symposium of Nonlinear Theory and Its Application 2016*, pages 638–641, 2016.

[170] Zeeshan Shareef and Ansgar Trächtler. Optimal trajectory planning for robotic manipulators using discrete mechanics and optimal control. In *2014 IEEE Conference on Control Applications (CCA)*, pages 240–245. IEEE, 2014.

[171] Zachary Manchester and Scott Kuindersma. Variational contact-implicit trajectory optimization. In *International Symposium on Robotics Research (ISRR), Puerto Varas, Chile*, 2017.

[172] Dominik Kern and Michael Groß. Variational integrators and optimal control for a hybrid pendulum-on-cart-system. *PAMM*, 18(1):e201800088, 2018.

[173] Robert I McLachlan and Stephen Marsland. Discrete mechanics and optimal control for image registration. *Anziam Journal*, 48:1–16, 2006.

[174] Herbert Goldstein, Charles Poole, and John Safko. Classical mechanics, 2002.

[175] J Argyris and D Scharpf. Finite elements in time and space. *The Aeronautical Journal*, 73(708):1041–1044, 1969.

[176] Melvin Leok and Tatiana Shingel. Prolongation–collocation variational integrators. *IMA Journal of Numerical Analysis*, 32(3):1194–1216, 2011.

[177] Himanshu Shukla and Mayuresh J Patil. Nonlinear state feedback control design to eliminate subcritical limit cycle oscillations in aeroelastic systems. *Nonlinear Dynamics*, 88(3):1599–1614, 2017.

[178] Nikolaj Nordkvist and Amit K Sanyal. A Lie group variational integrator for rigid body motion in se (3) with applications to underwater vehicle dynamics. In *Decision and Control (CDC), 2010 49th IEEE Conference on*, pages 5414–5419. IEEE, 2010.

[179] Luca Carlone, Roberto Tron, Kostas Daniilidis, and Frank Dellaert. Initialization techniques for 3d slam: a survey on rotation estimation and its use in pose graph optimization. In *2015 IEEE international conference on robotics and automation (ICRA)*, pages 4597–4604. IEEE, 2015.

[180] Boris T Polyak. Some methods of speeding up the convergence of iteration methods. *USSR Computational Mathematics and Mathematical Physics*, 4(5):1–17, 1964.

[181] Yurii E Nesterov. A method for solving the convex programming problem with convergence rate o (1/k^ 2). In *Dokl. akad. nauk Sssr*, volume 269, pages 543–547, 1983.

[182] Camillo J Taylor and David J Kriegman. Minimization on the Lie group so (3) and related manifolds. *Yale University*, 16(155):6, 1994.

[183] Mark D Plumbley. Lie group methods for optimization with orthogonality constraints. In *International Conference on Independent Component Analysis and Signal Separation*, pages 1245–1252. Springer, 2004.

[184] Traian E Abrudan, Jan Eriksson, and Visa Koivunen. Steepest descent algorithms for optimization under unitary matrix constraint. *IEEE Transactions on Signal Processing*, 56(3):1134–1147, 2008.

[185] Hongyi Zhang and Suvrit Sra. Towards riemannian accelerated gradient methods. *arXiv preprint arXiv:1806.02812*, 2018.

[186] Weijie Su, Stephen Boyd, and Emmanuel Candes. A differential equation for modeling nesterov's accelerated gradient method: Theory and insights. In *Advances in Neural Information Processing Systems*, pages 2510–2518, 2014.

[187] Andre Wibisono, Ashia C Wilson, and Michael I Jordan. A variational perspective on accelerated methods in optimization. *proceedings of the National Academy of Sciences*, 113(47):E7351–E7358, 2016.

[188] Lin Yang, Raman Arora, Tuo Zhao, et al. The physical systems behind optimization algorithms. In *Advances in Neural Information Processing Systems*, pages 4372–4381, 2018.

[189] Michael Muehlebach and Michael I Jordan. A dynamical systems perspective on nesterov acceleration. *arXiv preprint arXiv:1905.07436*, 2019.

[190] Guilherme França, Jeremias Sulam, Daniel P Robinson, and René Vidal. Conformal symplectic and relativistic optimization. *arXiv preprint arXiv:1903.04100*, 2019.

[191] T. Lee, M. Leok, and N. H. McClamroch. Lie group variational integrators for the full

body problem. *Computer Methods in Applied Mechanics and Engineering*, 196:2907–2924, May 2007.

[192] Melvin Leok. *Foundations of computational geometric mechanics*. PhD thesis, California Institute of Technology, 2004.

[193] Harsh Sharma, Mayuresh Patil, and Craig Woolsey. A review of structure-preserving numerical methods for engineering applications. *Computer Methods in Applied Mechanics and Engineering*, 366:113067, 2020.

[194] M. D. Shuster and S. D. Oh. Three-axis attitude determination from vector observations. *Journal of Guidance Control and Dynamics*, 4(1):70–77, 1981.

[195] Taeyoung Lee. Real harmonic analysis on the special orthogonal group. *arXiv preprint arXiv:1809.10533*, 2018.

[196] James H Wilkinson. Error analysis of floating-point computation. *Numerische Mathematik*, 2(1):319–340, 1960.

[197] JM Sanz-Serna. Backward error analysis of symplectic integrators. *Fields Inst. Comm*, 10:193–205, 1996.

[198] Ernst Hairer. Variable time step integration with symplectic methods. *Applied Numerical Mathematics*, 25(2-3):219–227, 1997.

[199] Mats Vermeeren. Modified equations for variational integrators. *Numerische Mathematik*, 137(4):1001–1037, 2017.

[200] Elliot R Johnson and Todd D Murphey. Scalable variational integrators for constrained mechanical systems in generalized coordinates. *IEEE Transactions on Robotics*, 25(6):1249–1261, 2009.

[201] Jeongseok Lee, C Karen Liu, Frank C Park, and Siddhartha S Srinivasa. A linear-time variational integrator for multibody systems. *arXiv preprint arXiv:1609.02898*, 2016.

[202] Taosha Fan, Jarvis Schultz, and Todd D Murphey. Efficient computation of higher-order variational integrators in robotic simulation and trajectory optimization. *arXiv preprint arXiv:1904.12756*, 2019.

[203] Marin Kobilarov. Solvability of geometric integrators for multi-body systems. In *Multibody Dynamics*, pages 145–174. Springer, 2014.

[204] S Leyendecker, P Betsch, and P Steinmann. Energy-conserving integration of constrained Hamiltonian systems–a comparison of approaches. *Computational Mechanics*, 33(3):174–185, 2004.

[205] Peter Betsch, Christian Hesch, Nicolas Sänger, and Stefan Uhlar. Variational integrators and energy-momentum schemes for flexible multibody dynamics. *Journal of Computational and Nonlinear Dynamics*, 5(3):031001/1–031001/11, 2010.